Bodine Journal

Volume 1 | Issue 1 Article 8

2008

Download Entire Bodine Journal Volume 1, Issue 1, 2008

Jefferson™ Kimmel Cancer Center
NCI-designated

Vol 1, Issue 1 | Fall 2008

BODINE JOURNAL

Inside

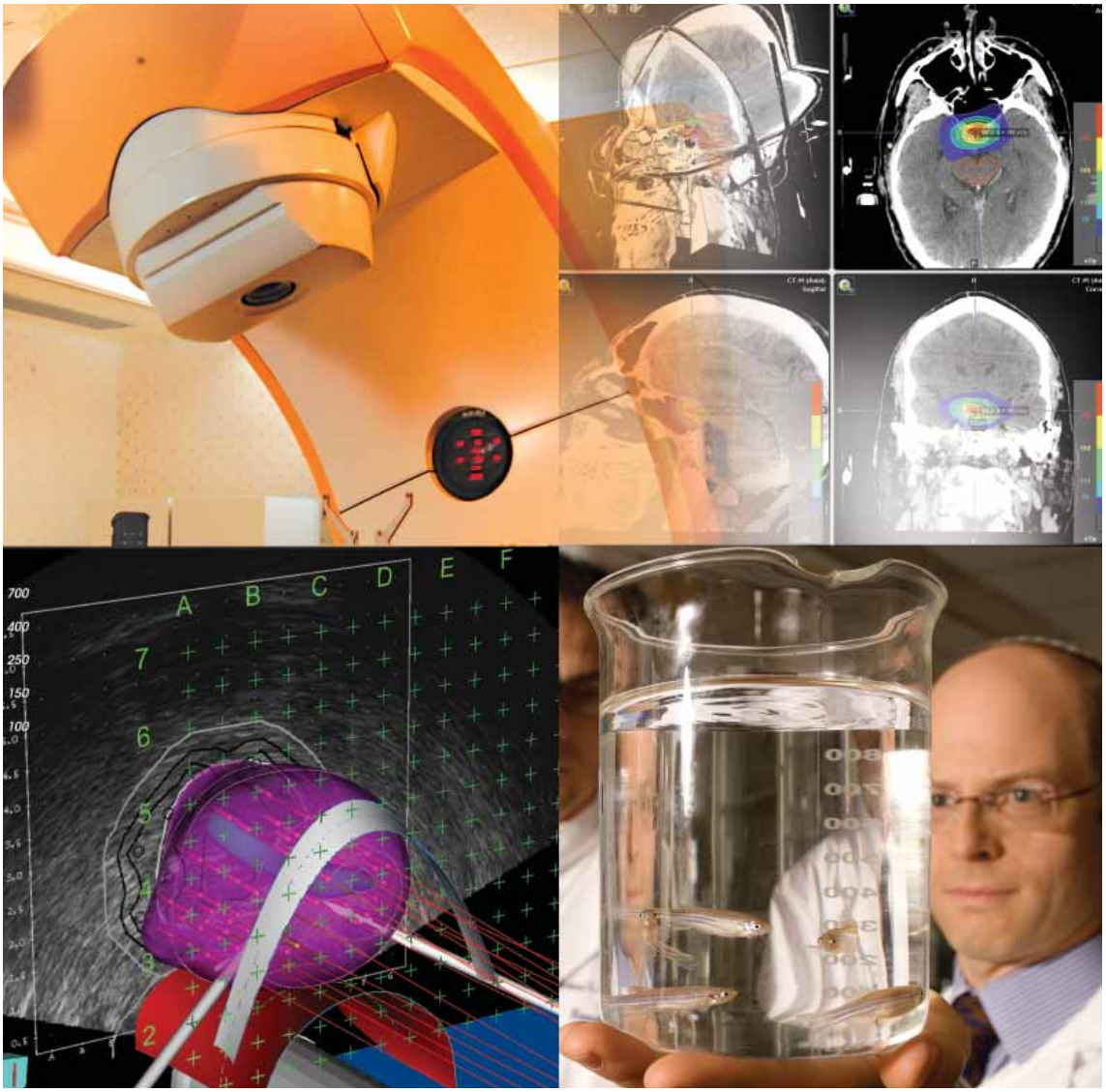

A publication of Thomas Jefferson University, Department of Radiation Oncology

NCI·CC
A Cancer Center Designated by the National Cancer Institute

BODINE JOURNAL

Vol 1, Issue 1 | Fall 2008

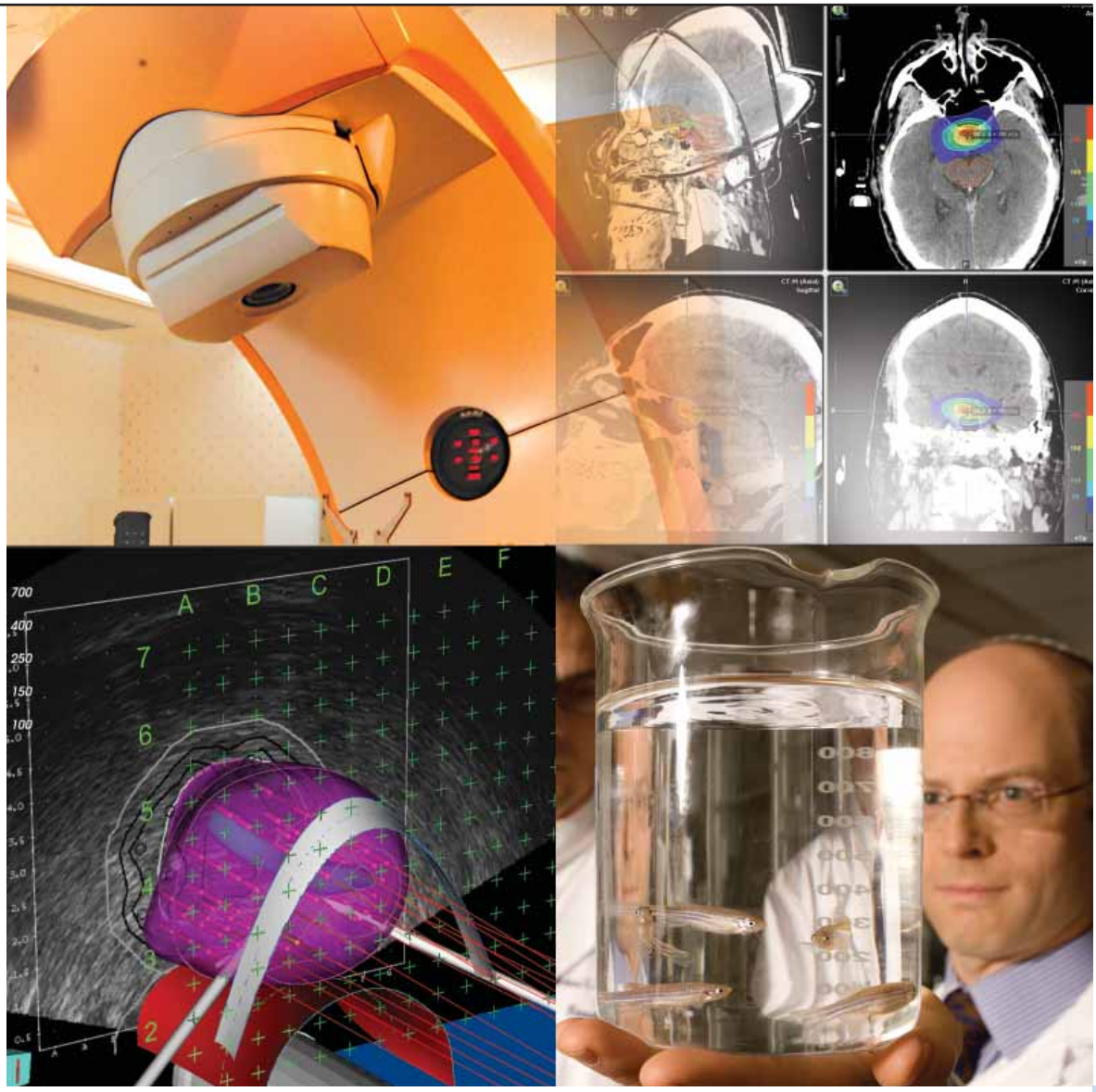

A publication of Thomas Jefferson University, Department of Radiation Oncology

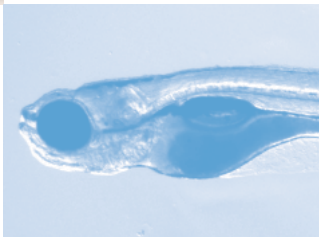

General Information
Correspondence, inquiries, or comments may be submitted to the Editor, Bodine Journal, Jefferson Kimmel Cancer Center – Bodine, 111 S. 11th St., Philadelphia, PA 19107 or email at: BODINEjournal@jeffersonhospital.org

www.kimmelcancercenter.org/kcc/radonc/bodine_journal/2008FallBodineJournal.pdf

Table of Contents

Articles

Departmental Information

Names in Bold: Members of the Department of Radiation Oncology, Thomas Jefferson University

Toxicity of Radiotherapy in Patients With Collagen Vascular Disease

Alexander Lin, MD,[1] Eyad Abu-Isa, MD,[1] Kent A. Griffith, MPH, MS[2]
Edgar Ben-Josef, MD[1]

[1]Department of Radiation Oncology, University of Michigan, Ann Arbor, Michigan.
[2]University of Michigan Cancer Center Biostatistics Core, Ann Arbor, Michigan.

The following article is reprinted with permission from John Wiley & Sons, Inc. It was originally published in CANCER, Volume 113, No. 3, pages 648-653, August 1, 2008.

Background
A diagnosis of collagen vascular disease (CVD) may predispose to radiotherapy (RT) toxicity. The objective of the current study was to identify factors that influence RT toxicity in the setting of CVD.

Methods
A total of 86 RT courses for 73 patients with CVD were delivered between 1985 and 2005. CVD subtypes include rheumatoid arthritis (RA; 33 patients), systemic lupus erythematosus (SLE; 13 patients), scleroderma (9 patients), dermatomyositis/polymyositis (5 patients), ankylosing spondylitis (4 patients), polymyalgia rheumatica/temporal arteritis (4 patients), Wegener granulomatosis (3 patients), and mixed connective tissue disorders (MCTD)/other (2 patients). Each patient with CVD was matched to 1 to 3 controls with respect to sex, race, site irradiated, RT dose (±2 Gray), and age (±5 years).

Results
There was no significant difference between CVD patients (65.1%) and controls (72.5%) experiencing any acute toxicity. CVD patients had a higher incidence of any late toxicity (29.1% vs 14%; $P = .001$), and a trend toward an increased rate of severe late toxicity (9.3% vs 3.7%; $P = .079$). RT delivered to the breast had increased risk of severe acute toxicity, whereas RT to the pelvis had increased risk of severe acute and late toxicity. RT administered in the setting of scleroderma carried a higher risk of severe late toxicity, whereas RT to SLE patients carried a higher risk of severe acute and late toxicity.

Conclusions
Although generally well tolerated, RT in the setting of CVD appears to carry a higher risk of late toxicity. RT to the pelvis or in the setting of SLE or scleroderma may predispose to an even greater risk of severe toxicity. These issues should be considered when deciding whether to offer RT for these patients. ***Cancer* 2008;113:648–53.** *©2008 American Cancer Society.*

Key Words: radiotherapy, collagen diseases, complications, adverse effects.

The decision of whether to offer therapeutic radiotherapy (RT) to patients with collagen vascular disease (CVD) continues to be a challenging one. It is believed that CVD may predispose patients to increased toxicity, and many practicing oncologists believe that a diagnosis of CVD is a relative contraindication to RT. However, to our knowledge, the available literature on this issue has been mixed. Early publications were largely case reports of CVD patients with increased toxicity from RT.[1-8] However, 2 separate matched control studies failed to observe any increased risk of acute or late complications in patients with CVD versus patients without CVD.[9,10] Other publications suggested that patients with nonrheumatoid arthritis CVD,[11,12] or patients with specific subtypes of CVD, may be at increased toxicity risk.[13-15] Further complicating the issue is the finding that some commonly prescribed medications, many of which are used in patients with CVD, may alter the radiation toxicity profile.[16–18] The goals of this matched control study were to determine whether patients with CVD were at a higher risk of RT-associated toxicity compared with patients without CVD and to identify factors that influence radiation toxicity in the setting of CVD, with particular emphasis on medications (antirheumatic drugs, nonsteroidal antiinflammatory drugs [NSAIDs], statins, and calcium channel blockers [CCBs]) that when taken concurrently may alter radiation toxicity.

Materials and Methods
After Institutional Review Board approval, 101 patients with a diagnosis of CVD treated in the Department of Radiation Oncology at the University of Michigan between 1985 and 2005 were identified. A total of 116 unique RT courses were delivered to these patients. A majority of these courses were delivered with 3-dimensional (3D) conformal techniques. Twenty-two cases were excluded because the diagnosis of CVD was made after the completion of RT. Of the remaining 94 RT courses, 8 courses could not be matched with a control. This left an analyzable sample of 86 CVD RT courses for 73 unique patients. Thirty-three patients had rheumatoid arthritis (RA), 13 had systemic lupus erythematosus (SLE), 9 had scleroderma, 5 had dermatomyositis/polymyositis, 4 had ankylosing spondylitis, 4 had polymyalgia rheumatica/temporal arteritis, 3 had Wegener granulomatosis, and 2 had mixed connective tissue disorders (MCTD)/other. Neither polymyalgia rheumatica/temporal arteritis nor Wegener granulomatosis are defined as a CVD; however, their inclusion was based on the systemic vasculitis noted with these diseases and its potential impact on RT toxicity. The mean age of the patients at time of RT was 58.2 years (range, 23-84 years) and the majority of patients were women (73.3%). Sixty patients received only a single RT course, with 13 patients receiving 2 RT courses in this dataset. Their medical records were reviewed for the following characteristics: age, sex, race, CVD type and activity, date of CVD diagnosis, concurrent medications, cancer diagnosis, chemotherapy treatment details, site and dose schedule of RT, acute and late toxicity, pattern of failure, and survival.

Of the total 86 RT courses, 15 were delivered to the thorax, 14 to the skin, 12 to the head and neck, 11 to bone, 11 to the pelvis, 8 to the breast, 6 to total body, 4 to the central nervous system, 4 to the abdomen, and 1 to an extremity.

Each CVD patient was then matched with a control patient without CVD for sex, race, site of disease treated by RT, dose delivered (±2 Gray [Gy]), and age at time of RT delivery (±5 years). For CVD patients with many matching controls, the controls with the smallest difference with regard to RT dose and age at

RT were chosen, with importance placed on minimizing the difference in RT dose over the difference in age at RT. An attempt was made to find 3 matching controls for each CVD RT course. Fifty-nine courses were matched to 3 controls, 18 courses were matched to 2 controls, and 9 courses were matched to a single control.

Acute toxicity was defined as toxicity from the time of commencement of RT through Day 90 after treatment and was scored using the Radiation Therapy Oncology Group (RTOG) common toxicity criteria.[19] Late toxicity was defined as occurring after Day 90 posttreatment, and was scored according to the RTOG/European Organization for Research and Treatment of Cancer (EORTC) late radiation morbidity scoring schema.[20] Severe acute or late toxicity was defined as ≥grade 3.

Because this is a match-pairs, case-control analysis, conditional logistic regression techniques were used. Because sex, age at RT, anatomic site treated, and RT dose were matched for by the design, these covariates were not adjusted for in the modeling process because their impact has been adjusted for by the study design. The remaining covariates of interest were as follows: concurrent infusional chemotherapy administration, and the use of steroids, NSAIDS, statins, CCBs, antimalarial antirheumatic drugs, and oral cytotoxic antirheumatics. Many of the medications apply only to the CVD cases and could not be adjusted for in the overall model. The medication list is therefore most appropriately used to help predict toxicity in the CVD group separately.

Overall crude rates for toxicity are reported by the anatomic site of RT delivery and by CVD subtype of the cases. Although these rates are instructive, formal comparison at the matched case-control level has not been attempted because of the small sample size. Formal comparisons were limited to the entire population. *P* values ≤.05 are considered statistically significant.

There were 4 endpoints of interest: any acute toxicity, severe acute toxicity, any late toxicity, and severe late toxicity.

Results

Acute Toxicity

With a median follow-up time of 1.3 years for each group, overall, there was no significant difference noted with regard to the incidence of acute toxicity between CVD and control cases, with 65.1% of CVD patients experiencing any acute toxicity, compared with 72.5% of control patients (Table 1). The incidence of severe acute toxicity was similar in both groups (10.5% vs 10.4%).

Table 1. Acute and Late Toxicity by CVD Status

	Toxicity Grade						Any	Severe
Frequency (percent)	**0**	**1**	**2**	**3**	**4**	**5**	***P*†**	***P*†**
Acute Toxicity*								
CVD cases	30 (34.9)	19 (22.1)	28 (32.6)	9 (10.5)	0	0	—	—
Control Cases	61 (27.5)	63 (28.4)	75 (33.8)	23 (10.4)	0	0	.97	.075
Late Toxicity‡								
CVD cases	61 (70.9)	10 (11.6)	7 (8.1)	4 (4.7)	2 (2.3)	2 (2.3)	—	—
Control Cases	191 (86.0)	14 (6.3)	9 (4.1)	7 (3.2)	1 (0.5)	0	.0010	.079

CVD indicates collagen vascular disease.

* Acute toxicity was defined as toxicity from the commencement of radiotherapy through Day 90 after treatment, and was scored using the Radiation Therapy Oncology Group (RTOG) common toxicity criteria.[19]

† Exact P value was derived from conditional logistic regression analysis.

‡ Late toxicity was defined as that occurring after Day 90 after treatment, and was scored according to the RTOG/European Organization for Research and Treatment of Cancer (EORTC) late radiation morbidity scoring schema.[20]

Late Toxicity

Overall, patients with a CVD diagnosis had a significantly higher incidence of any late toxicity (29.1% vs 14%; *P* =.001), with a trend toward increased severe late toxicity (9.3% vs 3.7%; *P* =.079) (Table 1).

Table 2. Acute and Late Toxicity by Anatomic Site of Radiotherapy Delivery

Frequency (Percent)	Acute toxicity grade*					
	0	**1**	**2**	**3**	**4**	**5**
Bone						
Cases (n = 11)	11 (100.0)	0	0	0	0	0
Controls (n = 28)	20 (71.4)	4 (14.3)	4 (14.3)	0	0	0
Breast						
Cases (n = 8)	1 (12.5)	1 (12.5)	4 (50.0)	2 (25.0)	0	0
Controls (n = 20)	0	6 (30.0)	14 (70.0)	0	0	0
Head and neck						
Cases (n = 12)	0	4 (33.3)	6 (50.0)	2 (16.7)	0	0
Controls (n = 32)	5 (15.6)	8 (25.0)	12 (37.5)	7 (21.9)	0	0
Pelvis						
Cases (n = 11)	0	1 (9.1)	6 (54.6)	4 (36.4)	0	0
Controls (n = 28)	2 (7.1)	7 (25.0)	16 (57.1)	3 (10.7)	0	0
Skin						
Cases (n = 14)	0	10 (71.4)	4 (28.6)	0	0	0
Controls (n = 35)	1 (2.9)	17 (48.6)	14 (40.0)	3 (8.6)	0	0
Thorax						
Cases (n = 15)	6 (40.0)	3 (20.0)	6 (40.0)	0	0	0
Controls (n = 41)	14 (34.2)	12 (29.3)	8 (19.5)	7 (17.1)	0	0
Other Sites†						
Cases (n = 15)	12 (80.0)	0	3 (20.0)	0	0	0
Controls (n = 38)	19 (50.0)	9 (23.7)	6 (15.8)	4 (10.5)	0	0

	Late toxicity grade‡					
	0	**1**	**2**	**3**	**4**	**5**
Bone						
Cases (n = 11)	11 (100.0)	0	0	0	0	0
Controls (n = 28)	27 (96.4)	1 (3.6)	0	0	0	0
Breast						
Cases (n = 8)	5 (62.5)	1 (12.5)	2 (25.0)	0	0	0
Controls (n = 20)	13 (65.0)	4 (20.0)	3 (15.0)	0	0	0
Head and neck						
Cases (n = 12)	6 (50.0)	2 (16.7)	2 (16.7)	2 (16.7)	0	0
Controls (n = 32)	24 (75.0)	2 (6.3)	2 (6.3)	3 (9.4)	1 (3.1)	0
Pelvis						
Cases (n = 11)	4 (36.4)	2 (18.2)	1 (9.1)	1 (9.1)	2 (18.2)	1 (9.1)
Controls (n = 28)	21 (75.0)	2 (7.1)	3 (10.7)	2 (7.1)	0	0
Skin						
Cases (n = 14)	10 (71.4)	4 (28.6)	0	0	0	0
Controls (n = 35)	35 (100.0)	0	0	0	0	0
Thorax						
Cases (n = 15)	11 (73.3)	1 (6.7)	2 (13.3)	1 (6.7)	0	0
Controls (n = 41)	36 (87.8)	4 (9.8)	1 (2.4)	0	0	0
Other Sites†						
Cases (n = 15)	14 (93.3)	0	0	0	0	1 (6.7)
Controls (n = 38)	36 (94.7)	0	0	2 (5.3)	0	0

CVD indicates collagen vascular disease.

* Acute toxicity was defined as toxicity from the commencement of radiotherapy through Day 90 after treatment, and was scored using the Radiation Therapy Oncology Group (RTOG) common toxicity criteria.[19]

† Other sites included the abdomen, central nervous system, extremities, and total body.

‡ Late toxicity was defined as that occurring after Day 90 after treatment, and was scored according to the RTOG/European Organization for Research and Treatment of Cancer (EORTC) late radiation morbidity scoring schema.[20]

Table 3. Distribution of Toxicity (Percent) by CVD Case/Control Status, by CVD Subtype

	Acute*				Late†			
	Any		Severe		Any		Severe	
CVD Subtype	CVD	Control	CVD	Control	CVD	Control	CVD	Control
Rheumatoid arthritis	64.9	76.2	10.8	9.9	29.7	13.9	2.7	4.0
Systemic lupus erythematosus	88.2	76.2	29.4	11.9	41.2	19.1	35.3	4.8
Dermatomyositis/polymyositis	66.7	91.7	0	8.3	16.7	8.3	0	0
Ankylosing spondylitis	0	0	0	0	0	0	0	0
Wegener granulomatosis	100	100	0	16.7	33.3	33.3	0	0
Scleroderma	30.0	53.9	0	11.5	20.0	15.4	10.0	3.9
Polymyalgia rheumatica/temporal arteritis	85.7	80.0	0	10.0	28.6	5.0	0	5.0
Mixed connective tissue disorder/other	50.0	83.3	0	16.7	50.0	16.7	0	0

CVD indicates collagen vascular disease.

* Acute toxicity was defined as toxicity from the commencement of radiotherapy through Day 90 after treatment, and was scored using the Radiation Therapy Oncology Group (RTOG) common toxicity criteria.[19]

† Late toxicity was defined as that occurring after Day 90 after treatment, and was scored according to the RTOG/European Organization for Research and Treatment of Cancer (EORTC) late radiation morbidity scoring schema.[20]

Toxicity by Irradiated Site

Although overall there was no significant difference noted with regard to the incidence of acute toxicity, CVD patients treated with RT to some anatomic sites were found to have a higher rate of severe acute toxicity (Table 2). RT to CVD patients produced higher crude rates of grade 3 acute toxicity when delivered to the breast (2 patients [25%] vs 0 patients [0%]) or pelvis (4 patients [36%] vs 3 patients [11%]). For the 2 CVD patients with severe breast acute toxicity, toxicity consisted of grade 3 skin desquamation. For the 4 CVD patients with severe pelvic acute toxicity, 3 had grade 3 skin desquamation alone, whereas the fourth patient had grade 3 skin desquamation, cystitis, and diarrhea/dehydration. However, given the small sample sizes per group and the matched case-control design of the study, formal statistical comparisons were not attempted.

RT to several anatomic sites produced a higher crude rate of any late toxicity in CVD patients (Table 2), including the head and neck (6 patients [50%] vs 8 patients [25%]), pelvis (7 patients [64%] vs 7 patients [25%]), skin (4 patients [29%] vs 0 patients [0%]), and thorax (4 patients [27%] vs 5 patients [12%]). The incidence of severe toxicity was greater mainly only in the pelvis subgroup, with 4 CVD patients (36%) experiencing grade 3+ toxicity (consisting of small bowel ulceration and dysuria), including 1 grade 5 event (intestinal perforation), versus 2 in the control group with severe toxicity (7%). RT to the other anatomic sites was found to be equally well tolerated by both CVD and control patients.

Toxicity by CVD Subtype

Table 3 summarizes the toxicity information when separated by CVD subtype. The only patients who had an appreciably higher crude incidence of any acute toxicity when compared with controls were patients with SLE (88.2% vs 76.2%). Patients with SLE were also the only CVD subset found to have a higher crude risk of severe acute toxicity (29.4% vs 11.9%), which was the highest rate of severe acute toxicity noted among all CVD subtypes. Otherwise, severe acute toxicity was uncommon.

Compared with controls, the incidence of any late toxicity was observed to be higher in several CVD subtypes: RA (29.7% vs 13.9%), SLE (41.2% vs 19.1%), dermatomyositis/polymyositis (16.7% vs 8.3%), polymyalgia rheumatica/temporal arteritis (28.6% vs 5.0%), and MCTD/other (50.0% vs 16.7%). The incidence of severe late toxicity was generally low among both CVD and control patients; however, patients with SLE (35.3% vs 4.8%) and scleroderma (10.0% vs 3.9%) had a higher risk of severe late toxicity versus controls.

Table 4. Medications and Frequency of Use for CVD Patients

	Cases (n = 86)	
Medication	Frequency	Percentage
NSAIDs	34	39.5
Corticosteroids	32	37.2
Antimalarials	25	29.1
CCB	20	23.2
Chemotherapy*	18	20.9
Oral cytotoxic, antirheumatic drugs	17	19.8
Statins	13	15.1

CVD indicates collagen vascular disease; NSAIDs, nonsteroidal antiinflammatory drugs; CCB, calcium-channel blocker.

* Concurrent with radiotherapy.

Concomitant Medication Use by CVD Patients

Table 4 lists several types of medications and their frequencies of use by CVD patients. Tables 5 and 6 list the distribution of acute and late toxicities for CVD cases, respectively. None of the following medications was found to be significantly associated with a risk of any acute or late toxicity: corticosteroids, NSAIDs, statins, CCBs, and antimalarials. The use of oral cytotoxic, rheumatologic agents was found to be significantly associated with a decreased risk of any acute toxicity (P = .0263), and concurrent infusional chemotherapy was found to be significantly associated with an increased risk of severe acute toxicity (P = .0022). Chemotherapy was the only concomitant medication that was found to be associated with increased risk of any (P = .009) or severe (P = .009) late toxicity.

Discussion

Delivering RT to patients with CVD continues to be a challenging clinical dilemma for radiation oncologists. The existing literature is difficult to interpret because of the heterogeneity in CVD subtype and activity, the variations in RT dose and site of treatment, as well as the potential role of concomitant medications in altering toxicity. Morris and Powell[11] reported that severe late effects were associated with CVD other than

Table 5.
Medications and Treatments by Acute Toxicity*: CVD Cases Only

	Toxicity Grade				Any	Severe
Frequency (percent)	0	1	2	3	P†	P†
Corticosteroids						
No	22 (40.7)	11 (20.4)	14 (25.9)	7 (13.0)		
Yes	8 (25.0)	8 (25.0)	14 (43.8)	2 (6.3)	.17	.47
NSAIDS						
No	17 (32.7)	11 (21.2)	18 (34.6)	6 (11.5)		
Yes	13 (38.2)	8 (23.5)	10 (29.4)	3 (8.8)	.65	~1
Statins						
No	28 (38.4)	13 (17.8)	23 (31.5)	9 (12.3)		
Yes	2 (6.7)	6 (46.2)	5 (38.5)	0	.13	.34
CCB						
No	23 (34.9)	15 (22.7)	21 (31.8)	7 (10.6)		
Yes	7 (35.0)	4 (20.0)	7 (35.0)	2 (10.0)	~1	~1
Antimalarials						
No	24 (39.3)	13 (21.3)	19 (31.2)	5 (8.2)		
Yes	6 (24.0)	6 (24.0)	9 (36.0)	4 (16.0)	.22	.44
Oral cytotoxics						
No	20 (29.0)	16 (23.2)	25 (36.2)	8 (11.6)		
Yes	10 (58.8)	3 (17.7)	3 (17.7)	1 (5.9)	.026	.68
Infusional chemotherapy						
No	23 (33.8)	19 (27.9)	23 (33.8)	3 (4.4)		
Yes	7 (38.9)	0	5 (27.8)	6 (33.3)	.78	.0022

CVD indicates collagen vascular disease; NSAID, nonsteroidal anti-inflammatory drug; CCB, calcium-channel blocker.
* Acute toxicity was defined as toxicity from the commencement of radiotherapy through Day 90 after treatment, and was scored using the Radiation Therapy Oncology Group (RTOG) common toxicity criteria.[19]
† *P* value was derived using the Fisher exact test.

Table 6.
Medications and Treatments by Late Toxicity*: CVD Cases Only

	Toxicity Grade						Any	Severe
Frequency (percent)	0	1	2	3	4	5	P†	P†
Corticosteroids								
No	37 (68.5)	6 (11.1)	5 (9.3)	3 (5.6)	2 (3.7)	1 (1.9)		
Yes	24 (75.0)	4 (12.5)	2 (6.3)	1 (3.1)	0	1 (3.1)	.63	.70
NSAIDS								
No	37 (71.2)	5 (9.6)	6 (11.5)	3 (5.8)	0	1 (1.9)		
Yes	24 (70.6)	5 (14.7)	1 (2.9)	1 (2.9)	2 (5.9)	1 (2.9)	~1	.71
Statins								
No	52 (71.2)	8 (11.0)	6 (8.2)	3 (4.1)	2 (2.7)	2 (2.7)		
Yes	9 (69.2)	2 (15.4)	1 (7.7)	1 (7.7)	0	0	~1	~1
CCB								
No	47 (71.2)	7 (10.6)	6 (9.1)	4 (6.1)	0	2 (3.0)		
Yes	14 (70.0)	3 (15.0)	1 (5.0)	0	2 (10.0)	0	~1	~1
Antimalarials								
No	45 (73.8)	6 (9.8)	6 (9.8)	3 (4.9)	0	1 (1.6)		
Yes	16 (64.0)	4 (16.0)	1 (4.0)	1 (4.0)	2 (8.0)	1 (1.0)	.44	.22
Oral cytotoxics								
No	48 (69.6)	7 (10.1)	7 (10.1)	4 (5.8)	2 (2.9)	1 (1.5)		
Yes	13 (76.5)	3 (17.6)	0	0	0	1 (5.9)	.77	~1
Infusional chemotherapy								
No	53 (77.9)	8 (11.8)	4 (5.9)	2 (2.9)	0	1 (1.5)		
Yes	8 (44.4)	2 (11.1)	3 (16.7)	2 (11.1)	2 (11.1)	1 (5.6)	.0087	.0089

CVD indicates collagen vascular disease; NSAIDs, nonsteroidal anti-inflammatory drugs; CCB, calcium-channel blocker.
* Late toxicity was defined as that occurring after Day 90 after treatment, and was scored according to the RTOG/European Organization for Research and Treatment of Cancer (EORTC) late radiation morbidity scoring schema.[20]
† *P* value was derived using the Fisher exact test.

RA, a finding that was also supported by a meta-analysis by Chon and Loeffler.[12] Other studies suggest that a diagnosis of scleroderma[13,14] or lupus[15] may increase the risk of RT associated toxicity. However, 2 separate matched control studies failed to observe any increased risk of acute or late complications in patients with CVD versus patients without CVD.[9,10]

To our knowledge, the current study is the largest matched-control analysis of acute and late complications in patients with CVDs receiving RT. Unlike the other matched control studies,[9,10] we did find that a diagnosis of a CVD increased the risk of having any late toxicity, with a trend toward increased severe late toxicity. We also examined a variety of factors that can potentially influence the toxicity profile. We found that there was little difference in toxicity profile for most irradiated sites. However, RT to the breast and pelvis were possible exceptions. Greater than one-third of all patients with RT to the pelvis experienced severe acute and late toxicity. Similar to previous studies,[11–15] we also found that patients with scleroderma or SLE were at the highest risk of experiencing severe acute or late complications. Morris and Powell[11] previously examined the impact of various medications on RT toxicity and found that patients undergoing NSAID therapy at the time of RT had a lower risk of late effects. Our findings demonstrated that most commonly used medications did not influence RT toxicity, but that concurrent chemotherapy was associated with increased severe acute and late toxicity.

There are strengths and limitations to the current study. Similar to previous publications on the subject, we were limited by the heterogeneity of CVD subtype, which thereby limited the number of patients analyzed for each subtype. Toxicity data was collected retrospectively, and there was no reliable method with which to assess CVD activity status at the time of RT. We were unable to analyze dose independently as a variable. Because dose was dependent on treatment site, it would require a range of RT doses at a given site and a reasonable sample size to make dose-specific comments. This was beyond the scope of our institutional patient experience. The strengths of this study lie in the total number of patients analyzed and the use of a 3:1 control:case match by age, sex, RT dose, and anatomic site. This approach allows for a more robust analysis of the risk profile, allowing us to determine that patients with scleroderma and SLE are at increased risk of severe toxicity. Although other CVD subtypes may also predispose to toxicity, the same conclusions cannot be made because of the limited sample size of patients with these subtypes in our study. It is also important to note that with a median follow-up of 1.3 years, the toxicity rates reported in our study may be underestimating the true rate of late toxicity. Another unique aspect of this study is the comprehensive analysis of concomitant medication use and its impact on the RT toxicity profile. Given the heterogeneity observed in CVD subtype and disease activity, and other variables such as RT dose and site, it is not likely that we will ever have prospective controlled data for these questions.

In summary, although a diagnosis of a CVD appears to predispose patients to a greater risk of late RT toxicity, treatment is generally well tolerated, with a relatively low incidence of severe acute or late toxicity. Other factors can impact the risk of toxicity, including CVD subtype, site of irradiation, RT dose, and the use of concurrent chemotherapy. In patients who may be at particularly high risk because of CVD subtype or RT site, careful attention to issues of toxicity is required. Treatment modifications such as reduction of fraction size, twice-daily treatment, or reduction of total dose for these patients may be considered. These factors should be taken into consideration in the risk-benefit analysis at the time of consultation.

References

1. Fleck R, McNeese MD, Ellerbroek NA, et al. Consequences of breast irradiation in patients with pre-existing collagen vascular disease. *Int J Radiat Oncol Biol Phys.* 1989;17:829–833.
2. Olivotto IA, Fairey RN, Gillies JH, et al. Fatal outcome of pelvic radiotherapy for carcinoma of the cervix in a patient with systemic lupus erythematosus. *Clin Oncol.* 1989;40: 83–84.
3. Ransom DT, Cameron FG. Scleroderma: a possible contraindication to lumpectomy and radiotherapy in breast carcinoma. *Australas Radiol.* 1987;31:317–318.
4. Robertson JM, Clarke DH, Pevzner MM, et al. Breast conservation therapy: severe breast fibrosis after radiation therapy in patients with collagen vascular disease. *Cancer.* 1991;68:502–508.
5. Teo P, Tai TH, Choy D. Nasopharyngeal carcinoma with dermatomyositis. *Int J Radiat Oncol Biol Phys.* 1989;16:471–474.
6. Varga J, Haustein UF, Creech RH, et al. Exaggerated radiation-induced fibrosis in patients with systemic sclerosis. *JAMA.* 1991;265:3292–3295.
7. Abu-Shakra M, Lee P. Exaggerated fibrosis in patients with systemic sclerosis (scleroderma) following radiation therapy. *J Rheumatol.* 1993;20:1601–1603.
8. Hareyama M, Nagakura H, Tamakawa M, et al. Severe reaction after chemoradiotherapy of nasopharyngeal carcinoma with collagen disease. *Int J Radiat Oncol Biol Phys.* 1995; 33:971.
9. Ross JG, Hussey DH, Mayr NA, et al. Acute and late reactions to radiation therapy in patients with collagen vascular diseases. *Cancer.* 1993;71:3744–3752.
10. Phan C, Mindrum M, Silverman C, et al. Matched-control retrospective study of the acute and late complications in patients with collagen vascular diseases treated with radiation therapy. *Cancer J.* 2003;9:461–466.
11. Morris MM, Powell SN. Irradiation in the setting of collagen vascular disease: acute and late complications. J Clin Oncol. 1997;15:2728–2735.
12. Chon BH, Loeffler JS. The effect of nonmalignant systemic disease on tolerance to radiation therapy. *Oncologist.* 2002;7:136–143.
13. Chen AM, Obedian E, Haffty BG. Breast-conserving therapy in the setting of collagen vascular disease. *Cancer J.* 2001;7:480–491.
14. Gold DG, Miller RC, Petersen IA, et al. Radiotherapy for malignancy in patients with scleroderma: the Mayo clinic experience. *Int J Radiat Oncol Biol Phys.* 2007;67:559–567.
15. Pinn ME, Gold DG, Petersen IA, et al. Systemic lupus erythematosus, radiotherapy, and the risk of acute and chronic toxicity: the Mayo Clinic experience. *Int J Radiat Oncol Biol Phys.* 2007 Dec 28 [Epub ahead of print].
16. Irwin B, Ben-Josef E, Tobi M. Calcium channel blockers may radiosensitize, statins and NSAIDs may radioprotect patients from radiation proctitis: a case control study. Presented at the American Gastroenterology Associations' Digestive Disease Week, Los Angeles, California, May 20–25, 2006.
17. Fuks Z, Smith KC. Effect of quinacrine on x-ray sensitivity and the repair of damaged DNA in Escherichia coli K-12. *Radiat Res.* 1971;48:63–73.
18. Voiculetz N, Smith KC, Kaplan HS. Effect of quinacrine on survival and DNA repair in x-irradiated Chinese hamster cells. *Cancer Res.* 1974;34:1038–1044.
19. Trotti A, Byhardt R, Stetz J, et al. Common toxicity criteria: version 2.0 an improved reference for grading the acute effects of cancer treatment: impact on radiotherapy. *Int J Radiat Oncol Biol Phys.* 2000;47:13–47.
20. LENT SOMA scales for all anatomic sites. *Int J Radiat Oncol Biol Phys.* 1995;31:1049–1091

A Cone Beam CT-Based Study For Clinical Target Definition Using Pelvic Anatomy During Post-Prostatectomy Radiotherapy

Timothy N. Showalter, MD, A. Omer Nawaz, MA, Ying Xiao, PhD, James M. Galvin DSc, Richard K. Valicenti MD

Department of Radiation Oncology, Kimmel Cancer Center, Thomas Jefferson University, Philadelphia, Pennsylvania

The following article is reprinted with permission from Elsevier Inc. It was originally published in the Int. J. Radiation Oncol. Biol. Physics, Volume 70, Issue 2, pages 431-436, Feb. 1, 2008.

Introduction

Radiation therapy (RT) is delivered after radical prostatectomy (RP) either as salvage treatment for an elevated prostate-specific antigen (PSA) level[1-6] or as adjuvant therapy for patients with high-risk pathologic features[7-8]. Recent prospective data demonstrated a disease-free survival benefit of adjuvant RT for pathologic T3N0 prostate cancer[9-10]. Despite literature supporting the delivery of post-RP RT to the prostatic fossa (PF), no clear target definition guidelines exist for intensity modulated radiation therapy (IMRT) or image-guided RT (IGRT)[11].

Visualization of the PF is limited on standard CT images, with significant interobserver variability and uncertainty in CTV definition[12]. Efforts to incorporate complementary imaging modalities such as MRI for PF target volume definition have generated neither demonstrably more reliable PF delineation, nor practical contouring guidelines[13]. Regardless of the imaging modality, direct visualization and delineation of the PF clinical target volume (CTV) is fraught with uncertainty. On the other hand, it is possible to distinguish the borders of important nearby pelvic structures, namely the bladder and the rectum. The reliability of rectal volume definition on helical CT is supported by analysis of rectal contours defined in a prospective trial, suggesting the feasibility of rectal dose-volume data collection in a multicenter setting[14]. Fiorino et al have described a correlation between PF CTV shift and anterior rectal wall shift for the cranial half of the rectum in their report of rectal and bladder movement during post-RP RT using weekly CT images[15]. These studies support the reliability of CT-defined rectum contours and a limited correlation between PF CTV and anterior rectal wall, an important tenet in the current study.

The data reported by Fiorino *et al.* are limited by the infrequency of image collection and the acquisition of images at a time and place separate from the treatment couch. Though PTV margin recommendations are not provided by Fiorino *et al.*, they state eloquently that 1), the anterior-posterior movements of rectum and bladder are more important than lateral motion; 2), the rectum trends anteriorly during an RT course; 3), there is significant correlation between the posterior CTV border and the anterior rectal wall for the cranial half of the rectum[15]. Through the use of CBCT images obtained during post-prostatectomy RT, the interfraction movement of the dose-limiting pelvic organs may be characterized further. This information may be used for the careful extrapolation of information regarding motion of the PF target volume. Prior reports have described the utility of online CBCT imaging during definitive, primary RT for prostate cancer using equipment similar to that utilized in the current study[16].

In our study, we approach the problem of PF target definition through analysis of real-time CBCT images during post-RP RT, studying the motion of the critical normal tissue structures that approximate the anterior and posterior anatomical boundaries of the prostatic fossa. Cone-beam CT images, obtained during a definitive course of RT, provided information regarding rectal and bladder movement. For the purpose of estimating appropriate anterior and posterior PF PTV definition guidelines, the posterior bladder border and the anterior rectum border were considered as radiographic surrogates for the anterior and posterior PF borders, respectively.

Methods and Materials

The pelvic anatomy of 10 consecutive prostate cancer patients undergoing post-RP RT was studied retrospectively using CBCT images obtained during the course of treatment. All patients received a radiation dose of 68.4 Gy (1.8 Gy/fraction), delivered with a four-field conformal RT plan. Planning CT (CT_{ref}) scans, with 3 mm slice thickness, were obtained in the supine position with contrast dye cystograms and urethrograms. Patients were instructed to follow a strict preparatory regimen before the CT_{ref} and during RT in order to ensure consistent filling and emptying of the bladder and rectum, respectively. The attending physician (R.V.) reviewed and approved CTV, rectum, and bladder CT_{ref} volumes on the helical CT scans for each patient as a component of standard RT planning and delivery. At our institution, a standard 1.0 cm PTV margin is added to the prostatic fossa CTV, an empirically chosen guideline. The standard post-RP treatment policy in our department includes at least every-other-day CBCT scans for position verification, with corrective shifts for 5 mm or more. Image registration using CBCT scans is performed based upon bony anatomy including femoral heads, pubic arch, sacrum, ischium and ilium. CBCT images were obtained 2-5 times weekly immediately before treatment using the Elekta Synergy® cone beam system.

CBCT scans (exported with a 1 mm slice thickness) were registered in relation to the planning CT using the mutual information algorithm on the CMS FocalSim®. The automatically co-registered images were evaluated for accuracy by a single observer (T.S.); manual adjustments

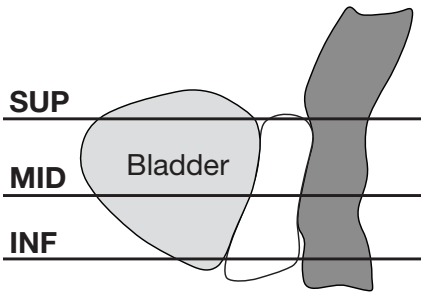

Figure 1. Rectum and bladder motion were recorded at three points along the distance from seminal vesicle stump to bladder-urethral junction.

Table 1. Characteristics of 10 patients receiving radiotherapy to PF after radical prostatectomy

Age (years)	
Mean	57
Range	44-69
Time from surgery to RT	
Median (months)	8.2
≤ 9 months (n)	6
> 9 months (n)	4
Pre-RT PSA (n)	
≤ 0.4	6
> 0.4	4
Gleason Score (n)	
GS = 6	2
GS = 7	8
Pathologic Tumor Stage (n)	
pT2	5
pT3	5
Extracapsular extension (n)	
Yes	6
No	4
Margin status	
Positive	4
Negative	6

were made when necessary to produce an optimal fusion of images in relation to the bony pelvic anatomy. The same observer contoured bladder and rectal volumes on all CBCT images of satisfactory quality for the identification of the rectal and bladder borders. Rectal and bladder motion was measured from the seminal vesicle stump (SVS) to the bladder-urethral junction (BUJ) (Figure 1). This region was chosen since it represents the volume at risk for subclinical disease and it includes the relevant, potentially dose-limiting organs-at-risk (OAR). For each patient, 3 cross-sectional levels were studied: 1) superior (SUP), one slice caudal to the SVS; 2) inferior (INF), one slice cranial to the BUJ; and 3) middle (MID), midway between SUP and INF levels. In the cross-sectional plane, midsagittal coordinates were measured at the anterior rectal border and the posterior bladder border and compared to the planning CT volumes and the mean organ position to obtain interfraction motion. Lateral shifts were not assessable with this technique, and were not studied due to minimal impact on RT dose delivered to adjacent organs at risk (bladder and rectum) relative the anterior and posterior shifts. Inter-organ distance (IOD), the midsagittal difference between bladder and rectum, was also recorded at each measurement level, as this quantity may approximate crudely the anteroposterior PF distance. Data regarding organ volume and movement were collected for each CT_{ref} and CBCT. The mean and the standard deviation of organ border motion were calculated relative to both CT_{ref} and mean organ position.

In order to assess the reproducibility of the rectum and bladder by volume definition, repeat contours of the rectum and bladder were performed for 2 patients. In separate contouring sessions, the same observer (T.S.) repeated the organ definition steps using all CBCT scans for both patients. Repeat measurements of the anterior rectal border and the posterior bladder border were recorded, and movement relative to CT_{ref} was collected. The difference between the two sets of CBCT organ contours was calculated to determine the intraobserver variability for bladder and rectum

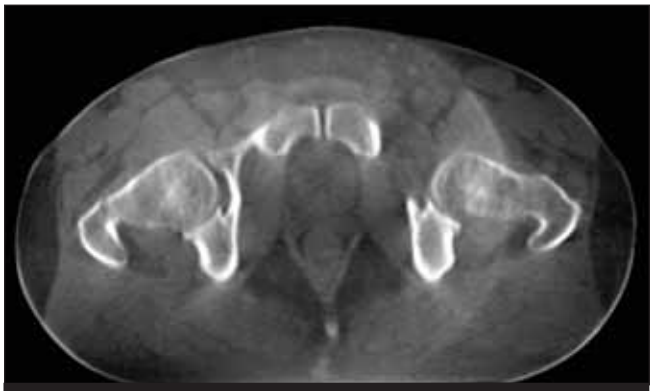

Figure 2. Representative cone-beam CT scan obtained on the treatment couch immediately prior to RT.

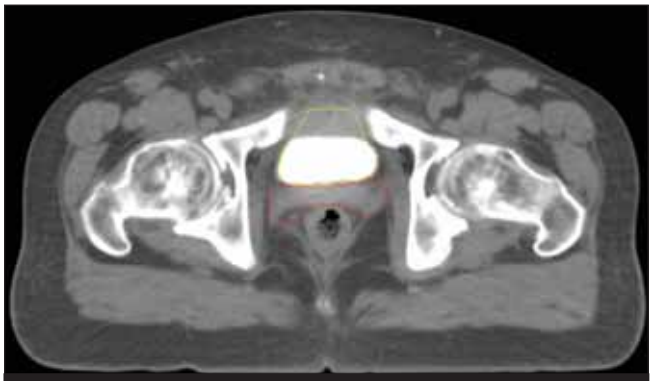

Figure 3. Sample treatment planning CT scan (CT_{ref}) obtained prior to initiation of RT.

motion measurements. A similar process was followed for rectum and bladder volume measurements to determine intraobserver variation in organ volume.

Anterior and posterior PTV margins were calculated by applying a formula ($2\Sigma + 0.7\sigma$) that includes systematic error (Σ) and random error (σ) of target volume position[17], using measured organ border shifts relative to CT_{ref} for each CBCT scan. Interfraction motion of the posterior bladder border and the anterior rectum border were used in the analysis as substitutes for anterior and posterior PF motion in order to calculate estimated margin recommendations.

Results

Ten patients undergoing prostatic fossa RT to 68.4 Gy in 38 fractions were evaluable for this study. Demographic data is displayed in Table 1. A total of 176 CBCT study sets obtained 3-5 times weekly were analyzed. The rectal and bladder borders were reliably identified in 166 of 176 (93%) of CBCT images. Figure 2 shows a representative CBCT image. Figure 3 contains a typical CT image obtained for planning purposes.

Validation of Methods

Repeat contours and measurements for two patients reveal an average organ movement measurement discrepancy between contour sets of 1.2 ± 1.7 mm for bladder and 1.1 ± 1.0 mm for rectum for each of thirty CBCT

Table 2. Organ motion and suggested margin guidelines based on systematic and random error.

Observed Motion		Bladder Motion (mm)			Rectal Motion (mm)		
Relative to	Mean	SUP	MID	INF	SUP	MID	INF
CT_{ref} (+ = anterior, − = posterior)	SD	+0.1 4.4	+0.4 3.7	+1.5 4.0	-2.6 6.0	-1.6 6.3	-2.7 5.8
Relative to mean organ position for all scans (absolute values)	Mean SD	3.3 2.9	2.9 2.4	3.1 2.9	4.7 4.6	4.8 4.4	4.5 4.6
Systematic Error (Σ)		2.4	2.1	2.1	3.5	3.5	3.1
Random Error (Σ)		3.3	2.8	2.4	4.0	4.5	3.5
Calculated PTV Margin (2Σ + 0.7Σ)		7.1	6.2	5.9	9.8	10.2	8.6

study sets analyzed. Average variation at SUP, MID, and INF levels for bladder was 1.0 ± 1.4 mm, 1.0 ± 1.3 mm, 1.5 ± 2.5 mm, and, for rectum, 1.1 ± 1.2 mm, 1.1 ± 0.8 mm, and 1.1 ± 1.1 mm, respectively. Mean difference in bladder volume between the CBCT contours was 2.4 mL (2.6% of mean organ volume); for rectal volume, 2.5 mL (4.6% of mean organ volume).

Organ Motion

There was a tendency towards posterior movement of the anterior rectal wall and anterior tendency in the position of the posterior bladder border during the RT course relative to the CT_{ref}. Organ border motion values at SUP, MID, and INF levels are displayed in Table 2. The calculated posterior margin for PF PTV creation ranged from 8.6 to 10.2 mm, while the calculated anterior margin for PF PTV ranged from 5.9 to 7.1 mm (Table 2). The mean IOD observed on CT_{ref} images was 8.0 ± 5.7 mm, 6.8 ± 5.1 mm, and 5.6 ± 3.5 mm for the SUP,MID and INF levels, respectively. The average CBCT IOD, based on mean IOD for all patients, was 11.4 ± 6.7 mm, 9.4 ± 3.1 mm, and 10.4 ± 4.2 mm for the SUP, MID and INF levels, respectively.

Organ Volume

The bladder and rectum CBCT volumes measured during the course of RT were smaller than those obtained on the planning CT. The average CT_{ref} rectum volume was 67.6 ± 50.5 mL , while the average CBCT volume was 59.5 ± 11.3 mL (8.1 mL difference). For the bladder, the average CT_{ref} volume was 152.3 ± 103.3 mL, while the average CBCT volume was 93.1 ± 26.8 mL (59.2 mL difference). When patients with greater than 50% difference between CT_{ref} and average CBCT organ volume were removed from analysis (2 patients for bladder and 2 patients for rectum), the mean difference between average CT_{ref} and CBCT volumes decreased to 2.9 mL for rectum and to 40.7 mL for bladder.

Volume and Motion Relationships

Pearson correlation coefficients were calculated to analyze interrelationships among mean organ motion at SUP, MID, and INF levels, as well as the average of all levels, mean organ volume, and mean IOD. Correlation coefficient values are displayed in Table 3, revealing that the largest correlation exists between the anterior rectum border position and the distance between the rectum and bladder, with a correlation coefficient of 0.71 between the average interorgan distance and the average rectal wall position. Figure 4 displays the relationship between rectal motion and rectal volume.

Table 3. Pearson correlation coefficients among mean organ motion and mean organ volume.

	Bladder Volume	Rectum Volume	IOD	Rectum Motion
Rectum Motion				
SUP	-0.15	0.37	-0.68	X
MID	-0.01	0.25	-0.56	X
INF	-0.05	0.29	-0.69	X
AVG	-0.07	0.33	-0.71	X
Bladder Motion				
SUP	-0.14	0.18	0.29	0.42
MID	-0.14	0.17	0.18	0.43
INF	-0.06	0.11	0.44	0.23
AVG	-0.12	0.18	0.10	0.45
IOD				
SUP	0.04	-0.26	X	X
MID	-0.07	-0.21	X	X
INF	0.01	-0.26	X	X
AVG	0.01	-0.28	X	X

Discussion

The normal tissue anatomy (bladder and rectum) adjacent to the PF CTV was readily definable throughout the course of post-RP RT using CBCT. Relative to the planning CT, a mean posterior shift of the anterior rectal wall was observed on the CBCT images. The mean rectal volume as contoured on CBCT images during RT was less than the mean CT_{ref} volume. The rectum border shift and rectal volume change noted in this study may be related to a trend towards reduced rectal volume over time during prostate RT[18-19]. Our adjusted analysis of rectum volumes, which showed smaller mean variations in rectum volume after the removal of two large, outlying values, suggests that strict adherence to the bowel preparatory regimen may produce a planning CT that is more representative of the rectum during RT. The recommendation that patients in the current study present to clinic for RT with a full bladder and an evacuated rectum may have contributed to the small level of rectum volume variation observed.

In their study of nine patients receiving weekly CT scans during post-RP RT, Fiorino *et al* report a mean anterior shift of the anterior rectal wall throughout the cranial half of the rectum, but no shift within the caudal half of the rectum[15]. In our study, measurements of rectum and

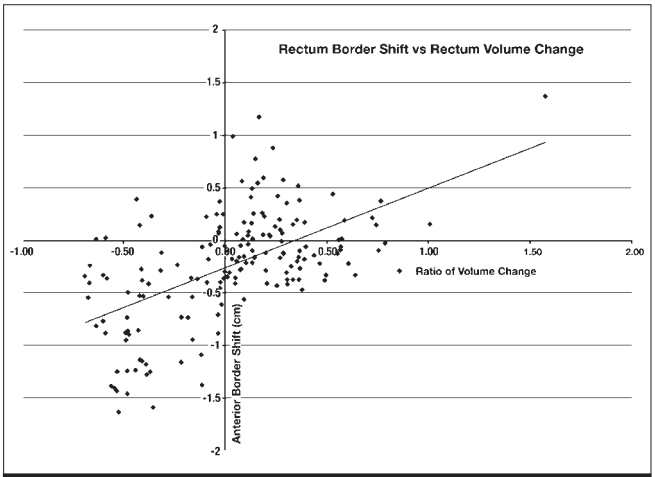

Figure 4. Scatter plot of rectum motion and change in rectum volume.

bladder shifts were performed only at levels that included the PF CTV. The mean posterior shift of the anterior rectum wall relative to CT_{ref} in the current study (1.6-2.7 mm) was small. The standard deviation of the rectal wall position on CBCT relative to the CT_{ref} (5.8-6.3 mm) demonstrates important interfraction variation in rectal wall position, noted throughout the region of rectum relevant to the PF CTV, despite the small average shift observed. Variations in rectal volume appear to impact the position of the anterior rectum wall (Figure 4). In addition, the interorgan distance, which may serve as a rough approximation of the prostatic fossa, correlates more strongly with anterior rectal motion than with other factors (Table 3), supporting the influence of rectal border motion on PF CTV delineation.

We recommend the use of a nonuniform margin for PTV definition, consisting of a 5.9 to 7.1 mm bladder border margin and an 8.6 to 10.2 mm rectal border margin. A published report of significant correlation between the anterior rectal wall and the prostatic fossa CTV supports, in part, the rationale of the current study's approach, though the reported relationship between rectal and CTV motion occurred only with the cranial portion of the rectum[15]. Although the influence of OAR motion on PF PTV margin definition seems sensible, the extrapolation of target information from organ motion should be approached with caution. The use of 3D conformal RT after RP has been shown to reduce toxicity relative to conventional delivery techniques[20]. In addition, rectal dose-volume histograms (DVHs) for patients undergoing post-RP RT have been shown to correlate significantly with risk for late complications[21]. Retrospective analyses of patients undergoing salvage post-RP RT suggest a benefit from RT doses 64.8 Gy or higher[2-3]. As higher RT doses are delivered to the prostatic fossa, the ability to minimize toxicity of adjacent tissues rests upon an understanding of motion of both CTV and OARs during treatment. Intensity-modulated radiation therapy (IMRT) may allow safe dose-escalation for post-RP RT[22], but its application requires detailed target definition guidelines[1]. CBCT may allow tighter RT margins when used to conduct IGRT with daily corrections[16], potentially allowing for higher total doses without parallel increases in OAR dose and treatment-related toxicity.

The current study provides approximate anterior and posterior margins for PF PTV definition based on calculations using pelvic organ motion information. Lateral margins were not calculated, as lateral movement is less significant than anteroposterior motion[9] and is unlikely to influence dose delivered to the adjacent organs at risk (bladder and rectum). Due to uncertainty in direct definition of the PF CTV, an indirect approach was utilized based on interfraction rectal and bladder motion. This approach acknowledges the uncertainty of CTV definition[12, 23] while incorporating the additional anatomic information provided by on-line CBCT imaging during the RT course. The bladder and the rectum were easily identified on most CBCT images in the current study. A small number of CBCT images collected in the current study (7%) were unusable for organ definition due to poor image quality, which may be attributed to technical errors in image acquisition. The use of bladder and rectum movements as determinants for PTV margin guidelines may provide a reliable approach, as rectal contouring has been shown to be reproducible using helical CT scans[14]. These data and similar future studies should be pursued to better define target-definition guidelines for post-RP conformal RT. Avenues for future applications of CBCT images in post-RP RT may include daily online localization with manual soft-tissue registration and subsequent corrective shifts in patient position, as well as off-line adaptive RT based upon a set of CBCT scans obtained during the first week of RT in a fashion similar to that described previously by Yan *et al*[24]. The current work may be used in future attempts to develop off-line adaptive strategies for RT that rely upon conformal avoidance of the rectum and bladder to target the PF CTV for post-prostatectomy patients.

In conclusion, normal tissue anatomy (bladder and rectum) used to define the anterior and the posterior border of the prostatic fossa was readily definable by CBCT imaging throughout the course of post-RP RT. In the absence of direct, target-based treatment guidelines available, CBCT definition of bladder and rectum volumes may be used to pursue anterior and posterior PTV margin recommendations.

References

1. Hayes SB, Pollack A. Parameters for treatment decisions for salvage radiation therapy. *J Clin Oncol* 2005;23:8204-8211.
2. Macdonald OK, Schild SE, Vora SA, *et al.* Radiotherapy for men with isolated increase in serum prostate specific antigen after radical prostatectomy. *J Urol* 2003;170:1833-1837.
3. Valicenti RK, Gomella LG, Ismail M, *et al.* Effect of higher radiation dose on biochemical control after radical prostatectomy for pT3N0 prostate cancer. *Int J Radiat Oncol Biol Phys* 1998;42:501-506.
4. Stephenson AJ, Shariat SF, Zelefsky MJ, *et al.* Salvage radiotherapy for recurrent prostate cancer after radical prostatectomy. *JAMA* 2004;291:1325-1332.
5. Song DY, Thompson TL, Ramakrishnan V, *et al.* Salvage radiotherapy for rising or persistent PSA after radical prostatectomy. *Urology* 2002;60:281-287.
6. Morris MM, Dallow KC, Zeitman AL, *et al.* Adjuvant and salvage irradiation following radical prostatectomy for prostate cancer. *Int J Radiat Oncol Biol Phys* 1997;38:731-736.
7. Chawla AK, Thakral HK, Zietman AL, *et al.* Salvage radiotherapy after radical prostatectomy for prostate adenocarcinoma: Analysis of efficacy and prognostic factors. *Urology* 2002;59:726-731.
8. Valicenti RK, Gomella LG, Ismail M, *et al.* The efficacy of early adjuvant radiation therapy for pT3N0 prostate cancer: A matched pair analysis. *Int J Radiat Oncol Biol Phys* 1999;45:53-58.
9. Bolla M, Van Poppel H, Collette L, *et al.* Postoperative radiotherapy after radical prostatectomy: a randomized controlled trial (EORTC trial 22911). *Lancet* 2005;366:572-578.
10. Thompson IM Jr, Tangen CM, Paradelo J, *et al.* Adjuvant radiotherapy for pathologically advanced prostate cancer: a randomized clinical trial. JAMA 2006;296:2329-2335.
11. ASTRO Consensus Panel. Consensus statements on radiation therapy of prostate cancer: Guidelines for prostate re-biopsy after radiation and for radiation therapy with rising prostate-specific antigen levels after radical prostatectomy. J Clin Oncol 1999;17:1155-1163.
12. Symon Z, Tsvang L, Pfeffer R, *et al.* Prostatic fossa boost volume definition: Physician bias and the risk of planned geographical miss. Scientific Paper, RSNA 2004. [abstract]
13. Jani AB, Spelbring D, Hamilton R, *et al.* Impact of radioimmunoscintigraphy on definition of clinical target volume for radiotherapy after prostatectomy. *J Nucl Med* 2004;45:238-246.
14. Foppiano F, Fiorino C, Frezza G, *et al.* The impact of contouring uncertainty on rectal 3D dose-volume data: results of a dummy run in a multicenter trial (AIROPROS01-02). *Int J Radiat Oncol Biol Phys* 2003;57:573-579.
15. Fiorino C, Foppiano F, Franzone P, *et al.* Rectal and bladder motion during conformal radiotherapy after radical prostatectomy. *Radiother Oncol* 2005;74:187-195.
16. Létourneau D, Martinez AA, Lockman D, *et al.* Assessment of residual error for online cone-beam CT-guided treatment of prostate cancer patients. *Int J Radiat Oncol Biol Phys* 2005;62:1239-1246.
17. ICRU. International Commission on Radiation Units and Measurements, Prescribing, Recording, and Reporting Electron Beam Therapy, ICRU Report 71 (International Commission on Radiation Units and Measurements, Bethesda); 2004.
18. Zelefsky MJ, Crean D, Magera GS, *et al.* Quantification and predictors of prostate position variability in 50 patients evaluated with multiple CT scans during conformal radiotherapy. *Radiother Oncol* 1999;50:225-234.
19. Lebesque JV, Bruce AM, Kroes APG, et al. Variation in volumes, dose-volume histograms, and estimated normal tissue complication probabilities of rectum and bladder during conformal radiotherapy of T3 prostate cancer. *Int J Radiat Oncol Biol Phys* 1995;33:1109-1119.
20. Cozzarini C, Fiorino C, Mandelli D, et al. 3D conformal radiotherapy significantly reduces toxicity of post-prostatectomy adjuvant or salvage irradiation. *Int J Radiat Oncol Biol Phys* 2000;1 (suppl. 1):248.
21. Cozzarini C, Fiorino C, Ceresoli GL, *et al.* Significant correlation between rectal DVH and late bleeding in patients treated after radical prostatectomy with conformal or conventional radiotherapy (66.6-70.2 Gy). *Int J Radiat Oncol Biol Phys* 2003;55:688-694.
22. Bastasch MD, Teh BS, Mai Wy, *et al.* Post-nerve-sparing prostatectomy, dose-escalated intensity-modulated radiotherapy: Effect on erectile function. *Int J Radiat Oncol Biol Phys* 2000;48:369-375.
23. Fiorino C, Reni M, Bolognesi A, *et al.* Intra- and inter-observer variability in contouring prostate and seminal vesicles: implications for conformal treatment planning. *Radiother Oncol* 1998;47:285-92.
24. Yan D, Lockman D, Brabbins D, *et al.* An off-line strategy for constructing a patient-specific planning target volume in adaptive treatment process for prosate cancer. Int *J Radiat Oncol Biol Phys* 2000;48:289-302.

VEGF Trap In Combination With Radiotherapy Improves Tumor Control In U87 Glioblastoma

Phyllis R. Wachsberger, PhD,* Randy Burd, PhD,§ Chris Cardi, MS,† Mathew Thakur, PhD,† Constantine Daskalakis, ScD,‡ Jocelyn Holash, PhD,¶ George D. Yancopoulos, PhD,¶ And Adam P. Dicker, MD, PhD,*

Departments of *Radiation Oncology, †Radiology, ‡Pharmacology and Experimental Therapeutics, Thomas Jefferson University, Philadelphia, PA; §Department of Nutritional Sciences, University of Arizona, Tucson, AZ; and ¶Novartis, Emeryville, CA

The following article is reprinted with permission from Elsevier Inc. It was originally published in the Int. J. Radiation Oncol. Biol. Physics, Volume 67, Issue 5, pages 1526-1537, 2007.

Purpose

To determine the effect of vascular endothelial growth factor VEGF Trap (Regeneron Pharmaceuticals, Tarrytown, NY), a humanized soluble vascular endothelial growth factor (VEGF) receptor protein, and radiation (RT) on tumor growth in U87 glioblastoma xenografts in nude mice.

Methods and Materials

U87 cell suspensions were implanted subcutaneously into hind limbs of nude mice. VEGF Trap (2.5–25 mg/kg) was administered every 3 days for 3 weeks alone or in combination with a single dose of 10 Gy or fractionated RT (3 x 5 Gy). In addition, three scheduling protocols for VEGF Trap plus fractionated RT were examined.

Results

Improved tumor control was seen when RT (either single dose or fractionated doses) was combined with the lowest dose of VEGF Trap (2.5 mg/kg). Scheduling did not significantly affect the efficacy of combined therapy. Although high-dose VEGF Trap (10 mg/kg or 25 mg/kg) significantly reduced tumor growth over that of RT alone, there was no additional benefit to combining high-dose VEGF Trap with RT.

Conclusions

Vascular endothelial growth factor Trap plus radiation is clearly better than radiation alone in a U87 subcutaneous xenograft model. Although high doses of VEGF Trap alone are highly efficacious, it is unclear whether such high doses can be used clinically without incurring normal tissue toxicities. Thus, information on lower doses of VEGF Trap and ionizing radiation is of clinical relevance. © 2007 Elsevier Inc.

Key Words: Vascular endothelial growth factor Trap, Radiotherapy, Anti-angiogenic, U87 glioblastoma.

Introduction

Radiation (RT) therapy is an important treatment modality for many cancers; however, its therapeutic success is impeded by dose-limiting normal tissue toxicities and the development of radioresistance. Recent studies emphasize the importance of the tumor microvascular response in addition to the tumor cell response in determining tumor radioresistance[1, 2]. Ionizing radiation can directly induce endothelial cell apoptosis[1, 3], which can inhibit tumor growth and lead to radiosensitization. However, in opposition to endothelial cell damage, radiation also induces signal transduction cascades, which contribute to radiation resistance through upregulation of proliferative, survival, and angiogenic pathways[4]. In particular, radiation induces vascular cytokines, such as vascular endothelial growth factor (VEGF)[5, 6], one of the most potent endothelial cell survival factors[7], which functions as a powerful antiapoptotic factor for endothelial cells in new blood vessels[8, 9]. Radiation-induced VEGF results in tumor radioresistance through vascular radioprotection[2, 10].

Inhibition of VEGF activity or disabling the function of VEGF receptors is therefore a potential strategy for improving radiation outcome. The VEGF blockade alone has been shown to inhibit both tumor growth and metastasis in a variety of animal tumor models[11]. Currently, three approaches are in clinical development to target the VEGF/VEGFR-signaling pathway: *(1)* monoclonal antibodies directed against VEGF or its receptors[12–15], *(2)* small molecule inhibitors of the VEGFR-2 tyrosine kinase enzyme[16–19], and *(3)* soluble decoy receptors created from the VEGFR1 receptor which selectively inhibit VEGF[20, 21]. The relative benefits of these strategies have yet to be determined clinically.

Tumor cures are rare when VEGF blockers are used as the sole method of treatment; in general, antiangiogenics appear to work best in combination with cytotoxic therapies[22]. A number of preclinical studies suggest that radiotherapy in combination with VEGF targeting agents enhances the radiotherapeutic ratio (see reviews;[23, 24]). The best way to incorporate VEGF inhibition strategies into current radiotherapy regimens remains unknown.

Because of the role that angiogenesis plays in the radiation response, the objective of this study was to determine whether VEGF Trap (Regeneron Pharmaceuticals, Tarrytown, NY), a potent anti-VEGF angiogenesis inhibitor that traps circulating VEGF in the bloodstream and in the extracellular space, would enhance radiation therapy in the human U87 glioblastoma (GBM) tumor model. Because GBM tumors are among the most radioresistant and vascular of neoplasms and are known to secrete high levels of VEGF[25], U87 GBM was deemed an appropriate model to assess the effects of VEGF Trap and radiation. It was hypothesized that inhibition of VEGF signaling by VEGF Trap would improve the human U87 glioblastoma model response to radiotherapy.

The administration of decoy soluble VEGF receptors has been found to be a very effective way to block the VEGF signaling pathway[26–29]. VEGF Trap is a unique human fusion protein comprising portions of human VEGF recep-

tor 1 (VEGFR1) and human VEGF receptor 2 (VEGFR2) extracellular domains fused to the constant region (Fc) of human IgG1[21]. VEGF Trap has greater affinity for the VEGF ligand than anti-VEGF monoclonal antibodies (mab) do (dissociation constant <1 pMol/L for VEGF Trap vs. 0.1–10 nMol/L for mab)[30]. VEGF Trap has been shown to inhibit neoangiogenesis and tumor growth in tumor xenografts and metastases, as well as reduce the formation of malignant ascites[14, 21, 31].

Methods and Materials

Analysis of VEGF levels in U87 tumor cells in culture

U87 glioblastoma cells (American Type Culture Collection) were maintained in alpha MEM (Sigma-Aldrich, St. Louis, MO) with 10% fetal bovine serum (Atlanta Biologicals, Norcross, GA). U87 cells were irradiated at doses between 2 and 20 Gy in the presence or absence of 40 nM VEGF Trap and incubated for 48 h. Using a commercially available human VEGF immunoassay kit (R&D Systems, Minneapolis, MN), VEGF was assayed from culture supernatants.

Animal and tumor model

U87 cell suspensions (5 x 10^5 cells in 100 µL phosphate buffered saline) were implanted subcutaneouly (SC) into the right hind limbs of athymic NCR NUM mice (Taconic Farms, Hudson, NY). A SC xenograft model was chosen to facilitate radiation dosing and ease of tumor measurements in the more than 200 mice measured in this study. Mice were not pretreated before tumor implantation. U87 tumors were allowed to grow for approximately 14 to 18 days until reaching an approximate diameter of 4 to 5 mm before treatment.

Drug and irradiation treatment

In an initial pilot study, VEGF Trap was administered at two doses, a high dose (25 mg/kg) or low dose (2.5 mg/kg), every 3 days, up to 3 weeks, with or without a single dose of radiation (10 Gy) given on Day 0. VEGF Trap was administered every 3 days because it has a half-life of 72 h in mouse serum (drug pharmacokinetics communicated by Regeneron). Drug was administered 2 h before radiation. When fractionated radiotherapy was used, VEGF Trap was combined at 2.5 mg/kg (low dose) or 10 mg/kg (intermediate dose) with fractionated radiotherapy (three fractions of 5 Gy each) on Days 0, 1, and 2. Scheduling of VEGF Trap was either 1 week before fractionated radiation and continuing for a period of 3 weeks, concurrent with radiation and continuing for a period of 3 weeks, or 3 days postradiation treatment and continuing for a period of 3 weeks. Thus, the total number of drug doses was constant for each schedule (see Fig. 1 for dose and irradiation scheduling protocol).

Irradiation was performed on anesthetized mice using an X-ray machine (Gulmay Medical, Bethel, CT) operating at 250 kV, 10 mA, with a 2-mm aluminum filtration. The effective photon energy was ≈90 keV. Mice were anesthetized with a combination of ketamine and acepromazine at a concentration of 75 mg/kg and 0.35 mg/kg, respectively. Each mouse was confined in a lead casing with its tumor-bearing leg extended through an opening on the side to allow the tumor to be irradiated locally. Radiation was administered as three daily fractions of 5 Gy each as described earlier.

Tumor size was measured 4 to 5 times per week after treatment by direct measurement with calipers and calculated by the formula [(smallest diameter (2) x widest diameter) / 2]. Tumors were not allowed to grow beyond 2,000 mm^3 in accordance with Institutional Animal Care and Use Committee regulations.

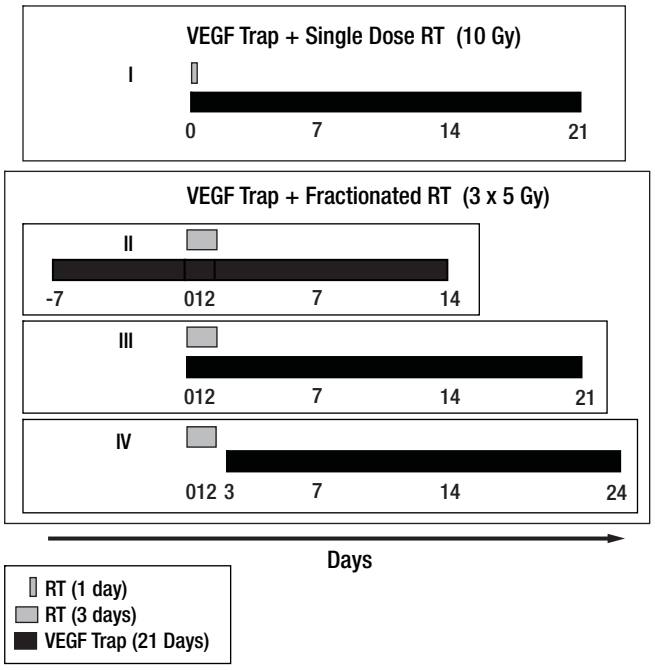

Figure 1. Scheduling protocols for vascular endothelial growth factor (VEGF) Trap administration in combination with radiation (RT). VEGF Trap was given at 2.5, 10, or 25 mg/kg every 3 days in four schedules: **(I)** VEGF Trap given on Day 0 concurrent with a single dose of RT (10 Gy) and continued up to 3 weeks; **(II)** VEGF Trap given on day –7 before RT (3 x 5 Gy) and continued for 3 weeks; **(III)** VEGF Trap given on Day 0 concurrent with RT (3 x 5 Gy) and continued up to 3 weeks; **(IV)** VEGF Trap given on Day 3 post RT (3 x 5 Gy) and continued up to 3 weeks. All three protocols received the same number of drug doses. Day 0 was always the start of radiation.

Positron emission tomography imaging

The MOSAIC PET scanner (Philips Medical Systems, Brisbane, CA) was used for PET studies. Before imaging, mice were anesthetized with ketamine (75 mg/kg) and acepromazine (0.35 mg/kg) via a SC injection. Once anesthetized 0.3 to 0.5 µCi of 18-fluorodeoxyglucose (FDG) was administered intravenously. Sixty to seventy min were allowed for uptake of the tracer. Mice were placed in a 50-mL specimen tube to facilitate multimodality stereotactic positioning. The PET data were acquired in a single position for 15 min. Volumes of interest (VOIs) were defined by drawing multislice regions of interest (ROIs) on the PET images using 50% of the full-width-at-half-maximum (FWHM) of the tumor to determine the tumor boundary. In the case of tumors with a core lacking FDG uptake, the tumor and core boundaries were defined by 50% FWHM of each wall adjacent to the core. Mice were divided into three groups (n = 3–6 animals per group): untreated; low-dose VEGF Trap–treated (2.5 mg/kg), and highdose VEGF Trap–treated (10 mg/kg).

Immunohistochemistry

Platelet–endothelial cell adhesion molecule 1 (PECAM-1) immunostaining for microvessel density (MVD): control, radiation-treated, VEGF Trap–treated tumors, and VEGF Trap plus radiation–treated tumors were immunostained with a rat antimouse PECAM-1 mAb (BD Biosciences, Boston, MA) and a rabbit antirat biotinylated secondary antibody (Vector Labs, Burlingame, CA). Enhanced horseradish peroxidase–conjugated streptavidin and a substrate chromogen, AEC (3-amino-9-ethyl carbazole), were used to visualize the signal. (HISTOSTAIN-*PLUS* kit, Invitrogen, Carlsbad, CA); slides were examined with a Nikon Eclipse E600 microscope to calculate MVD, the area occupied by the PECAM-1-positive microvessels, and total tissue area per section were quantified using National Institute of Health Image J software. Microvessel density was expressed as percent area of blood vessels stained per tissue section. Areas of necrosis were excluded from calculations. Four or five high-power fields were identified on each section with three to four sections per tumor and two tumors per endpoint.

Statistical analysis of tumor growth

Tumor size measurements over time were obtained from the following groups: control; radiation alone; VEGF Trap, low dose (2.5 mg/kg), intermediate dose (10 mg/kg), or high dose (25 mg/kg); and the corresponding two radiation plus VEGF Trap combinations (n = 10–14 animals per group). Tumor growth over the entire study follow-up period was modeled via mixed-effects linear regression. This approach fits a "random" growth curve to each animal's data and then statistically "averages" these curves within each treatment group to estimate an overall "fixed effect" for each group. It also properly handles unbalanced data (i.e., different number of measurements for different animals) and takes into account the correlation of each animal's measurements over time. Because tumors typically grow exponentially, the base-10 logarithm of tumor volume was modeled as a function of time and treatment. The interpretation of the linear model for the log of tumor volume is in terms of geometric means and geometric mean ratios (while the usual interpretation of a regression model for an untransformed outcome is in terms of arithmetic means and mean differences). The fitted linear growth curves fitted the data well. In addition, an allowance was made for the variance of the random effects to differ across groups to account for the larger variability of measurements in certain treated groups. All statistical analyses were conducted in SAS 8.2 (SAS Institute, Cary, NC, 1999–2001).

The mixed-effects regression has multiple advantages over analyses of tumor growth delay that typically compare groups with respect to the average time it takes tumors to reach some arbitrary size (e.g., 2,000 mm3). First, mixed-effects regression yields more general parameters of interest, such as average daily tumor growth rate and doubling time. Second, it can investigate (if necessary) treatment interactions and nonlinear patterns of tumor growth. Finally, it is more efficient because it used the repeated tumor size measurements obtained over the entire study period.

Results

Effect of VEGF Trap and radiation on VEGF secretion in U87 cells in culture

Levels of VEGF increased in U87 culture supernatants in a dose-dependent manner following irradiation (Fig. 2). The addition of VEGF Trap (40 nM) reduced free VEGF in the supernatant to undetectable levels.

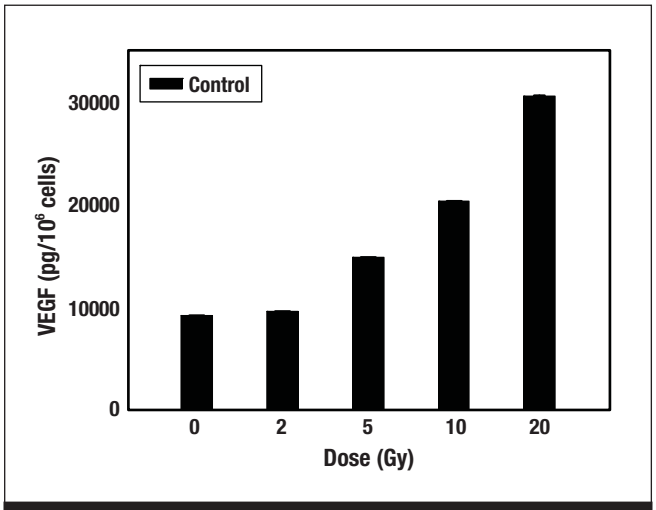

Figure 2. Effect of vascular endothelial growth factor (VEGF) Trap and radiation on VEGF secretion in U87 cells in culture. U87 cells were irradiated at doses between 2 and 20 Gy in the presence or absence of 40 nM VEGF Trap. Cell culture supernatants were assayed for VEGF secretion 48 h following treatment. VEGF secretion was undetectable in presence of 40 nM VEGF Trap.

Effect of VEGF Trap and radiation on U87 tumor growth inhibition

The linear models for the log-transformed tumor growth fitted the data quite well in all groups. The raw data for all treatment groups with regression lines are plotted in Figs. 3 through 6 with corresponding Tables 1 through 4. The average daily percent increase in tumor volume for the untreated control group was consistent across all protocols and ranged between 27% and 31%, corresponding to a tumor doubling time between 2.5 and 3.0 days (Tables 1–4). Radiation alone (both single or fractionated doses) or VEGF Trap alone (all doses) significantly reduced the tumor growth rate compared with control ($p < 0.001$, Figs. 3–6, Tables 1–4). Results with VEGF Trap in combination with single dose or fractionated radiotherapy are now summarized.

Effect of VEGF Trap and single dose radiation (10 Gy) on U87 tumor growth inhibition

Table 1 presents tumor growth data based on the mixed-effects linear regression analysis described in Methods and Materials, and Fig. 3 presents the original animal data. In this experiment, a low dose of VEGF Trap (2.5 mg/kg) initiated concurrently with a single dose of 10 Gy was compared with a 10x higher dose of VEGF Trap (25 mg/kg) plus 10 Gy. The six groups are compared in terms of average daily tumor growth and doubling time. It can be seen from Table 1 and Fig. 3 that both low-dose and high-dose VEGF Trap were effective inhibitors of daily percent increase in tumor volume (%Δ = 15% and 5%, respectively, vs. 31% for controls, $p = 0.001$). Although low-dose VEGF Trap was not significantly better than 10-Gy treatment alone, the combination of low-dose VEGF Trap and 10 Gy slowed daily tumor growth (%Δ = 12% vs. 18% for 10 Gy alone and 15% for low VEGF Trap alone). Thus, a less than additive enhancement in tumor control over either modality alone was observed. High-dose VEGF Trap, as a single treatment modality, was highly effective in slowing daily percent increase in tumor volume (5% vs. 18% for 10 Gy). Its efficacy was not improved by the addition of 10 Gy. This study

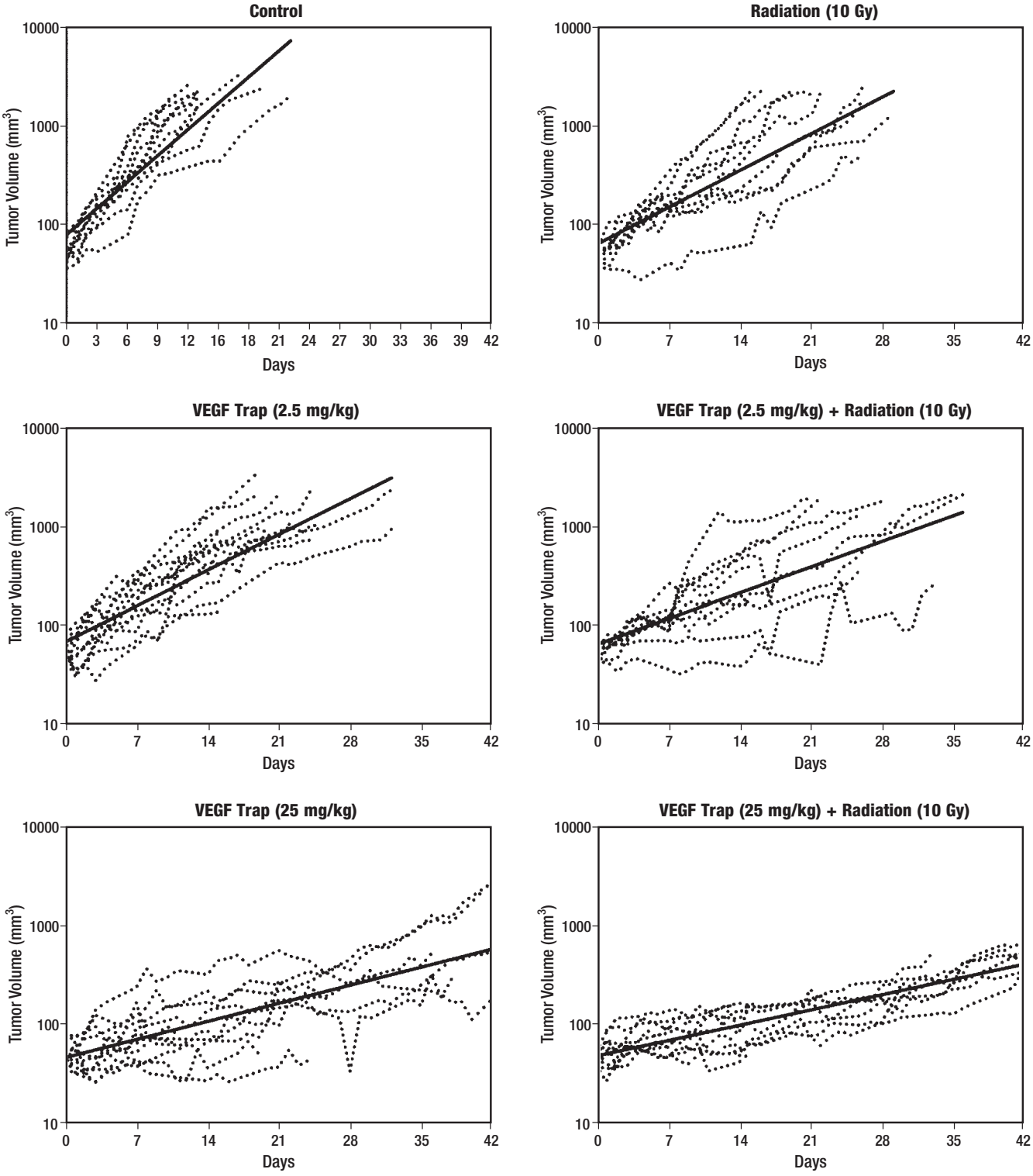

Figure 3. Effect of vascular endothelial growth factor (VEGF) Trap combined with single-dose radiation (10 Gy) on tumor growth in U87GBM. Individual mouse data for six treatment groups (n = 10–12 animals per group). VEGF Trap was given at 2.5 or 25 mg/kg starting on Day 0, concurrent with radiation and continuing every 3 days for 3 weeks (see schedule I, Fig. 1).

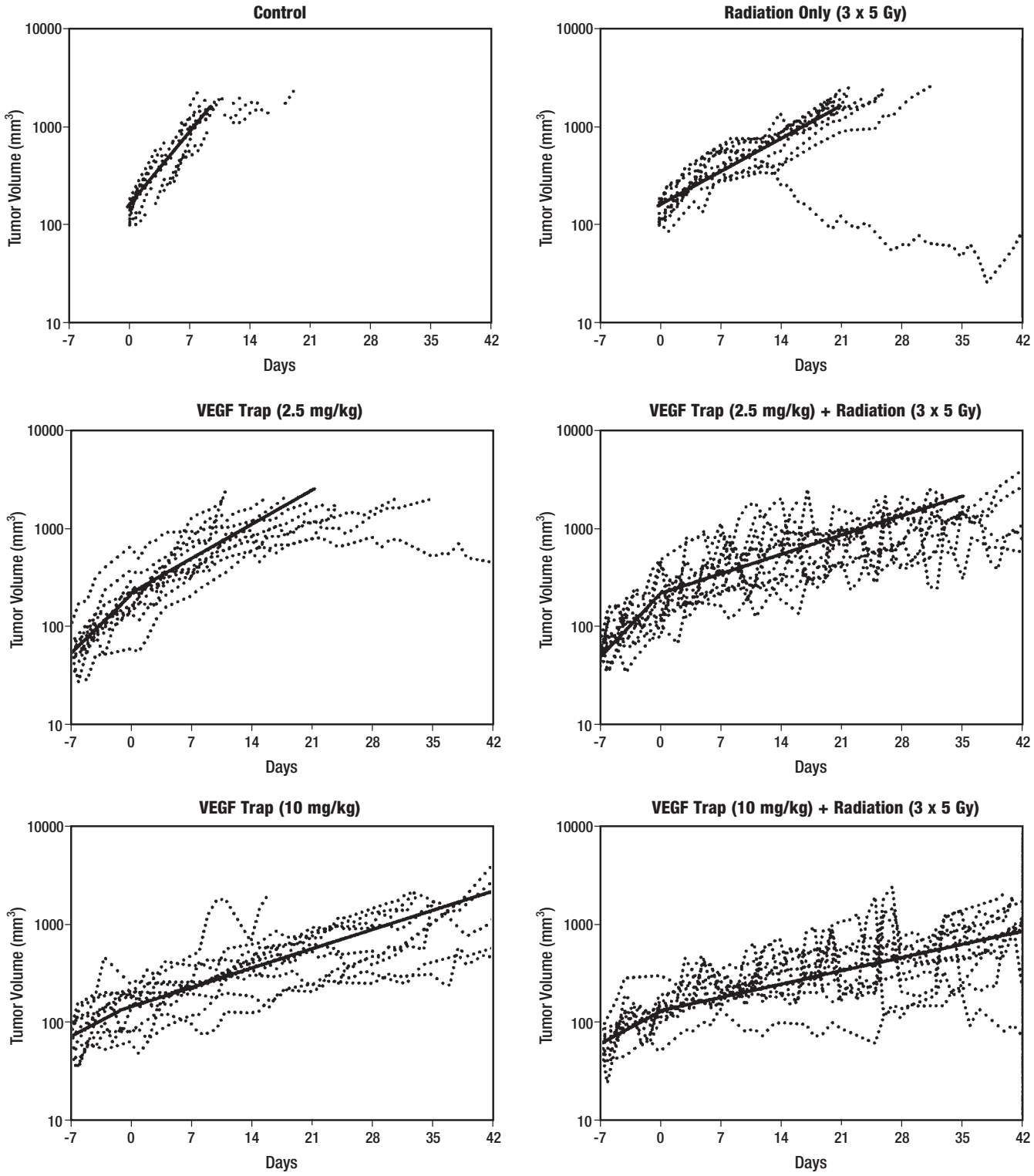

Figure 4. Effect of vascular endothelial growth factor (VEGF) Trap initiated before fractionated radiation (3 x 5 Gy) on tumor growth in U87 GBM. Individual mouse data for 6 treatment groups (n = 10–14 animals/group). VEGF Trap was given at 2.5 or 10 mg/kg starting on Day –7 and continuing every 3 days for 3 weeks (see schedule II, Fig. 2).

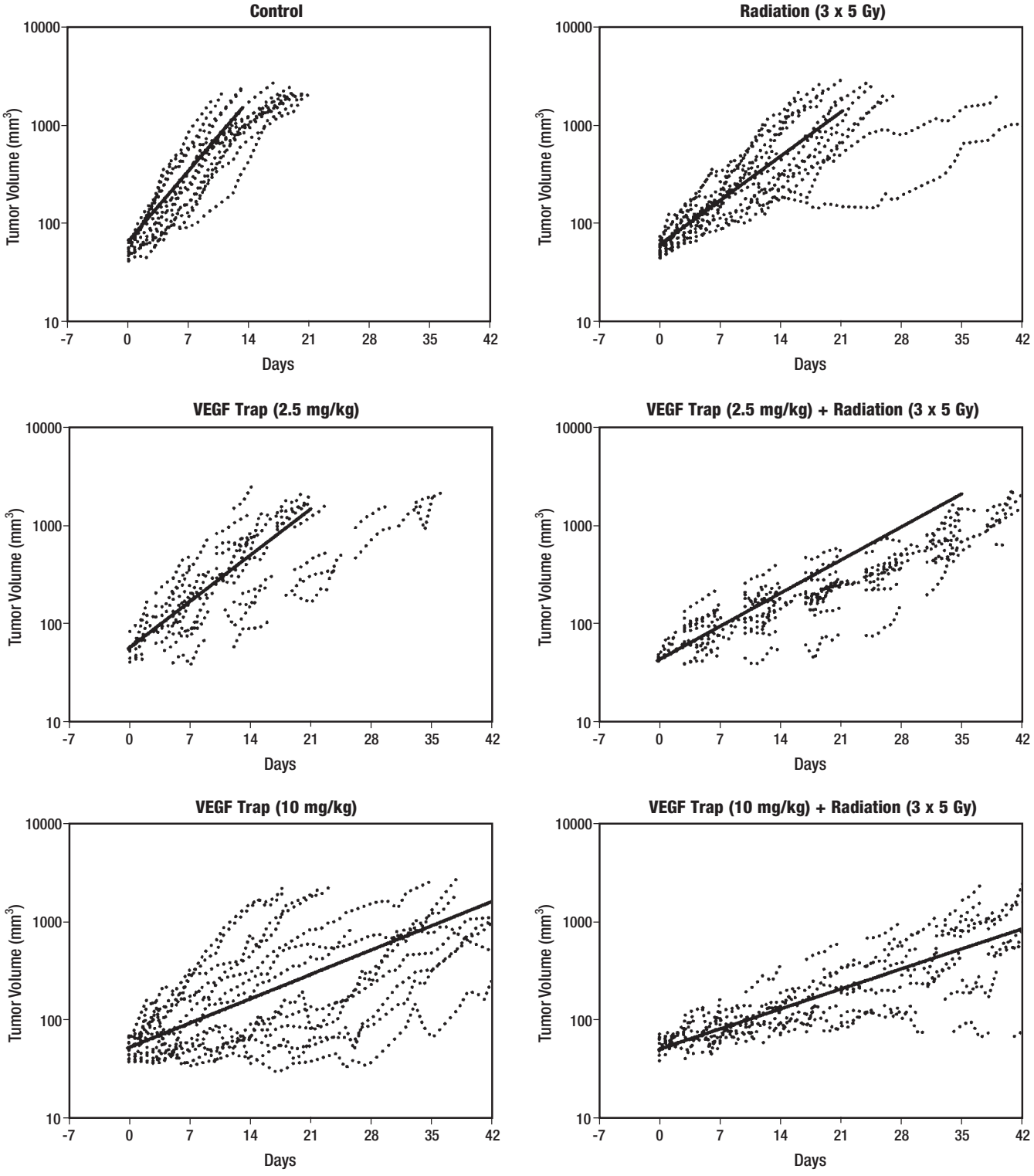

Figure 5. Effect of vascular endothelial growth factor (VEGF) Trap sequenced concurrent with fractionated radiation (3 x 5 Gy) on tumor Growth in U87 GBM. Individual mouse data for six treatment groups (n = 10–14 animals per group). VEGF Trap was given at 2.5 or 10 mg/kg starting on Day 0 and continuing every 3 days for 3 weeks (see schedule III, Fig. 3).

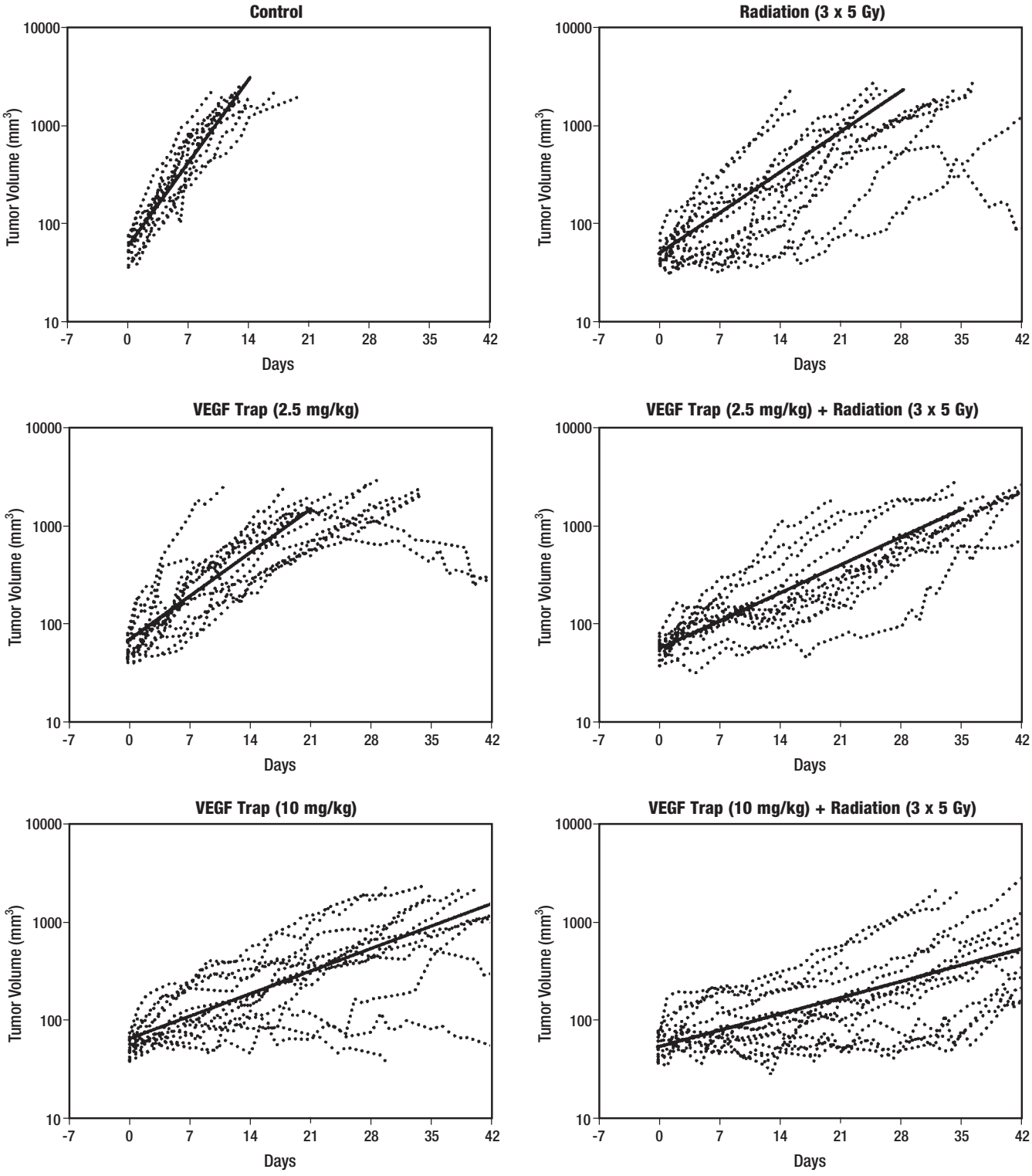

Figure 6. Effect of vascular endothelial growth factor (VEGF) Trap sequenced post–fractionated radiation (3 x 5 Gy) on tumor Growth in U87 GBM. Individual mouse data for six treatment groups (n = 10–14 animals/group). VEGF Trap was given at 2.5 or 10 mg/kg starting on Day 3 and continuing every 3 days for 3 weeks (see schedule IV, Fig. 4).

Table 1. Effect of VEGF Trap combined with single-dose radiation: Summary of tumor growth (Schedule I)

Treatment	%Δ	(95% CI)	T2x	*p* values
Control (human FC protein)	31.0	(27–35)	2.6	
RT (10 Gy)	18.0	(15–21)	4.2	0.001 vs. control, 0.19 vs. VEGF Trap (low)
VEGF Trap (2.5 mg/kg)	15.0	(13–28)	4.9	0.001 vs. control, 0.19 vs. RT alone
VEGF Trap (25 mg/kg)	5.0	(2–7)	15.2	0.001 vs. control, 0.001 vs. RT alone, 0.001 vs. VEGF Trap (low)
VEGF Trap (2.5mg/kg) + RT	12.0	(9–14)	6.3	0.003 vs. RT, 0.06 vs. VEGF Trap (low)
VEGF Trap (25 mg/kg) + RT	5.0	(2–7)	15.5	0.001 vs. RT, 0.417 vs. VEGF Trap (high), 0.96 vs. VEGF Trap (low) + RT

Abbreviations: %Δ = daily% increase in tumor volume; CI = confidence interval; RT = radiation; VEGF = vascular endothelial growth factor; T2x = average doubling time for tumor volume (in days).

suggests that low-dose VEGF Trap in combination with single-dose radiation has an enhanced effect on tumor cell kill. It was thought that this enhancement might be improved by varying dose and scheduling protocol. Additional studies were carried out in which low-dose VEGF Trap at 2.5 mg/kg was compared with an intermediate dose of 10 mg/kg (because VEGF Trap at 25 mg/kg appeared to have masked any additional benefit of radiation in enhancing tumor control) in combination with a more clinically relevant fractionated radiotherapy protocol. The results of these studies are reported in the following sections.

Effect of VEGF Trap and fractionated radiation on U87 tumor growth inhibition

VEGF Trap given before fractionated radiation: in this protocol, VEGF Trap was administered 7 days before radiation. The analyses allowed for separate tumor growth rates in the first and second periods (preradiation: Days –7 to 0; postradiation: Days 0+) for the groups that received radiation. The study's main aim was to compare tumor growth rates across treatment groups in the latter period, when all treatments had been applied. Table 2 summarizes the results of the tumor growth modeling analyses during this main study phase, and Fig. 4 presents the original animal data. The low-dose VEGF Trap group (2.5 mg/kg every third day, starting at Day –7) demonstrated a reduction in daily percent increase in tumor volume (12% vs. 27% for control; $p = 0.001$) that was similar to the first single-dose radiation study, whereas the high-dose VEGF Trap group (10 mg/kg every third day, starting at Day –7) had an even stronger effect (7%) that, again, was similar in trend to the first study. In the radiation only group, tumor daily growth was slowed to 11% ($p < 0.001$ vs. control). Although low-dose VEGF Trap was comparable to radiation alone ($p = 0.59$), the combination of low-dose VEGF Trap with radiation (7% average daily percent increase in tumor volume, Table 1) was significantly better than either radiation alone ($p = 0.036$) or low-dose VEGF Trap alone ($p < 0.005$). The combination of high-dose VEGF Trap with radiation (5% average percent daily increase in tumor volume) was also significantly better than radiation alone ($p = 0.002$) but not significantly better than high dose VEGF Trap alone ($p = 0.33$).

VEGF Trap given concurrently with fractionated radiation: Table 3 summarizes the results of the tumor growth modeling analyses based on original animal data shown in Fig. 5. High-dose VEGF Trap was significantly better than radiation in reducing daily percent increase in tumor volume (8.5% vs. 16.1% for radiation, $p = 0.001$). The combination of low-dose VEGF Trap with radiation (12% average daily increase in tumor volume) was significantly better than either radiation alone ($p = 0.029$) or low-dose VEGF Trap alone ($p = 0.012$). The combination of high-dose VEGF Trap (10 mg/kg) with radiation (7% average daily increase in tumor volume) was also significantly better than radiation alone ($p = 0.001$) but not high-dose VEGF Trap alone ($p = 0.417$).

VEGF Trap given postradiation: Table 4 summarizes the results of the tumor growth modeling analyses based on original animal data shown in Fig. 6. The results of this schedule followed the same pattern as seen in the previous two schedules with fractionated radiation as well as the first experiment with single-dose radiation. The benefit of combining VEGF Trap with radiation compared with single-modality treatments was once again seen with low-dose VEGF Trap plus radiation. High-dose VEGF Trap at 10 mg/kg plus radiation significantly reduced percent daily increase in tumor volume when compared with radiation alone but was not significantly different from VEGF Trap alone ($p = 0.187$).

In summary, improved tumor control was seen when radiation (either single dose or fractionated doses) were combined with the lowest dose of VEGF Trap (2.5 mg/kg) used in these studies. Scheduling did not significantly affectthe efficacy of combined therapy. The relative benefits of combined low-dose VEGF Trap plus fractionated radiation relative to radiation as judged by percent reduction in average daily increase in tumor volume were 36% for VEGF Trap given before radiation, 27% for

Table 2. VEGF Trap initiated before fractionated radiation: Summary of tumor growth (Schedule II)

Treatment	%Δ	(95% CI)	T2x	*p* values
Control (human FC protein)	27.0	(23–31)	3.0	
RT (3 x 5 Gy)	11.0	(8–15)	6.5	0.001 vs. control, 0.59 vs. VEGF Trap (low), 0.027 vs. VEGF Trap (high)
VEGF Trap 2.5 mg/kg)	12.0	(10-15)	5.9	0.001 vs. control, 0.59 vs. RT
VEGF Trap 10 mg/kg)	7.0	(4–9)	11	0.001 vs control, 0.027 vs. RT, 0.001 vs. VEGF Trap (low)
VEGF Trap (low) + RT	7.0	(4–9)	10.6	0.034 vs. RT, 0.004 vs. VEGF Trap (low)
VEGF Trap (high) + RT	5.0	(2–7)	15.3	0.002 vs. RT, 0.33 vs. VEGF Trap (high)

Abbreviations: %Δ = daily% increase in tumor volume; CI = confidence interval; RT = radiation; VEGF = vascular endothelial growth factor; T2x = average doubling time for tumor volume (in days).

Table 3. Trap sequenced concurrently with radiation: Summary of tumor growth (Schedule III)

Treatment	%Δ	(95% CI)	T2x	*p* values
Control (human FC protein)	27.0	(24–30)	2.9	
RT (3 x 5 Gy)	16.0	(13–19)	4.6	0.001 vs. control, 0.729 vs. VEGF Trap (low), 0.001 vs. VEGF Trap (high)
VEGF Trap (2.5 mg/kg)	17.0	(14–19)	4.5	0.001 vs. control, 0.729 vs. RT alone
VEGF Trap (10 mg/kg)	8.5	(6–11)	8.5	0.001 vs. control, 0.001 vs. RT alone, 0.001 vs. VEGT Trap (low)
VEGF Trap (low) + RT	12.0	(9–14)	6.3	0.020 vs. RT, 0.008 vs. VEGF Trap (low)
VEGF Trap (high) + RT	7.0	(5–9)	10.3	0.001 vs. RAD, 0.392 vs. VEGF Trap (high), 0.014 vs. VEGF Trap (low) + RT

Abbreviations: %Δ daily% increase in tumor volume; CI = confidence interval; RT = radiation; VEGF = vascular endothelial growth factor; T2x = average doubling time for tumor volume (in days).

concurrent treatment, and 32% for drug given postradiation treatment. Although high-dose VEGF Trap (either 10 mg/kg or 25 mg/kg) significantly reduced tumor growth over that of radiation alone, there was no added benefit to combining high dose VEGF Trap with radiation.

Effect of VEGF Trap and radiation on microvessel density

Immunoassaying for endothelial cells with PECAM-1 revealed an inhibition of tumor angiogenesis 3 weeks after treatment with VEGF Trap or VEGF Trap and radiation. Tumor MVD was similar in the control and radiation-treated tumors. Tumor MVD in the VEGF Trap treated tumors was decreased to between 43% to 57% of control or radiation-treated tumors ($p = 0.06$). Tumor MVD in VEGF and radiation-treated groups decreased to between 15% and 30% of control or radiation-treated groups ($p = 0.001$) (Fig. 7). There was no significant difference in MVD between high-dose VEGF Trap–treated with radiation vs. high dose VEGF Trap alone ($p = 0.29$). However, there was a significant difference in MVD between low-dose VEGF Trap-treated with radiation and low-dose VEGF Trap alone ($p = 0.01$, Fig. 8).

18-fluorodeoxyglucose–PET imaging of VEGF Trap–treated tumors

Figure 9a illustrates a series of images from a representative, untreated mouse. Figure 9b represents a series of images from a representative mouse treated with VEGF Trap dosed at or 10 mg/kg every 3 days (starting at Day 0) for 3 weeks. Tumor volume (mm^3) and days following start of treatment are indicated. Because of the difficulty in matching tumor volumes and time after treatment, the percent of metabolically inactive tumor volume (as measured by FDG uptake) was measured as a function of tumor volume and averaged over a range of tumor volumes between 900 and 1,600 mm^3. The percent of metabolically inactive tumor was significantly less in untreated tumors (2.46% ± 0.18%) than in tumors treated with 10 mg/kg VEGF Trap (8.7 ± 1.26%, $p = 0.01$) but not significantly different from tumors treated with 2.5 mg/kg VEGF Trap (3.36 ± 0.36%, $p = 0.13$) .

Discussion

This work demonstrated that VEGF Trap alone is an effective dose-dependent inhibitor of tumor growth in U87GBM. These findings agreed with previous studies of VEGF Trap in other preclinical animal models demonstrating efficacy in halting angiogenesis and shrinking tumors[30]. Because VEGF Trap was very potent by itself and could have potentially masked any additional benefits of radiation, both low-dose and high-dose scheduling of the drug were used with radiotherapy. In all scheduling protocols that were investigated, the combination of low-dose VEGF Trap with radiation was significantly better than either treatment modality alone. On the other hand, high-dose VEGF Trap was significantly better than radiation alone and therefore masked any additional benefit that may have resulted from combination therapy.

The benefit of combined treatment with low VEGF Trap and radiation relative to radiation alone was not influenced by scheduling protocol. This result was in contrast to earlier work demonstrating improved radiation response when a VEGFR2 blocker, DC101, was given 4 to 6 days before radiotherapy[32]. This earlier work suggested that tumor vasculature normalization occurred during pretreatment with the VEGFR2 blocker, a process in which pruning of immature and inefficient blood vessels occurs leading to improved tumor perfusion and oxygenation and improved radiation response. The current observations may reflect the absence of a normalization effect by VEGF Trap on U87 GBM vasculature or a missed window of opportunity for normalization because of the particular protocols used in this work. Because it is not known how tumor oxygenation levels may have varied throughout the course of combined treatment with VEGF Trap and radiation, additional studies are warranted to resolve the issue of normalization.

The observation that scheduling did not have an impact on efficacy of combined treatment with VEGF Trap and radiation in this study is also in contrast to recent studies in which VEGF blockade was obtained either by a VEGF receptor2 tyrosine kinase inhibitor, ZD6474, or indirectly by

Table 4. VEGF Trap sequenced post–fractionated radiation: Summary of tumor growth (Schedule IV)

Treatment	%Δ	(95% CI)	T2x	*p* values
Control (human FC protein)	31.5	(28–35)	2.5	
RT (3 x 5 Gy)	15.0	(13–17)	5.1	0.001 vs. control, 0.460 vs. VEGF Trap (low), 0.001 vs. VEGF Trap (high)
VEGF Trap (2.5 mg/kg)	16.0	(13–19)	4.7	0.001 vs. control, 0.460 vs. RT alone
VEGF Trap (10 mg/kg)	8.0	(5–10)	9.2	0.001 vs. control, 0.001 vs. RT alone, 0.001 vs. VEGT Trap (low)
VEGF Trap (low) + RT	10.0	(7–12)	7.4	0.011 vs. RT, 0.001 vs. VEGF Trap (low)
VEGF Trap (high) + RT	5.5	(3–8)	12.8	0.001 vs. RT, 0.187 vs. VEGF Trap (high), 0.013 vs. VEGF Trap (low) + RT

Abbreviations: %Δ daily% increase in tumor volume; CI = confidence interval; RT = radiation; VEGF = vascular endothelial growth factor; T2x = average doubling time for tumor volume (in days).

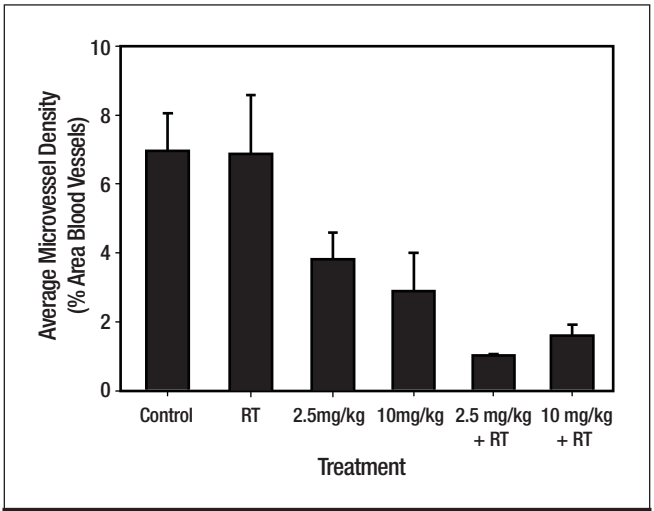

Figure 7. Effect of vascular endothelial growth factor (VEGF) Trap and radiation (RT) (Schedule II) on microvessel density (MVD). Tumor MVD in VEGF Trap–treated tumors was decreased to between 43% and 57% of control or RT-treated tumors ($p = 0.06$). Tumor MVD in VEGF Trap and RT-treated groups decreased to between 15% and 30% of control or RT-treated groups ($p = 0.001$). There was no significant difference in MVD between VEGF Trap–treated (high dose) + radiation vs. VEGF Trap (high dose) alone ($p = 0.29$). However, there was a significant difference in MVD between VEGF Trap (low dose) + radiation and VEGF Trap (low dose) alone ($p = 0.01$).

HIF-1 alpha blockade of VEGF secretion. In both these studies, optimal antitumor efficacy was obtained when VEGF blockers were sequenced following radiation[2, 33]. These studies suggested that prolonged suppression of radiation-induced angiogenesis account for enhanced efficacy of combined treatments with angiogenesis blockade and radiation. However, it is not clearly understood why there is a difference in the impact of scheduling among these agents.

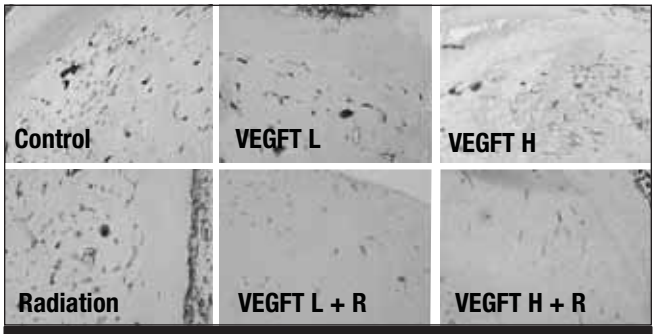

Figure 8. Platelet– endothelial cell adhesion molecule 1 (PECAM-1) staining in subcutaneous U87 glioblastoma xenografts treated with vascular endothelial growth factor (VEGF) Trap with and without radiation therapy (Schedule II). Lower microvessel density (MVD) and altered vessel morphology were observed in treated tumors. (VEGFT L = VEGF Trap low dose; VEGFT H = VEGF Trap high dose; *R* = radiation) Original magnification: X 100.

This work is encouraging in that it demonstrates for the first time a benefit in combining VEGF Trap with ionizing radiation in a highly resistant GBM tumor model. VEGF Trap is a unique human fusion protein with very potent binding affinity for VEGF A isoforms as well as placental growth factor (PIGF) and is currently in clinical trials. Its affinity for VEGF is potentially 100- to 1,000-fold higher than existing VEGF monoclonal antibodies such as bevacizumab[34]. This high-affinity blockade of VEGF differentiates VEGF Trap from other anti-VEGF strategies and therefore gives this drug the potential to enhance combination modality treatment with lower dosing.

Mechanisms of enhanced U87 tumor control by combined therapy with VEGF Trap and radiation most likely include inhibition of radiation-induced angiogenesis by VEGF Trap sequestration of circulating VEGF in the bloodstream and in the extracellular tumor space resulting from radiation-induced secretion. Indeed, in this study, a radiation-dose-dependent increase in VEGF secretion by U87 glioblastoma cells was observed and excess VEGF was bound in the presence of VEGF Trap. In addition, immunohistochemical findings indicated a reduction in MVD 3 weeks following treatment with VEGF Trap and radiation. Inhibition of radiation-induced angiogenesis was also observed indirectly through FDG–PET imaging, which revealed an increase in metabolically inactive tumor tissue after VEGF Trap treatment, possibly arising from the induction of tumor necrosis or apoptosis in the presence of angiogenesis inhibition. It is also of interest that in this study, a brief period of fraction-

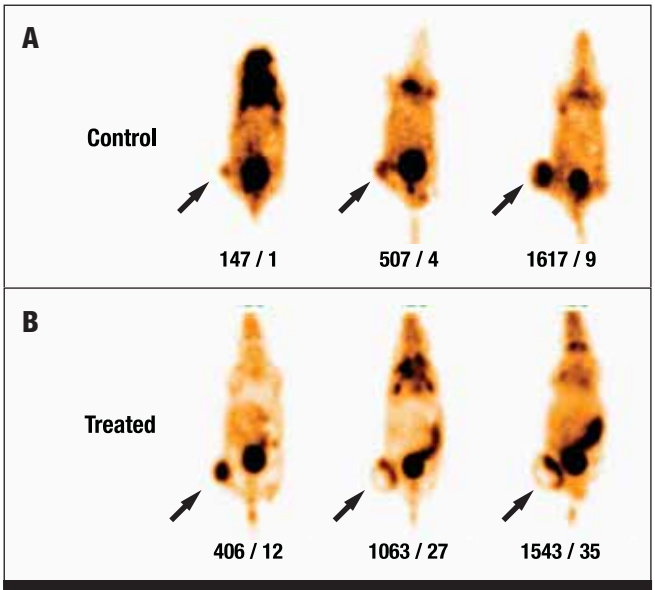

***Volume (mm3) / (days post-treatment)**

Figure 9. 18-fluorodeoxyglucose (FDG)–PET imaging of human U87 glioblastoma xenografts in nude mice. **(a)** A series of typical images from an untreated mouse. **(b)** A series of images from a mouse treated with vascular endothelial growth factor (VEGF) Trap dosed at 10 mg/kg every 3 days (starting at Day 0) for 3 weeks. Tumor volume (mm^3) and days following start of treatment are indicated. Imaging was performed as described in Methods and Materials. The percent of metabolically inactive tumor (as measured by FDG uptake) was significantly less in untreated tumors than in tumors treated with 10 mg/kg VEGF Trap.

ated radiotherapy with VEGF Trap resulted in tumor growth retardation but not remission. The lack of remission is probably related to continued production of VEGF after removal of drug and radiation and points to the need for chronic therapy with VEGF Trap, which is in agreement with what has been observed for the transient effects of other antiangiogenic agents on tumor control[23, 35].

In conclusion, these studies demonstrate that the combination of low-dose VEGF Trap and radiation is clearly better than radiation alone in a U87 subcutaneous xenograft model. Although high doses of VEGF Trap alone are highly efficacious, it is unclear whether such high doses can be used clinically without incurring normal tissue toxicities. Thus, information on lower doses of VEGF Trap and ionizing radiation are of clinical relevance.

It is understood that the SC xenograft model used in this study has shortcomings in that ectopic tumors implanted SC in the hind limb of animals do not duplicate the vascular microenvironment of orthotopic brain implants[36]. However, the use of hind limb injection is the standard approach for xenograft studies with radiation. In addition, human xenografts in immunocompromised nude mice, whether they be ectopic or orthotopic, both have deficiencies in that they can only approximate the human patient situation and seldom reflect accurately the glioblastoma multiforme histopathology seen in patients. This study is encouraging in that it demonstrates for the first time a benefit in combining VEGF Trap with ionizing radiation and warrants further investigations both preclinically and clinically.

References

1. Garcia-Barros M, Paris F, Cordon-Cardo C, *et al.* Tumor response to radiotherapy regulated by endothelial cell apoptosis. *Science* 2003;300:1155–1159.
2. Moeller BJ, Dreher MR, Rabbani ZN, *et al.* Pleiotropic effects of HIF-1 blockade on tumor radiosensitivity. *Cancer Cell* 2005;8:99 –110.
3. Paris F, Fuks Z, Kang A, *et al.* Endothelial apoptosis as the primary lesion initiating intestinal radiation damage in mice. *Science* 2001;293:293–297.
4. Dent P, Yacoub A, Contessa J, *et al.* Stress and radiation-induced activation of multiple intracellular signaling pathways. *Radiat Res* 2003;159:283–300.
5. Lanza-Jacoby S, Dicker AP, Miller S, *et al.* Cyclooxygenase (COX)-2-dependent effects of the inhibitor SC236 when combined with ionizing radiation in mammary tumor cells derived from HER-2/neu mice. *Mol Cancer Ther* 2004;3:417– 424.
6. Wachsberger P, Burd Marreron R, Rossetti D, *et al.* Improvement of fractionated radiation therapy by combination with a VEGF blocker, VEGF Trap. 96th Annual Meeting of the American Association of Cancer Research, Anaheim, CA, 2005.
7. Ferrara N. Role of vascular endothelial growth factor in regulation of physiological angiogenesis. *Am J Physiol Cell Physiol* 2001;280:C1358–C1366.
8. Benjamin LE, Golijanin D, Itin A, *et al.* Selective ablation of immature blood vessels in established human tumors follows vascular endothelial growth factor withdrawal. *J Clin Invest* 1999;103:159 –165.
9. Tran J, Master Z, Yu JL, *et al.*A role for survivin in chemoresistance of endothelial cells mediated by VEGF. *Proc Natl Acad Sci U S A* 2002;99:4349–4354.
10. Moeller BJ, Cao Y, Li CY, *et al.* Radiation activates HIF-1 to regulate vascular radiosensitivity in tumors: role of reoxygenation, free radicals, and stress granules. *Cancer Cell* 2004;5:429–441.
11. Hicklin DJ, Ellis LM. Role of the vascular endothelial growth factor pathway in tumor growth and angiogenesis. *J Clin Oncol* 2005;23:1011–1027.
12. Asano M, Yukita A, Matsumoto T, *et al.* An anti-human VEGF monoclonal antibody, MV833, that exhibits potent anti-tumor activity in vivo. *Hybridoma* 1998;17:185–190.
13. Kamiya K, Konno H, Tanaka T, *et al.* Antitumor effect on human gastric cancer and induction of apoptosis by vascular endothelial growth factor neutralizing antibody. *Jpn J Cancer Res* 1999;90:794–800.
14. Kim ES, Serur A, Huang J, *et al.* Potent VEGF blockade causes regression of coopted vessels in a model of neuroblastoma. *Proc Natl Acad Sci U.S.A.* 2002;99:11399 –11404.
15. Willett CG, Boucher Y, di Tomaso E, *et al.* Direct evidence that the VEGF-specific antibody bevacizumab has antivascular effects in human rectal cancer. *Nat Med* 2004;10:145–147.
16. Abdollahi A, Lipson KE, Han X, *et al.* SU5416 and SU6668 attenuate the angiogenic effects of radiation-induced tumor cell growth factor production and amplify the direct antiendothelial action of radiation in vitro. *Cancer Res* 2003;63:3755–3763.
17. 17. Drevs J, Hofmann I, Hugenschmidt H, *et al.* Effects of PTK787/ZK 222584, a specific inhibitor of vascular endothelial growth factor receptor tyrosine kinases, on primary tumor, metastasis, vessel density, and blood flow in a murine renal cell carcinoma model. *Cancer Res* 2000;60:4819–4824.
18. Fong TA, Shawver LK, Sun L, *et al.* SU5416 is a potent and selective inhibitor of the vascular endothelial growth factor receptor (Flk-1/KDR) that inhibits tyrosine kinase catalysis, tumor vascularization, and growth of multiple tumor types. *Cancer Res* 1999;59:99 –106.
19. Wedge SR, Ogilvie DJ, Dukes M, *et al.* ZD4190: An orally active inhibitor of vascular endothelial growth factor signaling with broad-spectrum antitumor efficacy. *Cancer Res* 2000;60:970–975
20. Hasumi Y, Mizukami H, Urabe M, *et al.* Soluble FLT-1 expression suppresses carcinomatous ascites in nude mice bearing ovarian cancer. *Cancer Res* 2002:62:2019 –2023.
21. Holash J, Davis S, Papadopoulos N, *et al.* VEGF-Trap: a VEGF blocker with potent antitumor effects. *Proc Natl Acad Sci U S A* 2002;99:11393–11398.
22. Kerbel R, Folkman J. Clinical translation of angiogenesis inhibitors. *Nat Rev Cancer* 2002;2:727–739.
23. Wachsberger P, Burd R, Dicker AP. Tumor response to ionizing radiation combined with antiangiogenesis or vascular targeting agents: exploring mechanisms of interaction. *Clin Cancer Res* 2003;9:1957–1971.
24. Wachsberger P, Burd R, Dicker AP. Improving tumor response to radiotherapy by targeting angiogenesis signaling pathways. *Hematol Oncol Clin North Am* 2004;18:1039–1057, viii.
25. Vajkoczy P, Schilling L, Ullrich A, et al. Characterization of angiogenesis and microcirculation of high-grade glioma: an intravital multifluorescence microscopic approach in the athymic nude mouse. *J Cereb Blood Flow Metab* 1998;18:510–520.
26. Ferrara N, Chen H, Davis-Smyth T, *et al.* Vascular endothelial growth factor is essential for corpus luteum angiogenesis. *Nat Med* 1998;4:336 –340.
27. Gerber HP, Kowalski J, Sherman D, *et al.* Complete inhibition of rhabdomyosarcoma xenograft growth and neovascularization requires blockade of both tumor and host vascular endothelial growth factor. *Cancer Res* 2000:60:6253– 6258.
28. Gerber HP, Hillan KJ, Ryan AM, *et al.* VEGF is required for growth and survival in neonatal mice. *Development* 1999;126:1149–1159.
29. Kuo CJ, Farnebo F, Yu EY, *et al.* Comparative evaluation of the antitumor activity of antiangiogenic proteins delivered by gene transfer. *Proc Natl Acad Sci U S A* 2001;98:4605– 4610.
30. Konner J, Dupont J. Use of soluble recombinant decoy receptor vascular endothelial growth factor trap (VEGF Trap) to inhibit vascular endothelial growth factor activity. *Clin Colorectal Cancer* 2004;4(Suppl. 2):S81–S85.
31. 31. Huang J, Frischer JS, Serur A, et al. Regression of established tumors and metastases by potent vascular endothelial growth factor blockade. Proc Natl Acad Sci U S A 2003;100:7785–7790.
32. Winkler F, Kozin SV, Tong RT, *et al.* Kinetics of vascular normalization by VEGFR2 blockade governs brain tumor response to radiation: role of oxygenation, angiopoietin-1, and matrix metalloproteinases. *Cancer Cell* 2004;6:553–563.
33. Williams KJ, Telfer BA, Brave S, *et al.* ZD6474, a potent inhibitor of vascular endothelial growth factor signaling, combined with radiotherapy: schedule-dependent enhancement of antitumor activity. *Clin Cancer Res* 2004;10:8587– 8593.
34. Bergsland EK. Update on clinical trials targeting vascular endothelial growth factor in cancer. *Am J Health Syst Pharm* 2004;61:S12–S20.
35. Klement G, Baruchel S, Rak J, *et al.* Continuous low-dose therapy with vinblastine and VEGF receptor-2 antibody induces sustained tumor regression without overt toxicity. *J Clin Invest* 2000;105:R15–R24.
36. Blouw B, Song H, Tihan T, *et al.* The hypoxic response of tumors is dependent on their microenvironment. *Cancer Cell* 2003;4:133–146.

Inhibition of p73 Function by Pifithrin-α as Revealed by Studies in Zebrafish Embryos

William Davidson,[1,2,*] Qing Ren,[1] Gabor Kari,[1] Ori Kashi,[1] Adam P. Dicker[1] and Ulrich Rodeck[3]

[1]Departments of Radiation Oncology, [2]Biochemistry & Molecular Biology; and [3]Dermatology and Cutaneous Biology; Thomas Jefferson University, Philadelphia, Pennsylvania, U.S.A.

The following article is reprinted with permission from Landes Bioscience. It was originally published in Cell Cycle, Volume 7, Issue 9, pp. 1224-1230.

Abreviations: MO, antisense morpholino oligonucleotide; PFTα, pifithrin-α; Hpf, hours post fertilization; Kd, knock down; IR, ionizing radiation

Key Words: zebrafish, development, radiation effects, tumor suppressor protein p53, tumor suppressor protein p73, pifithrin-α

The p53 family of proteins contains two members that have been implicated in sensitization of cells and organisms to genotoxic stress, i.e., p53 itself and p73. In vitro, lack of either p53 or p73 can protect certain cell types in the adult organism against death upon exposure to DNA damaging agents. The present study was designed to assess the relative contribution of p53 to radiation resistance of an emerging vertebrate model organism, i.e., zebrafish embryos. Consistent with previous reports, suppressing p53 protein expression using antisense morpholino oligonucleotides (MOs) increased survival and reduced gross morphological alterations in zebrafish embryos exposed to ionizing radiation. By contrast, a pharmacological inhibitor of p53 function [Pifithrin-α (PFTα)] caused developmental abnormalities affecting the head, brain, eyes and kidney function and did not protect against lethal effects of ionizing radiation when administered at 3 hours post fertilization (hpf). The phenotypic abnormalities associated with PFTα treatment were similar to those caused by antisense MO knock down (kd) used to reduce p73 expression. PFTα also inhibited p73-dependent transcription of a reporter gene construct containing canonical p53-responsive promoter sequences. Notably, when administered at later stages of development (23 hpf), PFTα did not cause overt developmental defects but exerted radioprotective effects in zebrafish embryos. In summary, this study highlights off-target effects of the pharmacological p53 inhibitor PFTα related to inhibition of p73 function and essential roles of p73 at early but not later stages of zebrafish development.

Introduction

The genotoxic stress response is one of the most widely studied phenomena in biology and the efforts of many groups have provided a detailed understanding of the molecular determinants of this homeostatic mechanism (reviewed in refs. 1–3). Yet, the current understanding of the effects of genotoxic stress on whole organisms is curtailed by the fact that many of the mechanistic insights are based on experiments with cultured cells. These shortcomings are compounded by pitfalls associated with the preferential use of immortalized or transformed cells.[4] In recognition of these problems, many groups have resorted to studying the DNA damage response in experimental animals, particularly genetically engineered mice. These efforts have contributed considerably to the understanding of molecular determinants of the in vivo genotoxic stress response including Ku,[5,6] DNA-PK,[7] DNA ligase IV,[8] ATM,[9] ATR,[10] Chk1[11] and Chk2.[12] In addition, these studies confirmed a central role of the tumor suppressor p53 in the genotoxic stress response (reviewed in refs. 13 and 14).

The present study was undertaken to explore molecular determinants of the genotoxic stress response in an emerging animal model system, i.e., zebrafish embryos. Zebrafish represents a vertebrate species with many similarities to mammals. Yet, they breed prolifically and are amenable to large-scale phenotypic screening facilitated by the fact that they are transparent during organogenesis. Importantly, 'knockdown' strategies using antisense MOs have been developed in this species to investigate protein function in the in vivo context. Zebrafish are attractive not only to model human diseases but also as tools in drug discovery.[15] We have previously reported that zebrafish embryos provide a rapid, facile system to identify pharmacological modifiers of the radiation response.[16] Here, we extend these studies to assess the contribution of endogenous modifiers of the radiation response to radiation-induced morbidity and mortality by focusing on pharmacological and genetic inhibition of p53 function.

Results and Discussion

Time- and dose-dependent effects of ionizing radiation on zebrafish embryo survival. Previously, we observed that radiation sensitivity of zebrafish embryos was different at distinct developmental stages and progressively decreased between 2 to 8 hours post fertilization (hpf).[16] Here, we extend this earlier study by assessing embryo survival after exposure to increasing radiation doses up to 72 h after radiation. These experiments confirmed progressive radioresistance at successive stages of development (not shown). To determine the consequences of inhibiting translation of specific gene products by antisense MO kd for radiation resistance of the developing embryo we performed all subsequent experiments in embryos which were irradiated at 24 hpf. This was based on the consideration that, at this time point, target protein expression is sufficiently suppressed by antisense MO kd and remains low for extended time periods up to 4 days post fertilization (dpf).[17] Dose-dependent survival upon radiation exposure at 24 hpf revealed 100% lethality scored at 6–7 dpf (40 Gy) with an LD_{50} of 20 Gy.[18] To monitor the effects of p53 expression on radiation sensitivity as it relates to both, mortality and tissue-specific effects, we thus performed experiments at 20 or 40 Gy.

Reduced p53 expression is associated with radioprotection of zebrafish embryos. Zebrafish embryos harboring homozygous missense p53 mutations exhibit increased resistance to the deleterious effects of ionizing radiation.[19] We determined whether suppressing

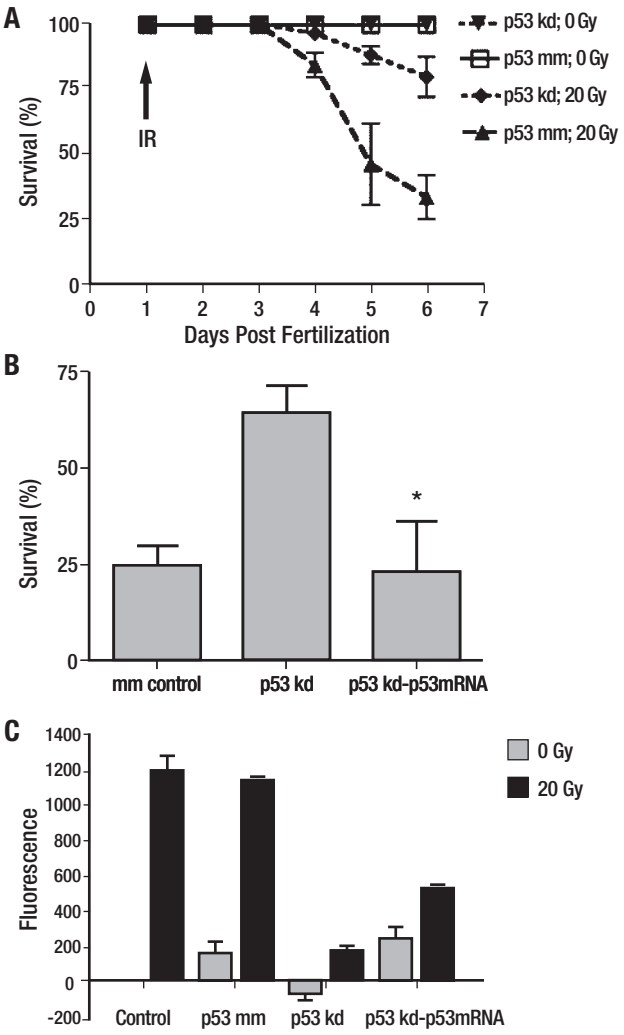

Figure 1. Antisense morpholino oligonucleotides (MOs) targeted to p53 increase embryo survival and reduce ionizing radiation-induced apoptosis evident in the head and trunk regions. **(A)** Embryo survival. Triplicate dishes of 60 embryos each were scored for live embryos daily after 20 Gy IR administered at 24 hpf. Necrotic dissolution or absent heartbeat were considered criteria for embryo death. **(B)** Restoration of IR sensitivity by restoring p53 expression using G-capped zebrafish p53 mRNA. Triplicate dishes of 60 embryos each were scored as described above at 6 dpf (5 days post IR). Asterix (*) p53kd vs p53kd-p53 mRNA; $p < 0.05$; t-test, one-tailed). **(C)** Attenuation of IR-induced apoptosis by p53 kd as assessed by quantification of acridine orange (AO) staining at 30 hpf. Sixty embryos per condition (Control, phenol red control; p53 mm, mismatch antisense MO; p53 kd, p53 antisense MO; p53 kd-p53mRNA, rescue coinjection with p53 antisense MO and p*53* G-capped mRNA) were pooled and stained with AO as described in Materials and Methods. Pooled embryos were transferred to 95% ethanol for 15 minutes to extract the AO for fluorescence determination. Triplicate measurements for each condition were performed on a FL600 microplate fluorescence reader (Bio-Tek) and normalized to control background fluorescence and reported as relative fluorescence units (RFU).

p53 expression by antisense MOs[20] similarly induced a radioresistant phenotype. We observed that *p53*-targeted MO kd markedly improved survival of zebrafish embryos irradiated with 20 Gy at 24 hpf (Fig. 1A) whereas coinjection of capped p53 mRNA restored radiation sensitivity (Fig. 1B). Similarly, *p53*-targeted MO kd markedly reduced the incidence and severity of radiation-induced morphological defects, notably defects in midline development that manifest as dorsal curvature of the body axis (Fig. S1). These results were similar to results by Duffy and Wickstrom published during preparation of this manuscript.[21] In addition, *p53*-targeted MO kd markedly reduced the extent of radiation-induced apoptosis as determined by acridine orange staining (Fig. 1C).

Effects of the pharmacological p53 inhibitor PFTα on development and radiation sensitivity of zebrafish embryos. PFTα was originally identified as an inhibitor of p53-dependent transcription[22] and it reduced the sensitivity of mice to the deleterious effects of ionizing radiation.[23] Based on these previous studies we tested whether PFTα also protected zebrafish embryos against radiation-associated toxicity (Fig. 2A). Unexpectedly, when added to zebrafish embryos at 3 hpf (sphere stage), PFTα (2 μM) caused malformations affecting the head region and led to the development of massive edema affecting the whole body of treated fish at later stages of development (Fig. 2B and Table 1). Furthermore, it has been described earlier that PFTα treatment also reduces overall survival of zebrafish embryos.[21] These results together raised the question whether PFTα exerted effects on molecular targets other than p53, which confound potential radioprotective properties of PFTα in the zebrafish embryo.

PFTα treatment mimics morphological effects associated with knockdown of p73 expression in zebrafish embryos. P73 is a likely candidate for off-target effects of PFTα because p73 binds to and transactivates p53 responsive promoters.[24] Thus, we determined whether suppression of p73 expression by antisense MO kd caused developmental defects similar to those observed in PFTα treated embryos. A previous report showed that targeting p73 adversely affected development of the head region, i.e., the olfactory system, the telencephalon and the pharyngeal arches of zebrafish embryos.[25] In addition, p73 is expressed at high levels in the developing kidneys.[26] We observed that *p73*-targeted antisense MO-mediated kd induced head region abnormalities (Fig. 3A) and led to liquid accumulation affecting the whole body of treated fish (Fig. 4 and Table 2). These changes were very similar to the morphological alterations observed in PFTα-treated fish (Fig. 2B). Furthermore, alcian blue staining revealed severe disturbances of branchial arch development associated with either PFTα treatment or *p73*-targeted antisense MO kd (Fig. 3B). These defects were, at least partially, reversed by coinjection of G-capped *p73* mRNA and not observed in embryos injected with *p73* mismatched antisense MO.

Impaired kidney function in zebrafish treated with PFTα and p73 morpholinos. This is the first report of edema formation upon treatment of developing embryos with *p73*-targeted antisense MO kd. We hypothesized that this phenotype was due to impaired renal clearance consistent with high-level expression of p73 in the developing kidneys.[26] To address this issue we used a renal function assay, which measures retention of a fluorescent dextran within 24 h after injection into the cardiac venous-sinus.[27] As compared to control fish receiving mismatch antisense MO, the *p73*-targeted antisense MO kd caused markedly reduced clearance of this contrast agent (Fig. 5). In contrast, control *p53*-specific antisense MO kd did not affect dextran retention. Importantly, PFTα treatment not only led to liquid accumulation in fish embryos in a manner similar to *p73*-targeted antisense MO kd but it also increased dextran retention in

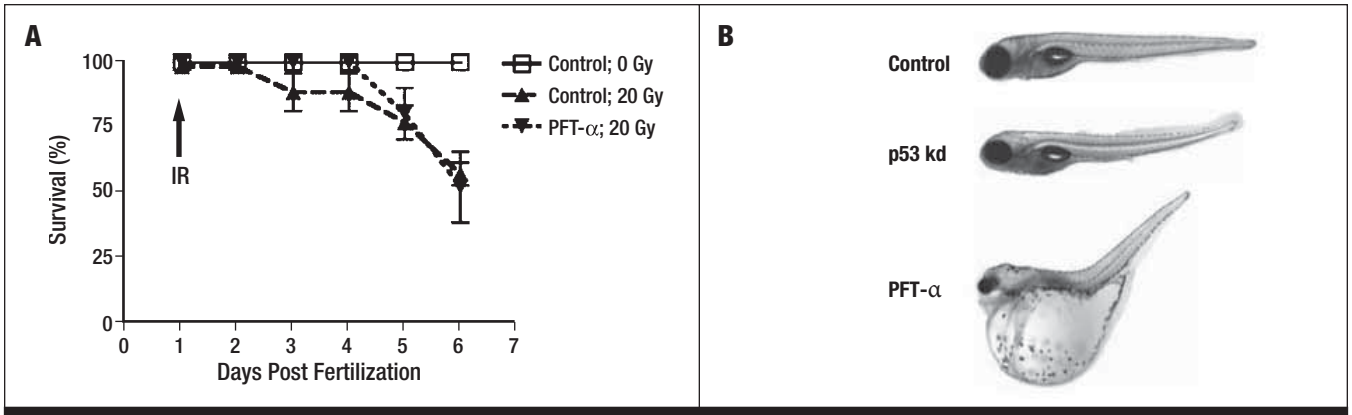

Figure 2. PFT-α (2 μM) administered to zebrafish embryos at 3 hpf does not protect against the lethal effects of IR and is associated with developmental abnormalities. **(A)** Embryo survival scored as described in Figure 1A. **(B)** Embryo morphology in the different experimental conditions as indicated. Representative embryos were digitally photographed at 4x magnification and processed using NIH ImageJ software.

Table 1.
Incidence of whole body edema caused by PFTα treatment

	Normal	Edema	Total	Edema (%)
Control	77	0	77	0
PFTα (2μM)	18	29	47	62

Triplicate dishes (30 embryos each per condition) of live embryos at 7 dpf were scored for edema as shown in Figure 2B and results expressed as percent edema.

a similar fashion. In these experiments, kidney function was tested at 3 dpf and prior to the development of edema to avoid confounding effects of the liquid accumulation on embryonal kidney function.

An alternative explanation for the profound edema in zebrafish embryos following IR exposure is that this effect was caused by reduced cardiac function.[28] To investigate this possibility, we performed time-lapse microscopy of cardiac contractility in control and irradiated fish embryos. Quantitative analysis of the images revealed only marginal effects of either PFTα treatment or *p73*-specific antisense MO kd on heart rate and blood flow (not shown). Collectively, these results suggest that the edema observed in PFTα and *p73 antisense* MO kd zebrafish embryos is due primarily to compromised renal function.

PFTα inhibits p73-dependent transactivation of a p53-responsive promoter construct. The striking similarities in developmental abnormalities caused by either PFTα treatment of suppression of p73 expression raised the question whether PFTα targeted not only p53-dependent but also p73-dependent transcription. Using a p53 responsive reporter gene construct and zebrafish p53 and p73 expression plasmids cotransfected into Saos-2 cells we observed that PFTα not only inhibited p53-dependent transcription but also p73-dependent transcription in a dose-dependent manner (Fig. 6).

It should be noted that administration of PFTα shortly before radiation (i.e., at 23 hpf) did not cause developmental abnormalities either of the craniofacial region or systemic edema and provided a measure of protection against radiation similar to that observed in *p53 antisense* MO kd fish (Fig. S1). This result indicates that p73 serves essential functions during the first 24 h of zebrafish development but is less relevant at later developmental stages and, presumably, in the adult organism. This circumstance also explains why inhibition of p73 function by PFTα has not been obvious in previous in vitro or in vivo studies in adult mice.

In summary, this report demonstrates the utility of the zebrafish model system in characterizing drug effects and highlights previously unrecognized effects of the p53 inhibitor PFTα related to inhibition of p73 function. Lack of either p53 or p73 function is associated with chemoresistance of transformed cells.[29] Furthermore, p73 is induced after DNA damage by the checkpoint kinases Chk1 and Chk2.[30] Based on these results, p73 has been considered as the "assistant" guardian of the genome that acts in concert with p53 to limit propagation of cells with damaged DNA.[31] Since we observed that PFTα inhibits not only p53-dependent but also p73-dependent transcription the overall radioprotective effect of PFTα as observed in mice may, thus, be due to inhibition of p53 and p73 function. Indeed, short-term pharmacological inhibition of both, p53 and p73 may be superior to inhibition of p53 alone to protect normal adult cells and tissues against deleterious effects of radiation.

Materials and Methods

Embryo harvesting and maintenance. Zebrafish husbandry, embryo collection, dechorionation and embryo maintenance were performed according to accepted standard operating procedures[32] and with approval by the Institutional Animal Care and Use Committee at Thomas Jefferson University. Zebrafish were maintained in the Zebrafish Core Facility of the Kimmel Cancer Center at Thomas Jefferson University at 28.5°C on a 14-h light/10-h dark cycle.

Zebrafish morphology by visual analysis. For visual analysis, zebrafish embryos were anesthetized with 0.003% tricaine, placed on 3% methylcellulose on a glass depression slide and analyzed using an Olympus BX51 microscope (Olympus, Melville, NY) at 4x magnification. Images were recorded using a SPOT camera and SPOT Advanced software (SPOT Diagnostic Instruments, Sterling Heights, MI).

Targeted knock down of gene expression. Antisense MO sequences targeting *p53, p73* and controls (5 base mismatches; p53 mm, p73 mm) were as described.[20,25] For microinjection, a 0.5 mM oligonucleotide solution was prepared in 10x phosphate-buffered saline solution, diluted 9:1

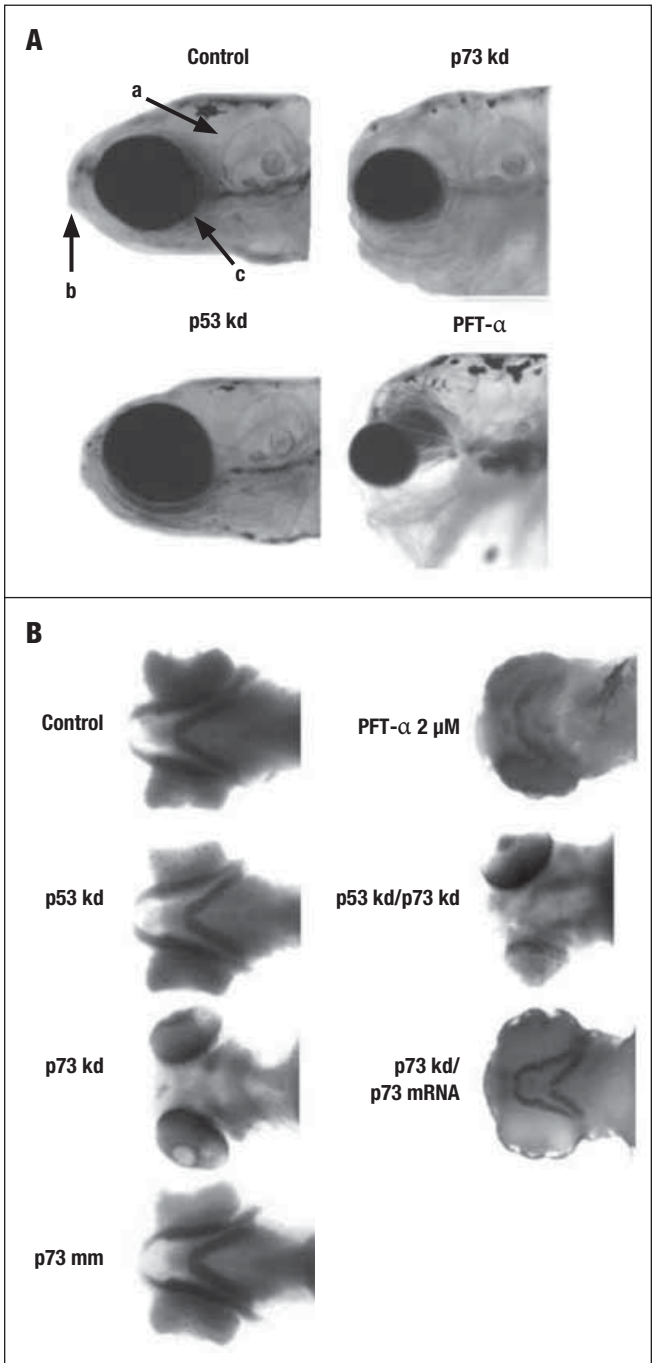

Figure 3. PFT-α treatment (2 μM at 3 hpf) affects cranio-facial development reducing brain, eye and auditory organ size. (A) Embryo head morphology at 6 dpf. Representative embryos were digitally photographed at 10x magnification and processed using NIH ImageJ software (a) snout, (b) eyes, (c) auditory cup. (B) Alcian blue staining (described in Materials and Methods) of cartilage shows markedly abnormal cranio-facial development associated with PFT-α treatment and with p73 antisense MO kd.

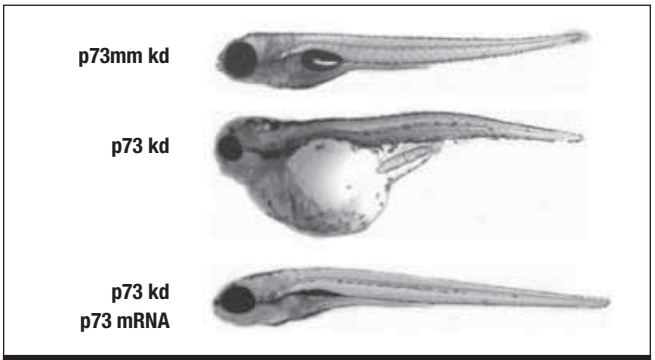

Figure 4. Phenotypic abnormalities associated with PFT-α treatment are similar to those caused by MO-mediated p73 kd. PFT-α was administered at 3 hpf. Embryo morphology and rescue by G-capped mRNA. Representative embryos were digitally photographed at 4x magnification and processed using NIH ImageJ software.

Table 2. Incidence of whole body edema caused by p73kd

	Normal	Edema	Total	Edema (%)
Control	219	1	220	0
p73 MO	121	126	247	51
p73 mm	64	4	68	6
p73 MO/mRNA	151	37	188	20

Live embryos at 7 dpf were scored for edema as described in Figure 4 and results expressed as percent edema.

(v:v) with Phenol Red dye, and ~1 nL injected into 1–4 cell embryos using a nitrogen gas pressure injector (Harvard Apparatus, Cambridge, MA). To account for non-specific effects of MO oligonucleotides, rescue experiments were carried out by coinjection of MOs with G-capped mRNA of the respective target gene. To this end, triplicate dishes of 60 embryos were injected with 4.5–7.5 pg of mRNA generated by cloning the zebrafish *p53* cDNA or p73 cDNA into the pCS2+ vector and producing mRNA with the mMessage-mMachine SP6 kit (Ambion, Austin, TX).

Radiation exposure and PFTα protection. Triplicate dishes (60 embryos each) were irradiated at 24 hpf (20 Gy) using 250 kVp X-rays (PanTak, East Haven, CT) at 50 cm source-to-skin with a 2-mm aluminum filter. Dosimetric calibration was performed before each experiment using a thimble ionization chamber (Victoreen; Elimpex-Medizintechnik, Moedling, Austria) with daily temperature and pressure correction. Pifithrin-α (EMD Biosciences, San Diego, CA) was solubilized in DMSO and diluted with embryo media. PFTα was applied 30 minutes prior to IR.

Kidney function assay. A 1% solution of rhodamine-labeled dextran (10 kDa; Molecular Probes) in PBS was injected (3 dpf) using glass micropipets into the cardiac venous sinus of embryos immobilized in 3% methyl cellulose. Prior to injection, embryos were anesthetized using a 0.003% tricaine solution in egg water.[33] After injection, the embryos were washed in egg water for 10 minutes and placed back into 3% methylcellulose on a glass depression slide. Fluorescence was quantitated using ImageJ software (NIH, USA). The analysis was repeated at 24 h after dextran injection. Percent dextran retention at 24 h was calculated using the formula: (intensity 24 h/intensity 0 h) X 100.

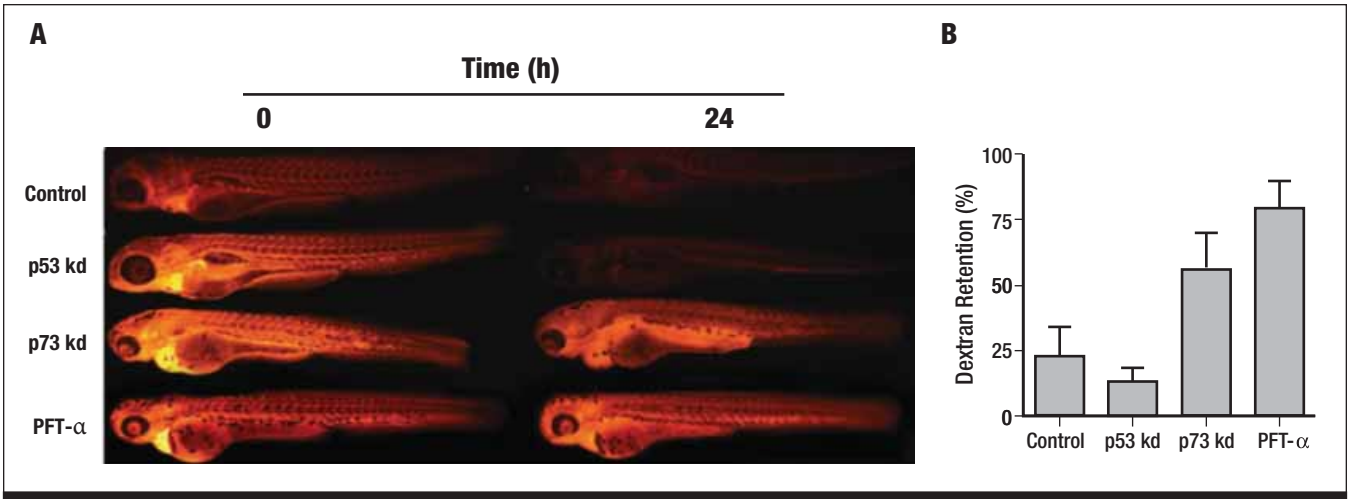

Figure 5. Reduced kidney function by either PFT-α treatment or p73 kd as determined by increased fluorescent dextran retention. **(A)** Rhodamine labeled dextran staining is described in Materials and Methods. Representative images are shown at 0 and 24 h. **(B)** Quantification of dextran label retention at 24 h after dye injection. Three embryos per condition were quantified for dye retention using NIH imageJ software.

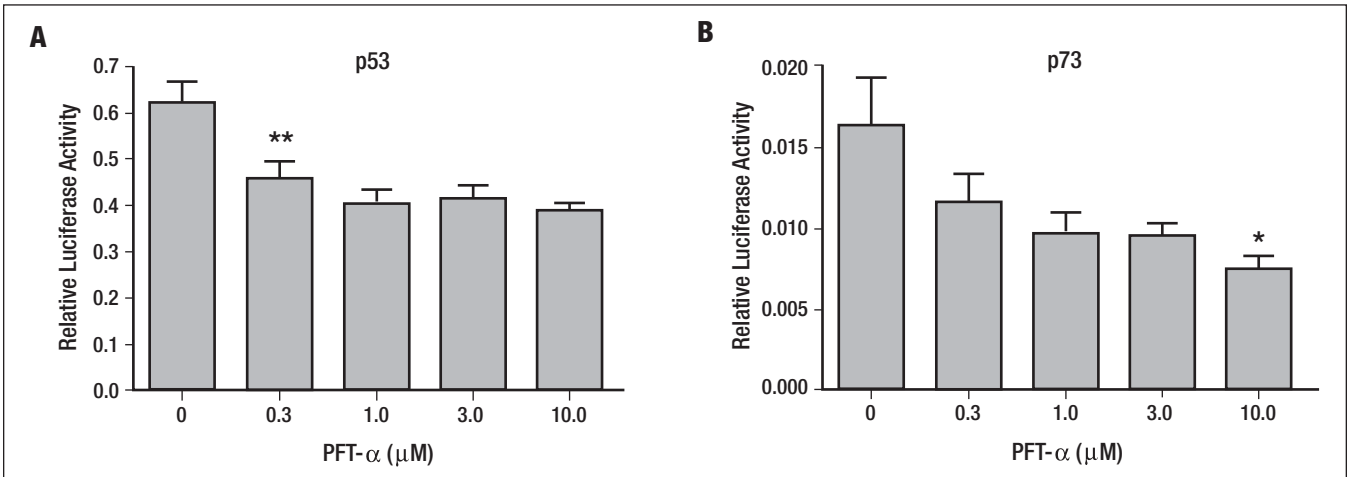

Figure 6. PFT-α inhibits p73-dependent transcription of a reporter gene construct. Triplicate wells (48-well plate) were transfected with pCMV-βgal and p53 pr-RLuc plasmids together with either a pCMV-zp53 **(A)** or a pCMV-zp73 plasmid. **(B)** Renilla luciferase activity was assayed 48 h post transfection and normalized to β-gal activity as described in the Materials and Methods. Cells were treated with PFT-α 15 minutes before transfection. Asterix (*) $p < 0.5$ (tukey test); **$p < 0.01$(tukey test).

Alcian blue staining. Alcian blue staining was performed according to Neuhauss *et al.*,[34] with the following modifications. Embryos (4 dpf) were fixed overnight in Davidson's Solution (Electron Microscopy Sciences, Hatfield, PA) and rinsed 3x for 10 min in PBS and transferred to neutral buffered formalin for 2 days at 4°C. The embryos were then transferred into distilled water and stored at 4°C. For Alcian blue staining, the samples were washed in PBT (0.1% Tween-20 in PBS) and transferred into 30% H_2O_2 (Sigma, St. Louis, MO) and bleached for 4–5 hours or until eyes became translucent. After bleaching, the embryos were rinsed in PBS for 15 min and transferred to filtered Alcian Blue solution (1% conc HCl, 70% Ethanol, 0.1% Tween-20) and stained overnight. The stain was cleared with acidic ethanol (5% conc HCl, 70% ethanol).

Acridine orange staining. Zebrafish embryos were dechorionated and placed in 50 μg/ml of acridine orange (Sigma) in fish water. After 30 min of staining, embryos were washed 3x for 10 min in PBS. Pooled embryos were transferred to 95% ethanol for 15 minutes to extract the AO for fluorescence determination. Triplicate measurements for each condition were performed on a FL600 microplate fluorescence reader (Bio-Tek) and normalized to control background fluorescence and reported as relative fluorescence units (RFU).

In vitro reporter gene assays. Saos-2 cells (ATCC Rockville, MD) were cultured in DMEM supplemented with 10% fetal calf serum. Cells were cultured to 60–70% confluence and transferred to 48-well plates at a density of 2.6×10^4 cells/well. Cells were transfected with three plasmids

using Fugene (Roche). The p53 reporter plasmid was constructed by inserting the synthetic p53-responsive promoter containing 14 tandem p53 enhancer elements and a TATA-box (Pathdetect p53-cis reporter, Stratagene) into the pRLnull plasmid (Promega) to drive the *Renilla* luciferase gene (p53 pr-RLuc). For normalization, a B-galactosidase reporter plasmid was used (pCMV-Bgal;[35]). *Renilla* luciferase activity was measured 48 hrs after transfection using the Dual-Luciferase Reporter Assay System (Promega, Madison, WI) and B-gal activity was measured using the Beta-Glo Reporter Assay System (Promega, Madison, WI) according to the manufacturer's specifications. Cells were treated with PFTα 15 minutes before transfection. Chemiluminescence was measured using a Veritas Microplate luminometer (Turner Biosystems, Sunnyvale, CA).

Acknowledgements

This research was supported by funding from the National Institutes of Health to UR (CA81008) and AD (CA10663) and by the Ruth L. Kirschstein fellowship to WRD (CA119951). Additional support was from the Tobacco Research Settlement Fund (State of Pennsylvania) and USDA. Assistance from the Zebrafish Core facility at Thomas Jefferson University supported by a Cancer Center Support Grant (P30-CA56036) is gratefully acknowledged.

Note

Supplementary materials can be found at: www.landesbioscience.com/supplement/DavidsonCC7-9-Sup.pdf

References

1. Zhou BB, Elledge SJ. The DNA damage response: putting checkpoints in perspective. *Nature* 2000; 408:433-9.
2. Iliakis G, Wang Y, Guan J, Wang H. DNA damage checkpoint control in cells exposed to ionizing radiation. *Oncogene* 2003; 22:5834-47.
3. Sancar A, Lindsey-Boltz LA, Unsal-Kacmaz K, Linn S. Molecular mechanisms of mammalian DNA repair and the DNA damage checkpoints. *Annual Review of Biochemistry* 2004;73:39-85.
4. Cimoli G, Malacarne D, Ponassi R, Valenti M, Alberti S, Parodi S. Meta-analysis of the role of p53 status in isogenic systems tested for sensitivity to cytotoxic antineoplastic drugs. *Biochimica et Biophysica Acta* 2004; 1705:103-20.
5. Zhu C, Bogue MA, Lim DS, Hasty P, Roth DB. Ku86-deficient mice exhibit severe combined immunodeficiency and defective processing of V(D)J recombination intermediates. *Cell* 1996; 86:379-89.
6. Nussenzweig A, Chen C, da Costa Soares V, Sanchez M, Sokol K, Nussenzweig MC, Li GC. Requirement for Ku80 in growth and immunoglobulin V(D)J recombination. *Nature* 1996; 382:551-5.
7. Kurimasa A, Ouyang H, Dong LJ, Wang S, Li X, Cordon-Cardo C, Chen DJ, Li GC. Catalytic subunit of DNA-dependent protein kinase: impact on lymphocyte development and tumorigenesis. *Proc Natl Acad Sci USA* 1999; 96:1403-8.
8. Frank KM, Sekiguchi JM, Seidl KJ, Swat W, Rathbun GA, Cheng HL, Davidson L, Kangaloo L, Alt FW. Late embryonic lethality and impaired V(D)J recombination in mice lacking DNA ligase IV. *Nature* 1998; 396:173-7.
9. Xu Y, Ashley T, Brainerd EE, Bronson RT, Meyn MS, Baltimore D. Targeted disruption of ATM leads to growth retardation, chromosomal fragmentation during meiosis, immune defects, and thymic lymphoma.[see comment]. *Genes Dev* 1996; 10:2411-22.
10. Brown EJ, Baltimore D. ATR disruption leads to chromosomal fragmentation and early embryonic lethality. *Genes Dev* 2000; 14:397-402.
11. Liu Q, Guntuku S, Cui XS, Matsuoka S, Cortez D, Tamai K, Luo G, Carattini-Rivera S, DeMayo F, Bradley A, Donehower LA, Elledge SJ. Chk1 is an essential kinase that is regulated by Atr and required for the G(2)/M DNA damage checkpoint. *Genes Dev* 2000; 14:1448-59.
12. Takai H, Naka K, Okada Y, Watanabe M, Harada N, Saito S, Anderson CW, Appella E, Nakanishi M, Suzuki H, Nagashima K, Sawa H, Ikeda K, Motoyama N. Chk2-deficient mice exhibit radioresistance and defective p53-mediated transcription. *Embo J* 2002; 21:5195-205.
13. Gudkov AV, Komarova EA. The role of p53 in determining sensitivity to radiotherapy. *Nature Reviews Cancer* 2003; 3:117-29.
14. Irwin MS. Family feud in chemosensitvity: p73 and mutant p53. Cell Cycle 2004; 3:319-23.
15. Rubinstein AL. Zebrafish: from disease modeling to drug discovery. *Current Opinion in Drug Discovery & Development* 2003; 6:218-23.
16. McAleer MF, Davidson C, Davidson WR, Yentzer B, Farber SA, Rodeck U, Dicker AP. Novel use of zebrafish as a vertebrate model to screen radiation protectors and sensitizers. *International Journal of Radiation Oncology, Biology, Physics* 2005; 61:10-3.
17. Heasman J. Morpholino oligos: making sense of antisense? *Developmental Biology* 2002; 243:209-14.
18. Daroczi B, Kari G, McAleer MF, Wolf JC, Rodeck U, Dicker AP. In vivo radioprotection by the fullerene nanoparticle DF-1 as assessed in a zebrafish model. *Clin Cancer Res* 2006; 12:7086-91.
19. Berghmans S, Murphey RD, Wienholds E, Neuberg D, Kutok JL, Fletcher CD, Morris JP, Liu TX, Schulte Merker S, Kanki JP, Plasterk R, Zon LI, Look AT. tp53 mutant zebrafish develop malignant peripheral nerve sheath tumors. *Proc Natl Acad Sci USA* 2005; 102:407-12.
20. Langheinrich U, Hennen E, Stott G, Vacun G. Zebrafish as a model organism for the identification and characterization of drugs and genes affecting p53 signaling. *Curr Biol* 2002; 12:2023-8.
21. Duffy KT, Wickstrom E. Zebrafish tp53 knockdown extends the survival of irradiated zebrafish embryos more effectively than the p53 inhibitor pifithrin-alpha. *Cancer Biol Ther* 2007; 6:675-8.
22. Komarov PG, Komarova EA, Kondratov RV, Christov Tselkov K, Coon JS, Chernov MV, Gudkov AV. A chemical inhibitor of p53 that protects mice from the side effects of cancer therapy. *Science* 1999; 285:1733-7.
23. Komarova EA, Neznanov N, Komarov PG, Chernov MV, Wang K, Gudkov AV. p53 inhibitor pifithrin alpha can suppress heat shock and glucocorticoid signaling pathways. *J Biol Chem* 2003; 278:15465-8.
24. Kaghad M, Bonnet H, Yang A, Creancier L, Biscan JC, Valent A, Minty A, Chalon P, Lelias JM, Dumont X, Ferrara P, McKeon F, Caput D. Monoallelically expressed gene related to p53 at 1p36, a region frequently deleted in neuroblastoma and other human cancers. *Cell* 1997; 90:809-19.
25. Rentzsch F, Kramer C, Hammerschmidt M. Specific and conserved roles of TAp73 during zebrafish development. *Gene* 2003; 323:19-30.
26. Satoh S, Arai K, Watanabe S. Identification of a novel splicing form of zebrafish p73 having a strong transcriptional activity. *Biochem Biophys Res Commun* 2004; 325:835-42.
27. Hentschel DM, Park KM, Cilenti L, Zervos AS, Drummond I, Bonventre JV. Acute renal failure in zebrafish: a novel system to study a complex disease. *American Journal of Physiology—Renal Fluid & Electrolyte Physiology* 2005; 288:923-9.
28. Incardona JP, Collier TK, Scholz NL. Defects in cardiac function precede morphological abnormalities in fish embryos exposed to polycyclic aromatic hydrocarbons. *Toxicology & Applied Pharmacology* 2004; 196:191-205.
29. Irwin MS, Kondo K, Marin MC, Cheng LS, Hahn WC, Kaelin WG Jr. Chemosensitivity linked to p73 function. *Cancer Cell* 2003; 3:403-10.
30. Urist M, Tanaka T, Poyurovsky MV, Prives C. p73 induction after DNA damage is regulated by checkpoint kinases Chk1 and Chk2. *Genes Dev* 2004; 18:3041-54.
31. Melino G. p73, the "assistant" guardian of the genome? *Annals of the New York Academy of Sciences* 2003; 1010:9-15.
32. Kimmel CB, Ballard WW, Kimmel SR, Ullmann B, Schilling TF. Stages of embryonic development of the zebrafish. *Dev Dyn* 1995; 203:253-310.
33. Westerfield M. *The zebrafish book.* University of Oregon Press, Eugene OR 1995.
34. Neuhauss SC, Solnica Krezel L, Schier AF, Zwartkruis F, Stemple DL, Malicki J, Abdelilah S, Stainier DY, Driever W. Mutations affecting craniofacial development in zebrafish. *Development* 1996; 123:357-67.
35. Jost M, Kari C, Rodeck U. An episomal vector for stable tetracycline-regulated gene expression. *Nucleic Acids Res* 31(4):e15 1997; 25:3131-4.

Increasing Tumor Volume Is Predictive of Poor Overall and Progression-Free Survival: Secondary Analysis of the Radiation Therapy Oncology Group 93-11 Phase I-II Radiation Dose-Escalation Study In Patients With Inoperable Non-Small-Cell Lung Cancer

Maria Werner-Wasik, MD,* R. Suzanne Swann, PhD,† Jeffrey Bradley, MD,‡ Mary Graham, MD,§ Bahman Emami, MD,‖ James Purdy, PhD,¶ and William Sause, MD#

*Department of Radiation Oncology, Jefferson Medical College, Thomas Jefferson University Hospital, Philadelphia, PA; †Radiation Therapy Oncology Group Headquarters, Philadelphia, PA; ‡Washington University, St. Louis, MO; §Phelps County Regional Medical Center, Rolla, MO;‖Loyola University Medical Center, Maywood, IL; ¶ University of California, Davis, Medical Center, Sacramento, CA; and #LDS Hospital, Salt Lake City, UT

The following article is reprinted with permission from Elsevier Inc. It was originally published in the Int. J. Radiation Oncology Biol. Physics, Volume 70, No. 2, pp. 385-390, 2008.

Purpose

Patients with non–small-cell lung cancer (NSCLC) in the Radiation Therapy Oncology Group (RTOG) 93-11 trial received radiation doses of 70.9, 77.4, 83.8, or 90.3 Gy. The locoregional control and survival rates were similar among the various dose levels.We investigated the effect of the gross tumor volume (GTV) on the outcome.

Methods and Materials

The GTV was defined as the sum of the volumes of the primary tumor and involved lymph nodes. The tumor response, median survival time (MST), and progression-free survival (PFS) were analyzed separately for smaller (≤45 cm^3) vs. larger (>45 cm^3) tumors.

Results

The distribution of the GTV was as follows: ≤45 cm^3 in 79 (49%) and >45 cm^3 in 82 (51%) of 161 patients. The median GTV was 47.3 cm^3. N0 status and female gender were associated with better tumor responses. Patients with smaller (≤45 cm^3) tumors achieved a longer MST and better PFS than did patients with larger (>45 cm^3) tumors (29.7 vs. 13.3 months, $p < 0.0001$; and 15.8 vs. 8.3 months, $p < 0.0001$, respectively). Increasing the radiation dose had no effect on the MST or PFS. On multivariate analysis, only a smaller GTV was a significant prognostic factor for improved MST and PFS (hazard ratio [HR], 2.12, $p = 0.0002$; and HR, 2.0, $p = 0.0002$, respectively). The GTV as a continuous variable was also significantly associated with the MST and PFS (HR, 1.59, $p < 0.0001$; and HR, 1.39, $p < 0.0001$, respectively).

Conclusions

Radiation dose escalation up to 90.3 Gy did not result in improved MST or PFS. The tumor responses were greater in node-negative patients and women. An increasing GTV was strongly associated with decreased MST and PFS. Future radiotherapy trials patients might need to use stratification by tumor volume. ©2008 Elsevier Inc.

Key Words: Tumor volume, Lung cancer, Radiotherapy dose escalation.

Introduction

The current American Joint Committee on Cancer staging system for the primary tumor in lung cancer is based mostly on the tumor extent and involvement of the neighboring structures (*e.g.*, pleura, chest wall, mediastinum, bone, esophagus, and proximal airways) rather than on tumor size or volume. A notable exception is Stage T1, in which a tumor surrounded completely by lung parenchyma cannot exceed 3 cm in the largest dimension. However, a Stage T2 tumor can measure 1.5 cm or 8 cm, as long as it invades the visceral pleura only, with sparing of the other structures. Evidence has been accumulating[1–11] that an increasing tumor volume has a significant effect on patient outcome, possibly even overriding the T stage assignment. Other factors influencing the American Joint Committee on Cancer stage assignment are nodal involvement and the presence of distant metastases.

In a recently published Radiation Therapy Oncology Group (RTOG) Phase I-II study[12] of radiation dose escalation for patients with inoperable non–small cell-lung cancer (NSCLC), the observed locoregional control rates and survival rates were similar between treatment groups, receiving escalated radiation doses (from 70.9 Gy to 90.3 Gy, depending on the volume of lung receiving ≥20 Gy [V_{20}]). A reasonable initial hypothesis would be, however, to expect that smaller tumors should demonstrate improved local control with greater radiation doses compared with larger tumors.

To investigate this hypothesis, we undertook a retrospective analysis of data from the RTOG 93-11 clinical trial in an attempt to demonstrate any benefit of radiation dose escalation for patients with smaller tumors and to determine any relationship between the initial tumor volume and patient outcome.

Methods And Materials

Patient population

The RTOG 93-11 study was a Phase I-II radiation dose escalation trial for patients with inoperable Stage I-III NSCLC treated with three-dimensional (3D) radiotherapy alone, without concurrent chemotherapy, although induction chemotherapy was allowed. The primary objective of the study was to determine the treatment-related morbidity and to determine the maximal tolerated radiation dose. The secondary objectives were to determine the local control and overall survival (OS) rates. The patient population consisted of subjects with NSCLC (inoperable Stage I, II, and IIIA and Stage IIIB; supraclavicular nodes involvement was not allowed; Table 1). Patients were treated according to the volumetric treatment planning computed tomography

findings and the gross tumor volume (GTV) included the primary tumor and any enlarged regional lymph nodes (>1 cm) with a minimal 3D margin of 1 cm. Noninvolved nodal areas were not irradiated, and no special effort was made to account for the respiratory motion, apart for assessing motion with fluoroscopy. Patients were placed into dose-escalation groups according to the V_{20} value in their radiotherapy (RT) plan, predicting the likelihood of treatment-related pneumonitis[13]. Patients with a V_{20} of <25% were assigned to Group 1 and received an escalated dose to 70.9, 77.4, 83.8, or 90.3 Gy. Patients with a V_{20} of 26–35% were assigned to Group 2 and received an escalated dose to 70.9, 77.4, or 83.8 Gy. Patients with a V_{20} of >35% were assigned to Group 3 and received an escalating dose to 64.5, 70.9, or 77.4 Gy. All fraction sizes were 2.15 Gy. The study accrued patients only to Groups 1 and 2. Group 3 enrollment was stopped because of poor accrual.

Table 1. Patient characteristics

Characteristic	Group 1 (*n* = 127)	Group 2 (*n* = 48)
Age (y)		
<60	18 (14)	5 (10)
≥60	109 (86)	43 (90)
Gender (*n*)		
Male	72 (57)	22 (46)
Female	55 (43)	26 (54)
KPS (*n*)		
70–80	85 (67)	30 (63)
90–100	42 (28)	18 (37)
Histologic type (*n*)		
Squamous cell carcinoma	51 (40)	21 (44)
Adenocarcinoma	42 (33)	17 (35)
Other	34 (21)	10 (21)
N stage (*n*)		
N0	83 (65)	17 (35)
N1	10 (8)	6 (13)
N2	32 (25)	22 (46)
N3	2 (1)	3 (6)

Abbreviation: KPS = Karnofsky performance status.
Data in parentheses are percentages.

Evaluation of local control, OS, and progression-free survival

A chest X-ray was obtained 4 weeks after RT completion. Computed tomography scans of the chest were obtained at 6 and 12 months and repeated yearly thereafter. Local control (complete response [CR] or partial response [PR] vs. stable or progressive disease) was reported by the enrolling institutions. No central review of the follow-up computed tomography scans was performed. OS and progression-free survival (PFS) were reported as measured from the date of registration in the study.

Statistical analysis

The GTV was defined as the sum of the volumes of the primary tumor and involved lymph nodes. In the 3D plans, the primary tumor volume and the involved nodal volume were outlined as one structure; no data are available in the RTOG electronic database to allow for separation of those two volumes. Therefore, in an attempt to at least partially correct this deficiency, nodal status (N0 vs. N1 or N2 or N3) was analyzed as one of the variables. This allowed for the separation of the effect of the tumor GTV vs. nodal GTV (at least for Stage I, or N0, patients). OS was defined as death from any cause; an event for PFS was local or regional progression, distant metastases, or death from any cause. For the purpose of this investigation, tumor response, OS, and PFS were analyzed separately for the smaller tumors (≤45 cm^3) vs. larger tumors (>45 cm^3), first among all patients and, later, within each radiation dose level. GTV was also analyzed as a continuous variable. The association of response (CR/PR vs. stable/progressive disease) and the GTV categorized by cutpoint was tested by Fisher's exact test. OS and PFS were estimated by the Kaplan-Meier method and tested using the log–rank test statistic. Univariate and multivariate analyses of OS and PFS with the GTV and other prognostic factors (age [<60 vs. ≥60], gender, Karnofsky performance status [90–100 vs. 70–80], histologic type [nonsquamous vs. squamous], stage [I-II vs. IIIA-IIIB], previous chemotherapy [yes vs. no], and maximal radiation dose to the lung) were done using the Cox proportional hazards model. Multivariate modeling used the stepwise selection method. When analyzed as a continuous variable, GTV was transformed using a $\log_{10}$ transformation to ensure normality. Patients with unknown tumor volumes were excluded from this analysis.

Results

Patient characteristics

A total of 176 patients were included in the original report of the study[12]. Of the 176 patients, 161 had available data on GTV and tumor response and were the subject of this secondary analysis. The patient characteristics are presented in Table 1. Overall, most patients were older (>60 years) with a Karnofsky performance status between 70 and 80. The patients in this analysis were approximately equally split between men and women and those in Group 1 were more likely to have node-negative disease than were those in Group 2. The distribution of the American Joint Committee on Cancer stage was Stage I in 67, Stage II in 12, and Stage III in 48 patients in Group 1 and Stage I in 10, Stage II in 3, and Stage III in 35 patients in Group 2.

Tumor response, OS, and PFS

The GTV was ≤45 cm^3 in 79 (49%) and >45 cm^3, 82 (51%) of 161 patients (median, 47.3; range, 1.9–1,039.9 cm^3); 14 patients had an unknown GTV. The tumor response rate (CR/PR) was better for smaller tumors (≤45 cm^3) than for larger tumors (>45 cm^3; 87% vs. 76%, respectively), as was stable/progressive disease (13% vs. 24%, respectively; p = 0.0691, Fisher's exact test). Results using a cutoff point of 30 cm^3 did not better distinguish between those patients with a tumor response and those with stable or progressive disease than using a cutoff point of 45 cm^3 (p = 0.0642). A cutoff point of 60 cm^3 did not discriminate between the two groups (p = 0.4139). When the GTV was analyzed as a continuous variable, on univariate analysis, it was borderline statistically significantly associated with tumor response (p = 0.0551); however, on multivariate analysis, N stage (N0 vs. N1-N3) and female gender were the only significant variables (p = 0.025 and p = 0.02, respectively). This can be explained by the greater rate of responses (70%) in patients with N0 disease vs. N1-N3 (30%).

Patients with smaller tumors (≤45 cm^3) achieved a longer median survival than did patients with larger tumors (>45 cm^3; 29.7 vs. 13.3 months, p < 0.0001; Fig. 1), as well as better median PFS (15.8 vs. 8.3 months; p < 0.0001; Fig. 2).

When a different GTV was chosen as a cutoff point (30 cm^3 or 60 cm^3), patients with smaller tumors (≤30 cm^3 or ≤60 cm^3) still achieved better OS (32.9 vs. 14.6 months for 30 cm^3, p = 0.0002; and 26.8 vs. 13.3 months for 60 cm^3, p = 0.0006), as well as better PFS (15.5 vs. 9.0 months for 30 cm^3, p = 0.0031; and 14.7 vs. 8.7 months for 60 cm^3, p = 0.0023).

When the effect of GTV was analyzed on univariate analysis, a smaller GTV was associated with improved OS, with significant hazard ratios (HRs) for cutoff points of 30 cm^3 (HR, 2.15; $p = 0.0002$); 45 cm^3 (HR, 2.14; $p < 0.0001$); and 60 cm^3 (HR, 1.91; $p = 0.0008$), as well as for GTV analyzed as a continuous variable (HR, 1.59; $p < 0.0001$). The other variables associated with improved OS on univariate analysis were female gender ($p = 0.0407$) and nodal status ($p = 0.067$, borderline significance). The same factors were significant for PFS on univariate analysis (data not shown).

On multivariate analysis of the factors associated with improved OS and PFS, only a smaller tumor volume was significantly prognostic for both endpoints (HR, 2.12; $p = 0.0002$; and HR, 2.0; $p = 0.0002$, respectively) when GTV was analyzed as a continuous variable. Age, gender, performance status, histologic type, N stage (N0 vs. N1-N3), previous chemotherapy, and maximal radiation dose were not significant (Tables 2 and 3). The other GTV cutoff points (≤30 cm^3, ≤45 cm^3, and ≤60 cm^3) retained their statistically significant association with improved OS and PFS on multivariate analysis and again were the only factors in the multivariate models using a stepwise selection method.

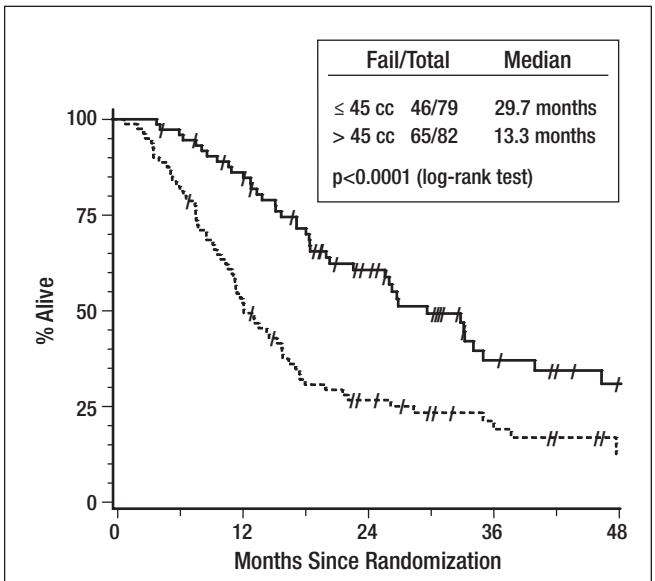

Figure 1. Five-year overall survival rate for patients with gross tumor volume ≤45 cm3 (solid curve) vs. those with gross tumor volume >45 cm^3 (dotted curve).

Effect of radiation dose escalation on tumor response, OS, and PFS by tumor volume

The primary research hypothesis of this study was that higher radiation doses would lead to increased efficacy in smaller tumors. Table 4 shows the frequencies and percentages of patients with a CR/PR and stable or progressive disease for each radiation dose and GTV combination using the 45 cm^3 cutoff point. No evidence was found in these data that the CR/PR rates increased as the radiation dose increases for the two categories of GTV ($p = 0.2213$). Increasing the radiation dose had no effect on OS or PFS (data not shown for PFS) when examined separately for smaller vs. larger tumors when the 45-cm^3 GTV cutoff point was used (Table 5). The results for the 30-cm^3 and 60-cm^3 cutoff points were similar (data not shown). The consistently statistically significant increase in the relative risk of death for all doses to a GTV >45 cm^3 can be attributed to the strong effect of a larger GTV on OS rather than the radiation dose. However, the analysis was not powered to detect a dose–tumor volume interaction, and it could not be ruled out on the basis of this analysis.

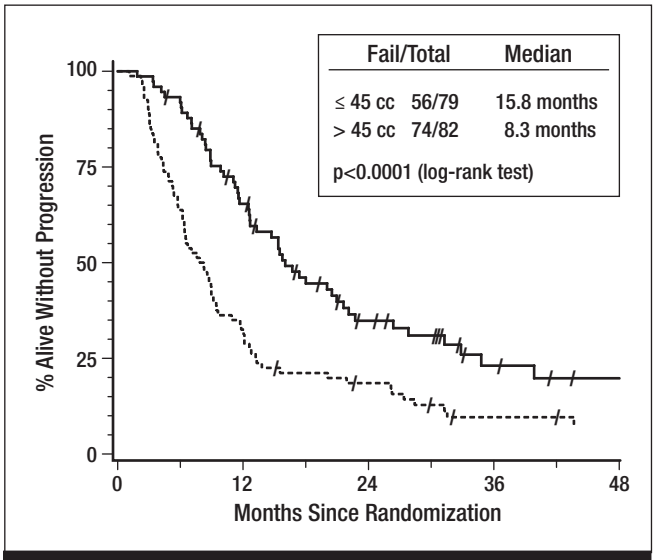

Figure 2. Five-year progression-free survival rate for patients with gross tumor volume ≤45 cm^3 (solid curve) vs. those with gross tumor volume >45 cm^3 (dotted curve).

Table 2. Multivariate analysis of overall survival for different gross tumor volumes used as cutoff point and as continuous variable

Model*	Comparison	Hazard ratio	95% CI	$p^{\dagger}$
GTV (cm^3)	<30 vs. ≥30	2.18	1.43–3.32	0.0003
GTV (cm^3)	≤45 vs. >45	2.12	1.43–3.13	0.0002
GTV (cm^3)	≤60 vs. >60	1.87	1.27–2.75	0.0015
GTV‡	Continuous	1.59	1.33–1.91	<0.0001

Abbreviation: CI = confidence interval; GTV = gross tumor volume; KPS = Karnofsky performance status.
*Following covariates did not meet entry criteria for any multivariate model: age (<60 vs. ≥60 y), gender (female vs. male), KPS (90–100 vs. 70–80), histologic type (nonsquamous vs. squamous), N stage (N0 vs. N1-N3), previous chemotherapy (no vs. yes), or maximal dose to lung (continuous).
†Chi-square test using Cox proportional hazards model; stepwise selection, with entry level of 0.05 and exit level of 0.10.
‡GTV transformed using log10 to ensure normalcy.

Discussion

The aim of RTOG 93-11 was to determine the dose-limiting toxicity of 3D RT. The radiation dose was safely escalated to 83.8 Gy for patients with V_{20} <25% and to 77.4 Gy for patients with a V_{20} of 25–36%. The 90.3-Gy dose level was too toxic. The observed locoregional control was similar among the study arms, without evidence that the higher doses eliminated or at least lowered the recurrence rates.

Our initial hypothesis was that patients with volumetrically smaller tumors would have improved survival with radiation dose escalation but not patients with larger tumors. However, we were not able to demonstrate that in this secondary analysis of the RTOG 93-11 trial, at least not with

Table 3. Multivariate analysis of progression-free survival for different gross tumor volumes used as cutoff point and as continuous variable

Model*	Comparison	Hazard ratio	95% CI	$p^{\dagger}$
GTV (cm^3)	<30 vs. ≥30	1.74	1.20–2.53	0.0039
GTV (cm^3)	≤45 vs. >45	2.00	1.40–2.86	0.0002
GTV (cm^3)	≤60 vs. >60	1.65	1.16–2.36	0.0056
GTV‡	Continuous	1.39	1.18–1.64	<0.0001

Abbreviations as in Table 2.
*Following covariates did not meet entry criteria for any multivariate model: age (<60 vs. ≥60 y), gender (female vs. male), KPS (90–100 vs. 70–80), histologic type (nonsquamous vs. squamous), N stage (N0 vs. N1-N3), previous chemotherapy (no vs. yes), or maximal dose to lung (continuous).
†Chi-square test using Cox proportional hazards model; stepwise selection, with entry level of 0.05 and exit level of 0.10.
‡GTV was transformed using log10 to ensure normality.

the small patient numbers that were available at each radiation dose level tested. It could be that doses >83.8 Gy in standard fractions are necessary to eliminate local failure. Additionally, the protracted overall treatment time of 7–9 weeks might have facilitated tumor repopulation and therefore attenuated any radiation dose response. Finally, the PTV margins were tight (1–1.5 cm around the GTV), which might have increased the likelihood for a marginal miss in mobile tumors, obliterating any potential benefit of dose escalation.

Such a benefit has been suggested in the Memorial Sloan-Kettering Cancer Center experience[4], with the observation of improved local control and survival in Stage III NSCLC patients with large (>100 cm^3) tumors treated with radiation doses >64 Gy compared with those who received lower radiation doses.

A significant interaction between radiation dose and tumor size was shown in the University of Michigan retrospective analysis[5] of 114 patients with medically inoperable Stage I and II NSCLC treated with 3D conformal RT in a dose-escalation study. Patients treated to a biologically equivalent dose of ≤79.2 Gy lived longer if their tumors did not exceed 51.8 cm^3 in volume. However, patients treated to a biologically equivalent dose of >79.2 Gy had the same overall survival, irrespective of tumor volume. With all the limitations of the retrospective study, a hypothesis has been raised that radiation dose escalation can result in improved outcome in NSCLC, at least in node-negative, early-stage tumors.

Table 4. Frequency of tumor response subdivided by radiation dose level and gross tumor volume cutpoint of 45 cm^3

	Incidence (n)		
GTV ≤45 cm^3	CR/PR	SD/PD	p^{*}
Dose 70.9 Gy	13 (93)	1 (7)	0.2736
Dose 77.4 Gy	14 (82)	3 (18)	
Dose 83.8 Gy	15 (88)	2 (12)	
Dose 90.3 Gy	23 (88)	3 (12)	
Dose 70.9 Gy	21 (70)	9 (3)	
Dose 77.4 Gy	19 (68)	9 (32)	
Dose 83.8 Gy	12 (92)	1 (8)	
Dose 90.3 Gy	8 (89)	1 (11)	

Abbreviation: CR = complete response; PR = partial response; SD = stable disease; PD = progressive disease; GTV = gross tumor volume.
Data in parentheses are percentages.
*Fisher's exact test.

Table 5. Multivariate analysis of overall survival subdivided by radiation dose level and gross tumor volume cutpoint of 45 cm^3

Model*	n	Hazard ratio	95% CI	$p^{\dagger}$
GTV ≤45 cm^3, dose 83.8 Gy	17	1.60	0.65–3.93	0.3058
GTV ≤45 cm^3, dose 77.4 Gy	17	1.10	0.43–2.82	0.8432
GTV ≤45 cm^3, dose 70.9 Gy	14	1.57	0.63–3.91	0.3301
GTV >45 cm^3, dose 90.3 Gy	9	4.20	1.52–11.64	0.0058
GTV >45 cm^3, dose 83.8 Gy	13	3.83	1.53–9.60	0.0041
GTV >45 cm^3, dose 77.4 Gy	28	2.41	1.06–5.48	0.0361
GTV >45 cm^3, dose 70.9 Gy	30	2.61	1.17–5.84	0.0193

Abbreviations as in Table 4.
Reference level: GTV ≤45 cm^3, dose 90.3 Gy.
*Chi-square test using Cox proportional hazards model.

In the reports of highly hypofractionated ("radioablative") RT using precise localization techniques to account for tumor motion, very high local control rates have been achieved in medically inoperable patients with Stage I NSCLC receiving 60 Gy in three fractions of 20 Gy each[10] or other hypofractionated regimens[11]. Such doses have not yet been tested in Stage III NSCLC and might be too dangerous for large and central tumors.

We found that the increasing tumor volume, defined as the sum of the primary tumor volume and the volume of the involved lymph nodes, was associated with a greater risk of local failure, with significantly better control achieved with tumors <45 cm^3 than with the larger tumors. The 45-cm^3 volume corresponds roughly to a spherical tumor diameter of 4.4 cm. It must be remembered that the "tumor volume" in our analysis denoted a sum of the volume of the primary tumor and the involved lymph nodes, if any. However, in the multivariate analysis of the tumor volume studied as a continuous variable, it was only the earlier nodal stage and female gender, not the tumor volume, that was associated with better local control. In reality, those two variables (volume and nodal stage) overlap to a large degree, because Stage I NSCLC is defined as a node-negative tumor measuring ≤3 cm in the largest dimension. Separate values for the primary GTV and the nodal GTV were not available in the RTOG 93-11 study; therefore, we were unable to isolate their respective influences on outcomes.

Because a rigorous evaluation of locoregional control was not performed in the RTOG 93-11 trial, local control was not assessed in an actuarial fashion and the radiographic responses might not reflect the true biologic tumor elimination; using survival as an endpoint is a more objective measure of the relevance of tumor volume. A strong association of increasing tumor volume with worsened survival and PFS was observed in our analysis, overriding other known prognostic factors for survival, such as lower disease stage.

Such an association has been previously reported[1–9]. In 207 patients with inoperable NSCLC (Stage I-III) treated at the Washington University with 3D-conformal thoracic RT[1], overall survival, cause-specific survival, and local tumor control were highly correlated with the GTV, and the GTV (and pathologic findings) were predictive for survival on multivariate analysis, but overall stage and nodal stage were not. Those patients with tumor volumes not exceeding 33 cm^3 appeared to have the best outcome.

Local response was evaluated volumetrically on 107 followup thoracic computed tomography scans of 22 patients (19 with Stage III NSCLC)

treated with definitive thoracic RT[2]. A volumeof ≤63cm^3 and a diameter of ≤4 cm were significantly associated with improved local control compared with larger volumes or diameters. In a large series from Wuerzburg[6], 784 scans of 136 patients were evaluated volumetrically, and a cutoffpoint of 100 cm^3 for tumor volume was a discriminating factor for local control, but not survival. In that study, the primary tumor volume and nodal volume were measured separately. The total tumor volume (tumor plus nodes), as well as primary tumor volume alone, was a significant prognostic factor for survival in a Japanese group experience[7].

Because most of the studies cited in our report included a significant proportion of patients with nodal involvement (N1-N3), the relative prognostic value of the "T" tumor volume vs. the "N" nodal volume needs to be elucidated. One would expect that worse survival and possibly lower local control would be associated with an increasing nodal volume rather than the primary tumor volume. However, contradictory data have been published on this issue. On univariate analysis of the factors associated with overall survival and failure-free survival in a Phase I-II radiation dose-escalation trial[3], only the increasing GTV (defined as tumor plus nodes), but not the nodal stage or the overall stage, were predictive. Similarly, in the Japanese experience[7] of 71 patients with Stage III NSCLC, on univariate analysis, the total tumor volume and the primary tumor volume were significant and the nodal volume was not. On multivariate analysis, the total tumor volume and primary tumor volume were both significant prognostic factors.

Investigators from Shanghai Medical University[8] created a prognostic index model predicting for local control in patients with NSCLC treated with RT. Patients with a smaller tumor volume (primary plus nodal), earlier clinical stage, and treated with higher total irradiation dose with a shortened overall treatment time had better local control.

In a Classification and Regression Tree analysis of the Thomas Jefferson University's 107 patients with Stage III NSCLC (9), an aggregate nodal volume >12.5 cm^3 (sum of volumes of the abnormal hilar and mediastinal lymph nodes), as well as a central tumor location, but not the primary tumor volume, were associated with a greater risk of nodal recurrence and shorter median survival time than a nodal volume of ≤12.5 cm^3 (MST 13.9 months vs. 17.1 months, respectively). We are not aware of other reports that have focused on the prognostic value of the involved nodal volume.

Conclusions

Our study is one of several publications demonstrating the importance of tumor volume in patients receiving thoracic RT for NSCLC. It is not fully clear whether patients with smaller tumors have better outcomes simply because of the lower number of clonogenic cells or whether smaller tumors are inherently more biologically favorable; however, the tumor volume may need to be considered in the staging system for lung cancer, once user-friendly volume assessment becomes commonplace in diagnostic studies.

References

1. Bradley JD, Ieumwananonthachai N, Purdy JA, *et al.* Gross tumor volume, critical prognostic factor in patients treated with three dimensional conformal radiation therapy for non–small-cell lung carcinoma. *Int J Radiat Oncol Biol Phys* 2002;52:49–57.
2. Werner-Wasik M, Xiao Y, Pequignot E, *et al.* Assessment of lung cancer response after non-operative therapy: Tumor diameter, bidimensional product, and volume – A serial CT scan-based study. Int J *Radiat Oncol Biol Phys* 2001;51:56–61.
3. Belderbos JS, Heemsbergen WD, DeJaeger K, *et al.* Final results of a phase I/II dose escalation trial in non–small-cell lung cancer using three-dimensional conformal radiotherapy. *Int J Radiat Oncol Biol Phys* 2006;66:126–134.
4. Rengan R, Rosenzweig KE, Venkatraman E, *et al.* Improved local control with higher doses of radiation in large-volume Stage III non–small-cell lung cancer. *Int J Radiat Oncol Biol Phys* 2004;60:741–747.
5. Zhao L, West B, Hayman JA, et al. High radiation dose may reduce the negative effect of large gross tumor volume in patients with medically inoperable early-stage non–small-cell lung cancer. *Int J Radiat Oncol Biol Phys* 2007;68:103–110.
6. Willner J, Baier K, Caragiani E, *et al.* Dose, volume and tumor control prediction in primary radiotherapy of non–small-cell lung cancer. *Int J Radiat Oncol Biol Phys* 2002;52:382–389.
7. Basaki K, Abe Y, Kondo H, *et al.* Prognostic factors for survival in Stage III non–small-cell lung cancer treated with definitive radiation therapy: Impact of tumor volume. *Int J Radiat Oncol Biol Phys* 2006;64:449–454.
8. 8. Chen M, Jiang GL, Fu XL, *et al.* Prognostic factors for local control in non-small cell lung cancer treated with definitive radiation therapy. *Am J Clin Oncol* 2002;25:76–80.
9. Werner-Wasik M, Peqignot E, Garofola B, *et al.* Volume of involved mediastinal lymph nodes and tumor location are predictive of tumor recurrence: Classification and regression tree (CART) analysis of patients with Stage III non-small cell lung cancer [Abstract]. *Proc ASCO* 2003;22:638.
10. Timmerman R, Papiez L, McGarry R, *et al.* Extracranial stereotactic radioablation: Results of a phase I study in medically inoperable Stage I non-small cell lung cancer. *Chest* 2003;124:1946–1955.
11. Onishi H, Araki T, Shirato H, *et al.* Stereotactic hypofractionated high-dose irradiation for stage I nonsmall cell lung carcinoma: Clinical outcomes in 245 subjects in a Japanese multiinstitutional study. *Cancer* 2004;101:1623–1631.
12. Bradley J, Graham MV, Winter K, *et al.* Toxicity and outcome results of RTOG 93-11:A phase I-II dose-escalation study using three-dimensional conformal radiotherapy in patients with inoperable non–small-cell lung carcinoma. *Int J Radiat Oncol Biol Phys* 2005;61:318–328.
13. Graham MV, Purdy JA, Emami B, *et al.* Clinical dose–volume histogram analysis for pneumonitis after 3D treatment for non–small-cell lung cancer. *Int J Radiat Oncol Biol Phys* 1999;45:323–329.

Factors Associated with Severe Late Toxicity After Concurrent Chemoradiation for Locally Advanced Head and Neck Cancer: An RTOG Analysis

Mitchell Machtay, MD[1], Jennifer Moughan, MS[2], Andrew Trotti, MD[3], Adam S. Garden, MD[4], Randal S. Weber, MD[5], Jay S. Cooper, MD[6], Arlene Forastiere, MD[7], K. Kian Ang, MD[4]

[1]Jefferson Medical College and Kimmel Cancer Center of Thomas Jefferson University, Philadelphia; [2]RTOG Headquarters and Statistical Center and the American College of Radiology, Philadelphia; [3]Moffitt Cancer Center of University of South Florida, Tampa; Departments of [4]Radiation Oncology and [5]Head and Neck Surgery at MD Anderson Cancer Center, Houston; [6]Maimonides Medical Center, New York; and [7]Johns Hopkins University Medical Center, Baltimore.

Purpose

Concurrent chemoradiotherapy (CCRT) for squamous cell carcinoma of the head and neck (SCCHN) increases both local tumor control and toxicity. This study evaluates clinical factors that are associated with and might predict severe late toxicity after CCRT.

Methods

Patients were analyzed from a subset of three previously reported RTOG trials of concurrent chemoradiotherapy for locally advanced SCCHN (RTOG 91-11; 97-03; and 99-14). Severe late toxicity was defined in this secondary analysis as chronic Grade 3-4 pharyngeal/laryngeal toxicity (RTOG/EORTC late toxicity scoring system) and/or requirement for a feeding tube ≥2 years after registration and/or potential treatment-related death (e.g. pneumonia) within 3 years. Case-control analysis was performed, with a multivariable logistic regression model that included pre-treatment and treatment potential factors.

Results

A total of 230 patients were evaluable for this analysis, 99 cases (patients with severe late toxicities) and 131 controls; thus 43% of evaluable patients had a severe late toxicity. On multivariable analysis, significant variables correlated with the development of severe late toxicity were older age (odds ratio 1.05 per year; p = 0.001); advanced T-stage (odds ratio 3.07; p=0.0036); larynx/hypopharynx primary site (odds ratio 4.17; p=0.0041); and neck dissection after chemo-RT (odds ratio 2.39; p=0.018).

Conclusions

Severe late toxicity following CCRT is common. Older age, advanced T-stage, and larynx/hypopharynx primary site were strong independent risk factors. Neck dissection after CCRT was associated with an increased risk of these complications.

Background/Introduction

Concurrent chemoradiotherapy (CCRT) is a standard treatment for patients with locally advanced squamous cell carcinoma of the head and neck (SCCHN) treated non-surgically. Meta-analyses show an improved 5-year survival by approximately 8% when CCRT is compared to radiotherapy alone[1, 2]. The advantage of this approach with respect to disease free survival and local-regional control is greater than 8%[3-6, 7-10].

While there are undisputed advantages to CCRT for local-regional control, it increases toxicity when compared to radiotherapy alone[11]. Many studies have focused on acute toxicity, particularly mucositis, as summarized in a meta-analysis by Trotti *et al.*[12]. Comprehensive data on late toxicity from randomized trials of RT +/- chemotherapy, however, are sparse. Late toxicity may include long-term severe dysphagia and its related effects, including dependence upon a feeding tube, and have a profound effect on quality of life. The increased incidence of these serious, potentially permanent effects after CCRT is concerning, leading some to question as to whether chemoradiotherapy is truly a major improvement in the therapeutic ratio over radiotherapy alone.[13]

Starting approximately 15 years ago, the RTOG conducted a series of prospective clinical trials using CCRT for locally advanced SCCHN. General data on efficacy and early and subacute toxicity have been reported[14-16]. It is likely, however, that each individual study is underpowered for a thorough analysis of late effects, given sample size and patient attrition due to mortality and other causes. Consequently, we performed a secondary analysis of severe late toxicities from these several trials, specifically focusing on late toxicities and mortality related to pharyngolaryngeal dysfunction. An analysis of potential factors associated with severe late toxicities was undertaken.

Materials/Methods

As noted above, the three prospective trials analyzed for this paper have been previously reported. All three studies required an acceptable performance status (60-100% by Karnofsky scale); non-metastatic stage III/IV SCCHN; and good hematologic, renal, hepatic and cardiovascular function.

Briefly, the three studies are**:**

RTOG 91-11[14]: A phase III trial of larynx-preserving radiotherapy or chemoradiotherapy for selected Stage III/IV larynx cancer. For this analysis, only the concurrent chemo-radiotherapy arm was studied; this treatment in this arm consisted of 70 Gy in conventionally fractionated radiotherapy (XRT) – 2 Gy once daily – plus three cycles of high dose

cisplatin (100 mg/m2, Weeks 1, 4, and 7). There were 172 patients in this arm from RTOG 91-11; 88 patients were evaluable for this analysis of late toxicity.

RTOG 97-03[17]: A Phase IIR trial of several novel regimens of concurrent chemoradiotherapy for stage III/IV head and neck cancer (excluding patients who were eligibile for RTOG 91-11). This study included three arms. Arms 1 and 3 utilized conventionally fractionated XRT as per 91-11. Arm 1 chemotherapy was infusional 5-FU and cisplatin, both given daily during the last two weeks of XRT. Arm 3 chemotherapy was once weekly cisplatin (20 mg/m2/week) and paclitaxel (30 mg/m2/week). Arm 2 chemoradiotherapy was modeled upon the prospective phase II trials performed by the University of Chicago. In Arm 2, although the total XRT dose remained 70 Gy in 2 Gy fractions, it was delivered over 13 weeks (week-on, week-off technique); chemotherapy in Arm 2 consisted of concurrent infusional 5-FU and hydroxyurea. There were 231 patients in RTOG 97-03; 102 patients were evaluable for this analysis of late toxicity.

RTOG 99-14[16]: A Phase II trial of accelerated radiotherapy with concurrent chemotherapy for stage III/IV head and neck cancer. This single arm phase II study consisted of accelerated concomitant boost radiotherapy to 72 Gy over 6 weeks (as per the concomitant boost arm of RTOG 90-03), with two cycles of high dose cisplatin (100 mg/m2 weeks 1 and 4). There were 76 patients in RTOG 99-14; 40 patients were evaluable for this analysis of late toxicity.

All of these studies used conventional radiotherapy techniques, mostly 2-dimensional planning and delivery. No patient received intensity modulated radiation therapy (IMRT). For this report, a severe late toxicity was defined as any or all of the following events:

- Grade 3 or greater toxicity (RTOG/EORTC Late Toxicity Criteria) present > 180 days after the start of XRT and clearly related to dysfunction of the larynx and/or pharynx (e.g. dysphagia)
- Requirement for a feeding tube/gastrostomy 2 years or longer after the start of XRT.
- Death without cancer progression and from an uncertain cause in which laryngeal dysfunction is suspected to be a contributing factor (e.g. pneumonia) ≤ 3 years from the date of randomization. Patients who died of unknown causes were included in this category. Review of these deaths was performed by one of the study authors (MM) in a manner blinded to any of the patient's clinical pre-treatment and/or treatment related characteristics.

Patients who suffered one or more qualifying severe late toxicity events were only considered to be one "case."

Patients with severe laryngopharynx dysfunction due to cancer, prior to the start of treatment, were excluded because of the potential confounding nature of tumor destruction of critical normal tissues (See Table 1). In RTOG 91-11, the determination of severe pre-treatment laryngopharynx dysfunction was based on patients' on-study data collection form, which scored airway obstruction and dysphagia on a 4-point scale (none, mild, moderate, severe/life-threatening); patients with severe/life-threatening airway obstruction and/or dysphagia based on this form were excluded. In RTOG 91-11, data on pre-treatment use of feeding tubes were not collected. In RTOG 97-03 and RTOG 99-14, pre-treatment feeding tube data were collected, and this was used as the primary means of defining patients with pre-treatment severe laryngopharynx dysfunction.

Patients with missing/inevaluable data or early death from acute toxicity were also excluded.

Statistical Analysis

Frequency tables with counts and percentages were used to describe pretreatment and treatment characteristics for each group. Univariate and multivariable logistic regression models were used to identify associations of pretreatment and treatment-related factors with severe late toxicity. All models were stratified by the 5 treatment arms described above. The following factors were studied: age (continuous variable); gender; race (non-black vs. black); KPS (60-80 vs. 90-100); hemoglobin (continuous variable); weight loss pre-treatment (continuous variable); T-stage (T1/2 vs. T3/4); N Stage (Nx/0/1 vs. N2 vs. N3); Tumor site (oral cavity/oropharynx vs. larynx/hypopharynx); radiotherapy dose received as assessed by late effects BED model (total RT dose multiplied by (1+ [dose/fraction size] ÷ 3): continuous variable); chemotherapy dose received (<85% of planned dose vs. > 85% of planned dose); and post-RT neck dissection (yes vs. no). Variables' levels were grouped in order to avoid small cell counts. A stepwise selection procedure was used to build the multivariable logistic regression model using the above pretreatment/treatment variables. Entry criterion was set at $p < 0.05$. The odds ratios (OR) for each variable in the final model along with their 95% confidence intervals and p-values are reported. The odds ratios estimate how much more (less) likely it is to be in the case group versus the control group among patients with the specific variable level's characteristic compared to those patients in the reference level (RL), after stratifying for treatment arm. The cumulative incidence method was used to estimate time to severe late toxicity and levels for pre-treatment/treatment-related variables were compared using the Gray's test [18, 19].

Table 1. Summary of Patients Excluded from this Analysis

	RTOG 91-11 (Original N=172)	RTOG 97-03 (Original N=231)	RTOG 99-14 (Original N=76)	Total (Original N=479)
Reason for Exclusion				
Severe Pre-treatment Airway Obstruction	15	—	—	15
Severe Pre-treatment Dysphagia	5	—	—	5
Pre-treatment Feeding Tube Dependence	—	62	18	80
Total Excluded due to Severe pre-treatment laryngopharynx dysfunction	20	62	18	100
Death from Acute toxicity	2	3	1	6
Tumor Recurrence/ death < 3 yrs followup.	52	62	16	130
Missing Data	10	2	1	13
Grand Total Excluded	84	129	36	249
Total Analyzable for this study	88	102	40	230

Abbreviations as in Table 4.
Reference level: GTV ≤45 cm^3, dose 90.3 Gy.
*Chi-square test using Cox proportional hazards model.

Table 2. Summary of patients with severe late toxicities (cases) and patients without severe late toxicities (controls)

	Case Group (n=99)	Control Group (n=131)
Age		
Median	60	56
Range	33-78	26-78
Age ≤ 70	85 (86%)	118 (90%)
Age > 70	14 (14%)	13 (10%)
Gender		
Male	78 (79%)	99 (76%)
Female	21 (21%)	32 (24%)
Race		
Non-Black	90 (91%)	120 (92%)
Black	9 (9%)	11 (8%)
KPS		
60-80	24 (24%)	20 (15%)
90-100	75 (76%)	111 (85%)
Hemoglobin		
Median	14.3	14.2
Range	7.1-18.2	9.9-18.2
Hgb ≤ 13.5 gm/dl	28 (28%)	43 (33%)
Hgb > 13.5 gm/dl	71 (72%)	88 (67%)
Weight Loss in Previous 6 months (kg)		
Mean	3.9	2.8
≤ 5 kg	78 (79%)	112 (86%)
> 5 kg	21 (21%)	19 (14%)
T Stage		
T1/T2	18 (18%)	39 (30%)
T3/T4	81 (82%)	92 (70%)
N Stage		
NX/N0/N1	47 (47%)	63 (48%)
N2	42 (42%)	58 (44%)
N3	10 (10%)	10 (8%)
Tumor Site		
Oral cavity/oropharynx	42 (42%)	71 (54%)
Oral Cavity	7 (7%)	5 (4%)
Oropharynx	35 (35%)	66 (50%)
Larynx/hypopharynx	57 (58%)	60 (46%)
Larynx	41 (41%)	51 (39%)
Hypopharynx	16 (16%)	9 (7%)
Radiotherapy Dose-Intensity delivered (BED)		
Mean	115 Gy	116 Gy
Median	117 Gy	117 Gy
Range	67-117 Gy	111-126 Gy
Neck Dissection after RT		
Yes	26 (26%)*	21 (16%)
No	73 (74%)	110 (84%)
Chemotherapy dose-intensity delivered		
< 85%	22 (22%)	29 (22%)
≥ 85%	77 (78%)	102 (78%)

*Two of these patients had their neck dissection after experiencing a severe late toxicity

Results

The original, potential patient population from these three studies was 479. However, there were 130 patients excluded because of local-regional failure or death due to cancer, 100 patients excluded because of severe pre-treatment laryngopharynx dysfunction due to tumor, 13 patients excluded because of missing data, and 6 patients excluded because of early death due to acute toxicity (see Table 1);. Thus, the overall evaluable sample size for this report was 230 patients. The median followup for the patient population is 2.96 years.

Of these 230 patients, 99 patients (cases) had severe late toxicity and 131 patients (controls) did not have severe late toxicity. This results in a crude rate of late toxicity of 43%. It should be noted that if the entire population of patients (N=479) from all three studies are analyzed (as is often performed for studies of late effects) the crude rate would appear to be 21%., considerably lower than the data reported here. An actuarial plot of "Time to Severe Late Toxicity" for all 230 evaluable patients is shown in Figure 1.

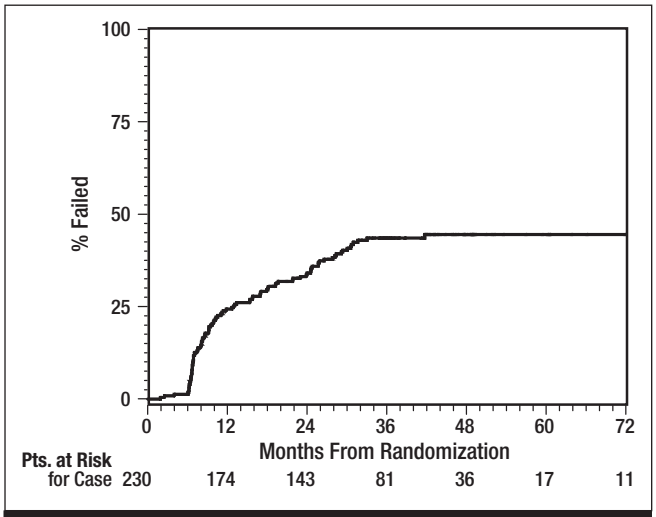

Figure 1. Time to Severe Late Toxicity Events – All Evaluable Patients.

Table 3. Types of late toxicity events seen by trial

	91-11	97-03	99-14	Total
Feeding Tube Dependence > 2 yrs. Post RT	—*	29*		29
Grade 3+ Pharyngeal Dysfunction (RTOG late toxicity criteria)	16	28	19	63
Grade 3+ Laryngeal Dysfunction (RTOG late toxicity criteria)	22	6	0	28
Death	11	9	2	22
Other (e.g. infection, fistula)	3	0	1	4
Any	38**	40**	21**	99**
No Severe late toxicity event (controls)	50	62	19	13

* Feeding tube data were not collected at all in RTOG 91-11.

** Numbers do not always add up along columns, due to some patients having more than one toxicity event.

Figure 2. Time to Severe Late Toxicity Subgoup Analyses based on Patient/Treatment Characteristics

(All graphs exclude 2 patients who had neck dissection after already experiencing a severe late toxicity.)

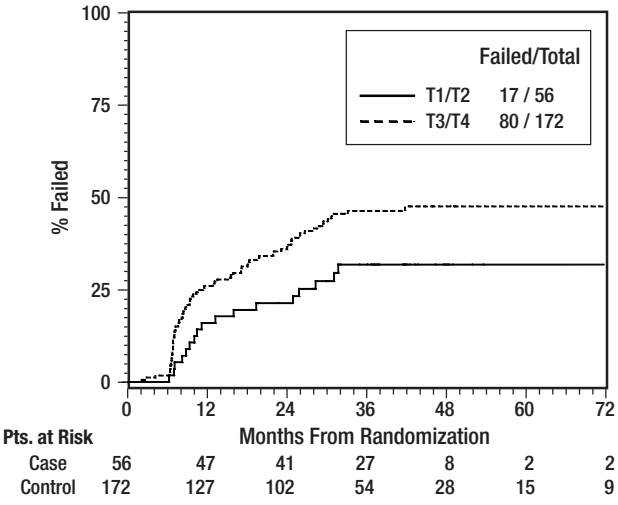

Figure 2a. Time to Severe Late Toxicity by T stage Advanced T stage is associated with a higher likelihood of severe late toxicity (p value from Gray's Test =0.031).

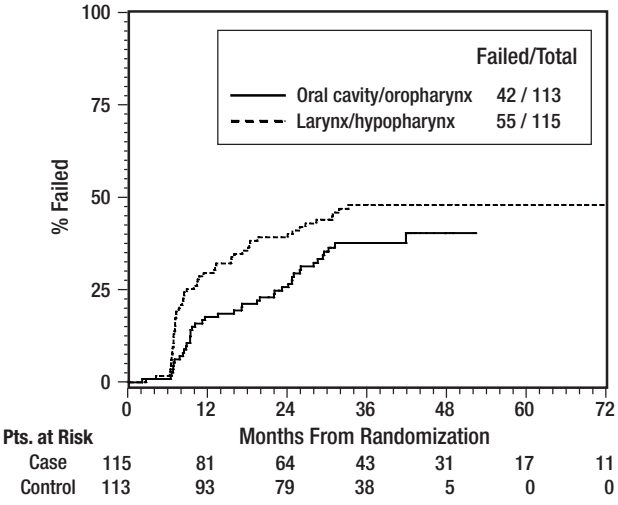

Figure 2b. Time to Severe Late Toxicity by Primary Tumor Site Larynx/Hypopharynx cancer is associated with a statistically non-significant higher likelihood of severe late toxicity (p value from Gray's Test =0.076).

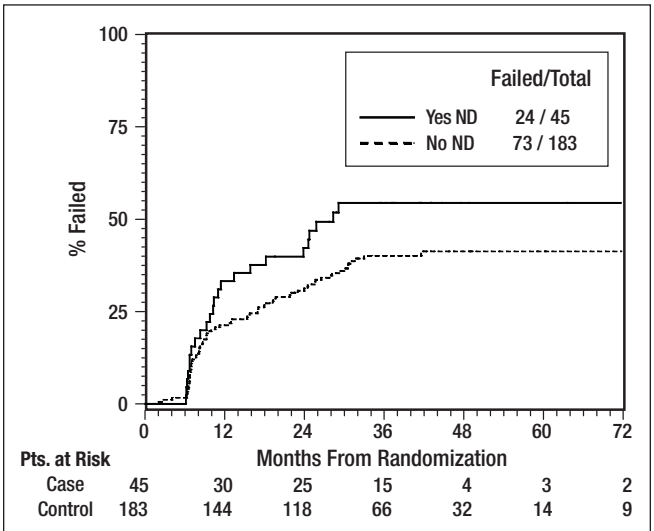

Figure 2c. Time to Severe Late Toxicity by Neck Dissection Neck dissection is associated with a statistically non-significant higher likelihood of severe late toxicity (p-value from Gray's Test =0.09).

The pre-treatment characteristics of these 230 patients are shown in Table 2, including both pre-treatment and treatment-related characteristics. Table 3 shows an accounting of the types of late toxicity events observed in this analysis; most were related to swallowing function (particularly in RTOG 97-03 and RTOG 99-14) or laryngeal dysfunction (RTOG 91-11).

Patients with severe toxicities (cases) were more likely to be older and/or to have larger T-stage and/or larynx/hypopharynx primary cancer. On univariate analysis, there were no statistically significant differences in the rates of late effects based on each individual study/arm.

Univariate logistic regression analysis of pre-treatment and treatment-related variables is shown in Table 4. Actuarial estimates of time to severe late toxicity as a function of T-stage, primary tumor site, and neck dissection are shown in Figures 2a to 2c, respectively. The most significant pre-treatment factor associated with severe late toxicity was age, analyzed as a continuous variable (p=0.0038) – older patients were significantly more likely to have severe late toxicity. T-stage (T3-4 more likely to have severe late toxicity) and tumor site (larynx/hypopharynx more likely to have severe late toxicity) were also statistically significant factors. On univariate analysis, none of the treatment-related variables were statistically significant except BED (p<0.0001), with a paradoxical negative association between BED and severe late toxicity. The p-value for potential association between severe late toxicity and neck dissection after RT was 0.145.

The results of a multivariable logistic regression model analysis are shown in Table 4. Age, T-stage and tumor site remained statistically significant. In addition, a positive association between post-treatment neck dissection and severe late toxicity was noted (p=0.02). Specifically, out of the 230 patients in this study, 47 (20%) underwent post-treatment neck dissection; this included 22% of the oral cavity/oropharynx patients and 19% of the larynx/hypopharynx patients. These 47 patients had a

Table 4. Univariate and Multivariable Logistic Regression Models to Identify Covariates that are associated with severe late toxicity.

	Univariate Analysis		Multivariate Analysis		
Covariates	Odds Ratio	p-value	Odds Ratio	95% confidence Interval	p value
Age					
Continuous variable	1.043*	0.0038	1.05*	[1.02,1.09]	0.001
Gender					
Female	RL				
Male	1.140	0.6846			
Race					
Non-Black	RL				
Black	1.165	0.7458			
KPS					
60-80	1.892	0.0612			
90-100	RL				
Hemoglobin (gm%)					
Continuous Variable	1.005	0.9528			
Weight loss (kg)					
Continuous Variable	1.018	0.3733			
T Stage					
T1/T2	RL		RL		
T3/T4	2.041	0.0349	3.07	[1.444,6.54]	0.0036
N Stage					
NX/N0/N1	RL				
N2	0.942	0.8464			
N3	1.297	0.6108			
Tumor Site					
Oral cavity/oropharynx	RL		RL		
Larynx/hypopharynx	2.955	0.0131	4.17	[1.57,11.03]	0.0041
BED (Toxicities) based on Actual Dose/Fx (Gy) Continuous Variable	0.842	<0.0001			
Neck dissection after RT**					
Yes	1.632	0.145	2.39	[1.16,4.92]	0.018
No	RL		RL		
Percent of chemotherapy received relative to the protocol amount					
< 85%	1.033	0.9216			
≥ 85%	RL				

Abbreviations: RL=reference level; RT=radiation therapy

* The odds ratio of 1.043 for age indicates that for each one year increase in age, patients have 1.043 times higher odds of being in the case group (having a severe late toxicity) than being in the control group (not having a severe late toxicity).

** This excludes 2 patients who had neck dissection after having already experiencing a severe late toxicity.

crude rate of severe late toxicity of 55% (compared with 40% for the 183 patients who did not undergo neck dissection).

Of note, besides neck dissection, other treatment-related factors were not associated with severe late effects. Although the most aggressive radiotherapy fractionation trial (RTOG 99-14, which used concomitant boost XRT + cisplatin) numerically had the highest crude rate of severe late toxicity (21/40 = 53%), there were no statistically significant differences among the trial arms.

As noted in Table 4, radiotherapy dose delivered (as analyzed as biologically equivalent dose [BED]) was significant on univariate analysis (with a paradoxical relationship in which lower RT dose was associated with higher risk) but fell out of the multivariable model. The amount of chemotherapy delivered was not statistically significant in either model.

Discussion

This retrospective analysis of several prospective trials shows that the rate of severe late toxicity after CCRT for SCCHN is high, particularly with the analysis methodology used here. Specifically, in this study, patients with severe pre-treatment laryngopharynx dysfunction and patients with early tumor recurrence were excluded a priori from this analysis. Thus, the number of patients "at risk" for a severe late toxicity event is much smaller than the original treated population. This technique closely approximates the use of actuarial analysis of late complications, a technique which yields a higher rate of complications than simply reporting crude rate of complications, as reported by Bentzen et al.[20] A true actuarial analysis of late complications in head and neck cancer is difficult, because it is not easy to ascertain a date of onset of a late complication in any one individual patient (Figures 2a-2c). Our sample size of 230 patients makes this one of the largest studies of late toxicity in the concurrent chemoradiotherapy era.

In this study, several factors that correlated with severe late toxicity were identified. Since this is a retrospective study, the data must be considered hypothesis-generating rather than definitive. Some caveats result from the fact that these studies were conducted over a 10-year time period (approximately 1991-2001), with variations in eligibility, treatment, and data collection techniques. A second problem inherent to retrospective studies like ours is that a number of potentially important factors may not have been collected at all. For example our database does not include information on tumor volume, cardiopulmonary co-morbidity, and amount of tobacco consumed in followup.

However, it is logical to believe that age, tumor site and tumor stage would predict for greater likelihood of severe late toxicity. The finding that post-treatment neck dissection was significantly associated with severe late toxicity was somewhat more surprising, although this has been reported previously. The number of patients undergoing post-treatment neck dissection was relatively small (20%, despite over 50% of the patients having N2-3 disease), and thus these data can not be considered conclusive. It is possible that selection bias could lead to this association; for example, patients with larger volume neck disease may be more likely to undergo neck dissection and may be more likely to have neck-tumor-related damage to adjacent normal tissues unrelated to the neck dissection. It is possible, though, that disturbance of the soft tissues of the neck via post-treatment neck dissection could cause added swallowing dysfunction, for example by increasing fibrosis in the neck and thus limiting the mobility of the laryngopharynx. It should be noted that a similar report of an association between severe late toxicity and post-treatment neck dissection was recently reported by researchers at

Fox Chase Cancer Center[21]. If these findings are validated in additional, larger datasets, there may be important implications with respect to the controversy regarding neck dissection following chemoradiotherapy for patients with advanced neck disease.

The lack of significant association between cumulative radiotherapy dose delivery (or chemotherapy dose delivery) and severe late toxicity may be due to the narrow dose range prescribed and the generally excellent compliance. We are currently analyzing the detailed radiotherapy records (simulation films, dosimetry and treatment records) available at RTOG headquarters in order to estimate the doses received by individual normal tissue sub-structures within the head and neck. Several recent single-institution studies have rigorously analyzed the relationships between radiotherapy dose-volume-histograms for normal structures and the risk and severity of toxicities[22, 23].

Considering the widespread acceptance of CCRT for SCCHN over the last 10 years, there are relatively few detailed studies of late toxicities. GORTEC reported long-term followup from their randomized trial of radiotherapy alone versus 5-FU/carboplatin/radiotherapy for oropharynx cancer; they did not find a significant difference in severe late toxicity[24]. However, there were fewer than 50 long-term survivors in that study. Staar reported that 51% of long-term survivors (> 2 years) after a very intense combination of accelerated fractionation radiotherapy and chemotherapy were dependent on feeding tubes[8]. With longer followup, that alarmingly high rate did decrease, and was not significantly worse than accelerated radiotherapy alone but the number of evaluable patients was relatively small[25]. Shiley reported that 4 of 13 (31%) cancer-free survivors (>1 year) after chemoradiotherapy required tube feedings for some or all of their nutrition[26].

These data suggest that the CCRT has reached the limits of acceptable long-term toxicity. Dose intensity can not be easily increased without some new and effective technique(s) of protection against late effects. In the future, these may include modern techniques in radiotherapy technology[27, 28], or biopharmacologic radioprotectors[29-31]. Presently, however, these techniques have only succeeded in reducing xerostomia, not severe late dysphagia. Emphasis should therefore be on careful patient selection for aggressive treatment and swallowing exercises before during and after radiotherapy[32, 33]. Some patients may benefit from more invasive procedures, such as dilatation of hypopharyngeal/esophageal stricture under anesthesia.

For some patient subpopulations the risks of concurrent chemoradiotherapy may outweigh the benefits. For example, subgroup analysis of a meta-analysis suggested that there was no significant survival benefit to CCRT in patients older than age 70[1]. Our data may add to the controversy regarding management of the elderly patient with head and neck cancer – if there is no significant survival benefit and a significant increase in late toxicity with concurrent chemoradiotherapy, should it be the standard of care in this patient population?

Our study has several limitations that should be discussed. First, it is a "meta-analysis" of three separate clinical trials, each of which had somewhat different eligibility criteria, chemoradiotherapy regimen, and year of activation. However, all of the patients did receive treatment that would be considered appropriate standard of care in today's oncology clinic. Second, our exclusion of patients with pre-existing severe laryngopharynx dysfunction from this analysis can be considered controversial. Although patients were excluded a priori, determining pre-existing severe laryngopharynx dysfunction is subjective. However, it should be noted that the determination of post-treatment severe laryngopharynx dysfunction (toxicity) is also subjective. It is extremely difficult to determine if severe dysfunction after treatment is the result of treatment or the result of the pre-existing cancer. By excluding patients with pre-treatment severe laryngopharynx dysfunction, we attempted to isolate the influence of treatment on outcomes. Third, our study is an exploratory analysis; while it is one of the larger series on late toxicity after chemoradiotherapy, the number of patients and number of events are relatively small. We plan to address this in the future with an analysis of the recently completed trial, RTOG 0129. This was a randomized trial of standard fractionation versus accelerated fractionation radiotherapy (with cisplatin in both arms). Preliminary acute and subacute toxicity data showed no significant differences between the two arms[34]. It is premature at this time to perform a detailed analysis of efficacy or late toxicity from that study. It is possible that with improved knowledge and experience with CCRT and supportive care available in the 21st century, outcomes may be improved in RTOG 0129 compared to historical controls.

Ultimately, it should be remembered that for most patients with head and neck cancer, the highest priority is cure and length of survival[35]. Excessive concern about treatment toxicity should not prevent the use of proven aggressive multimodality treatment, provided the patient is well informed about the potential late sequelae of these aggressive treatment regimens.

References

1. Bourhis J, LeMaitre A, Baujat B, *et al.* Individual patients' data meta-analyses in head and neck cancer. *Curr Opin Oncol* 2007;19(3):188-94.
2. Pignon JP, Bourhis J, Domenge C, Designe L. Chemotherapy added to locoregional treatment for head and neck squamous cell carcinoma: three meta-analyses of updated individual data. *Lancet* 2000;355:949-55.
3. Brizel DM, Albers MA, Fisher SR, *et al.* Hyperfractionated irradiation with or without concurrent chemotherapy for locally advanced head and neck cancer. *N Engl J Med* 1998;328:1798-804.
4. Wendt TG, Grabenbauer CG, Rodel CM, *et al.* Simultaneous radiochemotherapy versus radiotherapy alone in advanced head and neck cancer: a randomized multicenter study. *J Clin Oncol* 1998;16:1318-24.
5. Calais G, Alfonsi M, Bardet E, *et al.* Randomized study comparing radiation alone RT versus concomitant chemotherapy and radiation therapy for advanced-stage oropharynx carcinoma. *J Natl Cancer Inst* 1999;91:2081-6.
6. Adelstein DA, Lavertu P, Saxton JP, *et al.* Mature results of a phase III trial comparing concurrent chemoradiotherapy with radiation therapy alone in patients with stage III and IV squamous cell carcinoma of the head and neck. *Cancer* 2000;88:876-83.
7. Olmi P, Crispino S, Fallai C, *et al.* Locoregionally advanced carcinoma of the oropharynx: conventional radiotherapy vs. accelerated hyperfractionated radiotherapy vs. concomitant radiotherapy and chemotherapy – a multicenter randomized trial. *Int J Radiat Oncol Biol* 2003;55:78-92.
8. Staar S, Rudat V, Stuetzer H, *et al.* Intensified hyperfractionated accelerated radiotherapy limits the additional benefit of simultaneous chemotherapy -- results of a multicentric randomized German trial in advanced head and neck cancer. *Int J Radiat Oncol Biol Phys* 2001;50:1161-71.
9. Budach V, Stuschke M, Budach W., *et al.* Hyperfractionated accelerated chemoradiation with concurrent fluorouracil-mitomycin is more effective than dose-escalated hyperfractionated accelerated radiation therapy alone in locally advanced head and neck cancer: final results of the radiotherapy cooperative clinical trials group of the German Cancer Society 95-06 prospective randomized trial. *J Clin Oncol* 2005;23(6):1125-35.
10. Bensadoun RJ, Benezery K, Dassonville O, , *et al.* French multicenter phase III randomized study testing concurrent twice-a-day radiotherapy and cisplatin/5-fluorouracil chemotherapy (BiRCF) in unresectable pharyngeal carcinoma: Results at 2 years (FNCLCC-GORTEC). *Int J Radiat Oncol Biol Phys* 2006;64(4):983-94.
11. Henk JM. Controlled trials of synchronous chemotherapy with radiotherapy in head and neck cancer: overview of radiation morbidity. *Clin Oncol* (Royal Coll Radiol) 1997;9:308-12.
12. Trotti A, Bellm LA, Epstein JB, *et al.* Mucositis incidence, severity and associated outcomes in patients with head and neck cancer receiving radiotherapy with or without chemotherapy: a systematic literature review. *Radiother Oncol* 2003;66:253-62.
13. Stuben G, Thews O, Pottgen C, *et al.* Recombinant human erythropoietin increases the radiosensitivity of xenografted human tumours in anaemic nude mice. *J Cancer Res Clin Oncol* 2001;127:346-50.

14. Forastiere AA, Goepfert H, Maor M, *et al.* Concurrent chemotherapy and radiotherapy for organ preservation in advanced laryngeal cancer. *N Engl J Med* 2003;349:2091-8.

15. Garden AS, Harris J, Vokes EE, *et al.* Preliminary results of Radiation Therapy Oncology Group 97-03: a randomized phase II trial of concurrent radiation and chemotherapy for advanced squamous cell carcinomas of the head and neck. *J Clin Oncol* 2004;22:2856-64.

16. Ang KK, Harris J, Garden A, *et al.* Concomitant boost radiation plus concurrent cisplatin for advanced head and neck carcinomas: Radiation Therapy Oncology Group phase II trial 99-14. *J Clin Oncol* 2005;23(13):3008-15.

17. Garden AS, Pajak, T., Vokes, E., Forastiere, A., Ridge, J., Jones, C., Horwitz, E., Glisson, B., Nabell, L., Cooper, J., Demas, W., Gore, E. Preliminary results of RTOG 9703 – A Phase II Randomized Trial of Concurrent Radiation (RT) and Chemotherapy for Advanced Squamous Cell Carcinomas (SCC) of the Head and Neck (abstr.). *In: Proc Am Soc Clin Oncol* (ASCO); 2001; San Francisco; 2001.

18. Kalbfleisch JD, Prentice RL. The Statistical Analysis of Failure Time Data. New York: John Wiley & Sons; 1980:167-169.

19. Gray RJ. A class of K-sample tests for comparing the cumulative incidence of a competing risk. *Ann Statist*. 1988; 16: 1141-1154.

20. Bentzen SM, Vaeth M, Pedersen DE, Overgaard J. Why actuarial estimates should be used in reporting late normal tissue effects of cancer treatment . . . now! *Int J Radiat Oncol Biol Phys* 1995;32(5):1531-4.

21. Lango M, Ende K, Ahmad S, Feigenberg SJ, Ridge JA. Neck dissection following organ preservation protocols prolongs feeding tube dependence in patients with advanced head and neck cancer (abstr. #5525). In: 2006 ASCO annual meeting; 2006; Atlanta: *J Clin Oncol*; 2006.

22. Dornfeld K, Simmons JR, Karnell L, et al. Radiation doses to structures within and adjacent to the larynx are correlated with long-term diet- and speech-related quality of life. *Int J Radiat Oncol Biol Phys* 2007;68(3):750-7.

23. Eisbruch A, Schwartz M, Rasch C, *et al.* Dysphagia and aspiration after chemoradiotherapy for head and neck cancer: which anatomic structures are affected and can they be spared by IMRT? *Int J Radiat Oncol Biol Phys* 2004;60:1425-39.

24. Denis F, Garaud P, Bardet E, et al. Final results of the 94-01 French head and neck oncology and radiotherapy group randomized trial coparing radiotherapy alone with concomitant radiochemotherapy in advanced-stage oropharynx carcinoma. *J Clin Oncol* 2004;22(1):69-76.

25. Semaru R, Mueller RP, Stuetzer H, Staar S, *et al.* Efficacy of intensified hyperfractionated and accelerated radiotherapy and concurrent chemotherapy with carboplatin and 5-0fluorouracil: updated results of a randomized multicentric trial in advanced head and neck cancer. *Int J Radiat Oncol Biol Phys* 2006;64(5):1308-16.

26. Shiley SG, Hargunani C, Skoner JM, *et al.* Swallowing function after chemoradiation for advanced stage oropharyngeal cancer. *Otolaryngol Head Neck Surg* 2006;134(3):455-9.

27. Bucci MK, Bevan A, Roach Mr. Advances in radiation therapy: conventional to 3D, to IMRT, to 4D, and beyond. *CA Cancer J Clin* 2005;55(2):117-34.

28. Feng FY, Kim HM, Lyden TH, *et al.* Intensity-modulated radiotherapy of head and neck cancer aiming to reduce dysphagia: early dose-effect relationships for the swallowing structures. *Int J Radiat Oncol Biol Phys* 2007;2007:in press.

29. Kouvaris JR, Kouloulias VE, Vlahos LJ. Amifostine: the first selective-target and broad spectrum radioprotector. *Oncologist* 2007;12(6):738-47.

30. Ning S, Shuii C, Khan WB, al. e. Effects of keratinocyte growth factor on the proliferation and radiation survival of human squamous cell carcinoma cell lines in vitro and in vivo. *Int J Radiat Oncol Biol Phys* 1997;40:177-87.

31. Greenberger JS, Epperly MW. Review: antioxidant gene therapeutic approaches to normal tissue radioprotection and tumor radiosensitization. *In Vivo* 2007;21:141-6.

32. Mittal BB, Pauloski BR, Haraf DJ, *et al.* Swallowing dysfunction – preventative and rehabilitation strategies in patients with head and neck cancers treated with surgery, radiotherapy and chemotherapy: a critical review. *Int J Radiat Oncol Biol Phys* 2003;57(5):1219-30.

33. Rosenthal DI, Lewin JS, Eisbruch A. Prevention and treatment of dysphagia and aspiration after chemoradiation for head and neck cancer. *J Clin Oncol* 2006;24(17):2636-43.

34. Ang KK, Pajak T, Rosenthal D, *et al.* A phase III trial to compare standard versus accelerated fractionation in combination with concurrent cisplatin for head and neck carcinomas (RTOG 0129): Report of compliance and toxicity. *Proc. Am. Soc. Ther Rad Onc (ASTRO)*, 2007 Annual Meeting, Los Angeles, IJRBOP suppl.

35. List MA, Stracks J, Colangelo L, *et al.* How do head and neck cancer patients prioritize treatment outcomes before initiating treatment? *J Clin Oncol* 2000;18(4):877-84.

Departmental Information

Thomas Jefferson University
Jefferson Medical College
Department of Radiation Oncology

Kimmel Cancer Center – Bodine
111 S. 11th Street
Philadelphia, PA 19107
Telephone: 215-955-6700
www.kimmelcancercenter.org/kcc/radonc/bodine.htm

FACULTY

Clinicians

Adam P. Dicker, MD, PhD
Interim Chair

P. Rani Anné, MD
Jessie W. DiNome, MD
Scot A. Fisher, DO
Eric L. Gressen, MD
Arthur J. Harvey, MD
Alexander Lin, MD
Mitchell Machtay, MD
Jeffrey Rosenstock, MD
Shari B. Rudoler, MD
Merrill J. Solan, MD
Richard K. Valicenti, MD
Maria Werner-Wasik, MD

Division of Experimental Radiation Oncology

Adam P. Dicker, MD, PhD
Division Director

Ronald A. Coss, PhD
Dennis B. Leeper, PhD
Qing Ren, MD, PhD
Marlene Rochas DeQuadros, PhD
Phyllis R. Wachsberger, PhD

Division of Medical Physics

Yan Yu, PhD, MBA
Division Director

Jungshen Cao, MS
Lei Fu
James M. Galvin, DSc
Amy Harrison, MS
Jun Li, PhD
Haisong Liu, PhD
Harold Perera, PhD
Tarun Podder, PhD
Ying Xiao, PhD

Research
Department of Radiation Oncology

Clinical Research Studies/Grants

- Phase I Study of Combination of Sorafenib and Radiation Therapy For The Treatment of Patients With Brain Metastases and Primary Brain Tumors
- A Phase I Pilot Study of Samarium-153 Combined with Neoadjuvant Hormonal Therapy and Radiation Therapy in Men with Locally Advanced Prostate Cancer
- A Phase I Study of Pemetrexed (Alimta) and Carboplatin and Radiation Therapy in Patients with Inoperable Non-Small Cell Lung Cancer
- A Phase I Study of Combination Chemo-radiotherapy with Biologic Therapy for Advanced Head and Neck Cancer [Bevacizumab IND #12,907] Original: 1/26/06; Revised 3/24/06)
- A Randomized, Phase III, Open-Label Study of Oral Topotecan Plus Whole Brain Radiation Therapy (WBRT) Compared with WBRT Alone in Patients with Brain Metastases From Non Small Cell Lung Cancer HYT105962, Division: Worldwide Development, Retention Category: GRS019, Protocol Amendment Number: 01, Compound Number: SK&F-104864, Effective Date: 11-Apr-2007; including a Topotecan Oral Investigator Brochure, Compound Number: SK&F-104864, Approved Name: Hycamtin, Effective Date: 13-Jul-2006, Version number:8 dated July 2006
- Prospective, Longitudinal, Multi-Center, Descriptive Registry of Patients Receiving Therapy Other Than Surgical Resection Alone for Newly Diagnosed Head and Neck Carcinoma.
- A Phase 1, Open-Label, Dose-Escalation, Safety Study of the Combination of VELCADE and Chemoradiation for the Treatment of Patients with Cancer
- A Phase II Evaluation of Dose-Painted IMRT in Combination with 5-Fluorouracil and Mitomycin-C for Reduction of Acute Morbidity in Carcinoma of the Anal Canal
- A Randomized Prospective Active-controlled Study of the Epi-Rad90™ Opthalmic System for the Treatment of Subfoveal Choroidal Neovascularization Associated With Wet Age-related Macular Degeneration
- A Phase IB, Open-Label, Dose-escalation Safety Study of the Combination of Sunitinib and Radiation for the Treatment of Patients with Cancer.
- A Pilot Study Investigating Active Breathing Control (ABC) to Reduce Radiation Dose to Normal Structures in Breast Cancer Patients
- A Randomized Trial Comparing Two Forms of Immobilization of the Head for Fractionated Stereotactic Radiotherapy
- Phase I Dose Escalation Trial in Patients with Brain Metastases Using IMRT
- Exploratory Study of the Efficacy of the Cone Beam Computed Tomography (CBCT) Scanning During Radiation Therapy for Tumors of the Head and/or Neck
- A Phase III Protocol of Androgen Suppression (AS) and Radiation Therapy (RT) vs Androgen Suppression and RT Followed by Chemotherapy With Paclitaxel, Estramustine and Etoposide (TEE) for Localized, High Risk Prostate Cancer
- Waterfall Plots After Stereotactic Radiotherapy for Acoustic Neuroma: Assessing Response With a Novel Metric of Treatment Efficacy
- Stereotactic Fractionated Radiotherapy and Radiosurgery for the Treatment of Chordomas and Chondrosarchomas
- Retrospective Study of Esophageal Cancer Patients Treated With Surgery, Radiation Therapy, Chemotherapy Or Any Combination of the Three At Thomas Jefferson University Hospital
- Optimization of Radiation Therapy for Hypopharyngeal and Cervical Esophageal Cancers: A Comparison of Conventional and Three-dimensional Conformal Techniques
- Retrospective Analysis of Radiation Dose to Optic Structures Using Fractionated Stereotactic Radiotherapy: Determination of a Dose/Volume Relationship to Guide Safe Treatment of Tumors Near the Optic Apparatus
- Standardize Serum and Plasma Sample Collection and Cytokine Normal Values for RTOG Repository and Database

- A Prospective Phase II Trial of Transperineal Ultrasound-guided Brachytherapy for Locally Recurrent Prostate Adenocarcinoma Following External Beam Radiotherapy – RTOG 0526
- A Phase III Double Blind Placebo Controlled Study To Evaluate the Efficacy of Zometa for the Prevention of Osteoporosis and Associated Fractures In Patients Receiving Radiation Therapy and Long Term LHRH Agonists For High-grade and/or Locally Advanced Prostate Cancer – RTOG 0518
- RTOG #0012: A Randomized Phase II Trial of Preoperative Combined Modality Chemoradiation for Distal Rectal Cancer
- RTOG #0024: A Phase II Trial of Early Postoperative Paclitaxel Followed by Paclitaxel and Cisplatin Concurrent With Radiation Therapy for Resected, High-Risk Squamous Carcinoma of the Head and Neck
- RTOG #0126: A Phase III Randomized Study of High Dose 3D-CRT in Patients Treated for Localized Prostate Cancer
- RTOG #0129: A Phase III Trial of Concurrent Radiation and Chemotherapy for Advanced Head and Neck Carcinomas
- RTOG #0132: A Phase II Trial of Neoadjuvant/Adjuvant STI-571 (Gleevec NSC #716051) for Primary and Recurrent Operable Malignant Gist Expressing the Kit Receptor Tyrosine Kinase (CD117) (ACRIN 6665)
- RTOG #0211: A Phase I/ Study of an Oral Epidermal Growth Factor Receptor Tyrosine Kinase Inhibitor (EGFR-TK), ZD 1839 (IRESSA) (NSC #715055) With Radiation Therapy in Gliblastoma Multiforme
- RTOG #0214: A Phase III Comparison of Prophylactic Cranial Irradiation in Patients with Locally Advanced Non-Small Cell Lung Cancer
- RTOG #0225: A Phase II Study of Intensity Modulated Radiation Therapy (IMRT) +/- Chemotherapy for Nasopharyngeal Cancer
- RTOG #0227: A Phase I/II Study of Pre-Irradiation Chemotherapy with Methotrexate, Rituximab, and Temozolomide and Post-Irradiation Temozolomide for Primary Central Nervous System Lymphoma
- RTOG #0232: A Phase III Study Comparing Combined External Beam Radiation and Transperineal Interstitial Permanent Brachytherapy with Brachytherapy Alone for Selected Patients with Intermediate Risk Prostatic Carcinoma
- RTOG #0233: A Phase II Randomized Trial for Patients with Muscle-Invading Bladder Cancer Evaluating Transurethral Surgery and BID Irradiation Plus Either Paclitaxel and Cisplatin or 5 Fluorouracil and Cisplatin Followed by Selective Bladder Preservation and Gemcitabine/Paclitaxel/Cisplatin Adjuvant Chemotherapy
- RTOG #0236: A Phase II Trial of Stereotactic Body Radiation Therapy (SBRT) in the Treatment of Patients with Medically Inoperable Stage I/II Non Small Cell Lung Cancer
- RTOG #0241: A Phase I Study Of Irinotecan And Cisplatin In Combination With Twice Daily Thoracic Radiotherapy (45 Gy) or Once Daily Thoracic Radiotherapy (70 Gy) for Patients with Limited Stage Small Cell Lung Cancer
- RTOG #0247: A Randomized Phase II Trial of Neoadjuvant Combined Modality Therapy for Locally Advanced Rectal Cancer (Version: Activation 3/15/04)
- RTOG #0320: A Phase III Trial Comparing Whole Brain Radiation and Stereotactic Radiosurgery Alone Versus With Temozolomide or Erlotinib in Patients with Non-Small Cell Lung Cancer and 1-3 Metastases
- RTOG #0415: A Phase III Randomized Study of Hypofractionated 3D-CRT/IMRT Versus Conventionally Fractionated 3D-CRT/IMRT in Patients with Favorable-Risk Prostate Cancer
- RTOG #0420: A Phase II Study of Radiation Therapy Plus Low Dose Temozolomide Followed by Temozolomide Plus Irinotecan for Glioblastoma Multiform
- RTOG #0521: A Phase III Protocol of Androgen Suppression (AS) and 3DCRT/IMRT vs. AS and 3DCRT/IMRT Followed by Chemotherapy with Docetaxel and Prednisone for Localized, High-Risk Prostate Cancer
- A Randomized Phase III Trial of Concurrent Accelerated Radiation and Cisplatin Versus Concurrent Accelerated Radiation, Cisplatin, and Cetuximab (C225) [Followed by Surgery for Selected Patients] For Stage III and IV Head and Neck Carcinomas
- RTOG #0524: A Phase I/II Trial of a Combination of Paclitaxel and Trasuzumab with Daily Irradiation or Paclitaxel Alone with Daily Irradiation Following Transurethral Surgery for Non-Cystectomy Candidates with Muscle Invasive Bladder Cancer
- RTOG #0525: A Phase III Trial Comparing Conventional Adjuvant Temozolomide with Dose-Intensive Temozolomide in Patients with Newly Diagnosed Glioblastoma
- RTOG #0611-Urinary VEGF and MMP levels in patients receiving radiation therapy for glioblastoma multiforme: Prospective determination of a predictive value for recurrence

- A Randomized Phase III Comparison of Standard-Dose (60Gy) Versus High Dose (74Gy) Conformal Radiotherapy with Concurrent and Consolidation Carboplatin/Paclitaxel in Patients with Stage IIIA/IIIB Non Small Cell Lung Cancer; RTOG #0617/NCCTG N0628/CALGB 30609; Version Date: August 1, 2007; Updated Date: November 27, 2007; Activation Date: November 27, 2007
- RTOG #9003: A Phase III, Randomized Study to Compare Twice Daily Hyperfractionation, Accelerated Hyperfractionation With a Split and Accelerated Fractionation With Concomitant Boost to Standard Fractionation Radiotherapy for Squamous Cell Carcinomas of the Head and Neck
- RTOG #9019: A Phase III Study of the Treatment of Pathologic Stage C Carcinoma of the Prostate with Adjuvant Radiotherapy
- RTOG #9202: A Phase III Trial of the Use of Long-Term Total Androgen Suppression Following Neoadjuvant Hormonal Cytoreduction and Radiotherapy in Locally Advanced Carcinoma
- RTOG #9403: A Postoperative Evaluation of 5-FU By Bolus Injection vs. 5-FU By Prolonged Venous Infusion Prior to and Following Combined Prolonged Venous Infusion + Pelvis XRT vs. Bolus 5-FU + Leucovorin + Levamisole Prior to and Following Combined Pelvic XRT +Bolus 5-FU + Leucovorin in Patients with Rectal Cancer, Phase III
- RTOG #9406: A Phase I/II Dose Escalation Study Using Three Dimensional Conformal Radiation Therapy for Adenocarcinoma of the Prostate
- RTOG #9408: A Phase III Trial of the Study of Endocrine Therapy Used as a Cytoreductive and Cytostatic Agent Prior to Radiation Therapy in Good Prognosis Locally Confined Adenocarcinoma of the Prostate
- RTOG #9410: A Three-Arm, Phase III Study of Concomitant vs. Sequential Chemotherapy and Thoracic Radiotherapy for Patients With Locally Advanced Inoperable Non-Small Cell Lung Cancer
- RTOG #9413: A Phase III Trial Comparing Whole Pelvic Irradiation Followed by a Conedown Boost to Boost Irradiation Only and Comparing Neoadjuvant to Adjuvant Total Androgen Suppression (TAS)
- RTOG #9501: A Phase III Intergroup Trial of Surgery Followed by Radiotherapy vs. Radiochemotherapy for Resectable High Risk Squamous Cell Carcinoma of the Head and Neck
- RTOG #9512: A Randomized Study of Hyper-Fractionation vs. Conventional Fractionation in T2 Squamous Cell Carcinoma of the Vocal Cord
- RTOG #9601: A Phase III Trial of Radiation Therapy With or Without Casodex in Patients with PSA Elevation Following Radical Prostatectomy for pT3NO Carcinoma of the Prostate
- RTOG #9703: A Randomized, Phase II Trial of Concurrent Radiation and Chemotherapy for Advanced Squamous Cell Carcinomas of the Head and Neck
- RTOG #9708: A Phase II Study of Adjuvant Postoperative Irradiation Combined With Cisplatin/Taxol Chemotherapy Following TAH/BSO for Patients With High-risk Endometrial Cancer
- RTOG #9712: A Phase I/II Dose Escalation Study of Thoracic Irradation with Concurrent Chemotherapy for Patients with Limited Small Cell Lung Cancer
- RTOG #9801: A Phase III Study of Amifostine Mucosal Protection for Patients With Favorable Prognosis Inoperable Stage II-IIIA/B Non-Small Cell Lung Cancer (NSCLC) Receiving Sequential Induction and Concurrent Hyperfractionated Radiotherapy for Paclitaxel and Carboplatin
- RTOG #9802: A Phase II Study of Observation in Favorable Low-Grade Glioma and a Phase III Study of Refraction with or without PCV Chemotherapy in Unfavorable Low-Grade Glioma
- RTOG #9803: A Phase I/II Dose Escalation Study Applying Conformal Radiation Therapy in Supratentorial Glioblastoma Multiforme
- RTOG #9805: A Phase II Trial of Transrectal Ultrasound Guided Permanent Radioactive Implantation of the Prostate for Definitive Management of Localized Adenocarcinoma of the Prostate
- RTOG #9811: A Phase III, Randomized Study of 5-FU, Mitomycin-C and Radiotherapy vs. 5-FU, Cisplatin and Radiotherapy in Carcinoma of the Anal Canal
- RTOG #9813: A Phase I/III Randomized Study of Radiation Therapy and Temozolomide vs. Radiation Therapy and BCNU for Anaplastic Astrocytoma
- RTOG #9906: A Phase I/II in Patients With Muscle-Invading Bladder Cancer of Transurethral Surgery Plus Taxol, Cisplatin and BID Irradiation Followed by Either Selective Bladder Preservation or Radical Cystectomy and Adjuvant Chemotherapy
- RTOG #9910: A Phase III Trial to Evaluate the Duration of Neoadjuvant Total Androgen Suppression and Radiation Therapy in Intermediate-Risk Prostate Cancer

- RTOG #0235: Positron Emission Tomography Pre and Post Treatment Assessment for Locally Advanced Non Small Cell Lung Cancer (ACRIN #6668)
- RTOG #0413: A Randomized Phase III Study of Conventional Whole Breast Irradiation (WBI) versus Partial Breast Irradiation (PBI) for Women with Stage 0, I, II Breast Cancer (NSABP B-39)
- RTOG #0615: Phase II Study of Concurrent Chemoradiotherapy using Three-Dimensional Conformal Radiotherapy (3D-CRT) or Intensity-Modulated Radiation Therapy (IMRT) + Bevacizumab (BV) for Locally or Regionally Advanced Nasopharyngeal Cancer
- RTOG #0019: A Phase II Study of External Beam Radiation Therapy Combined With Permanent Source Brachytherapy for Intermediate Risk Clinically Localized Adenocarcinoma of the Prostate
- RTOG #0212: A Phase II/III Randomized Trial of Two Dose Schedules for Delivering Prophylactic Cranial Irradiation for Patients with Limited Disease Small Cell Lung Cancer
- A Phase II Randomized Trial of Surgery Followed by Chemoradiotherapy Plus C225 (CETUXIMAB) for Advanced Squamous Cell Carcinoma of the Head and Neck
- A Phase III Trial for Locally Recurrent, Previously Irradiated Head and Neck Cancer: Concurrent Re-Irradiation and Chemotherapy Versus Chemotherapy Alone
- RTOG #0424: A Phase II Study of a Temozolamide-Based Chemoradiotherapy Regimen for High Risk Low-Grade Gliomas
- A Phase II Trial of Preoperative Chemotherapy and Chemoradiotherapy for Potentially Resectable Adenocarcinoma of the Stomach

Basic Research Studies/Grants

- Improvement of Tumor Control by Combining an Inhibitor of the Epidermal Growth Factor Receptor (EGFR) with Radiation Therapy
- A New Role of MEPE/OF45 as a Co-factor of CHK1 for DNA Damage Response
- A New Target for Preventing Breast Cancer Metastasis to Bone
- The Mechanism of Excess Relative Risk on Carcinogenesis Induced High Let Radiation
- ACRIN Protocol 6688: PET Pre- and Post Treatment Assessment for Locally Advanced Non-Small Cell Lung Carcinoma
- Ethyl Pyruvate As A Radiation Mitigator – In Vivo Characterization And Mechanistic Studies
- Multichannel Robotic System for Concurrent Delivery and Immobilization of Interstitial Therapeutic Agents
- Molecular Determinants of Glioblastoma Response to ZD6474 Combined With Radiotherapy And Temozolamide
- Improvement of Fractionated Radiation Therapy by Combination with SU11248 - Impact of Scheduling
- Molecular Determinants of Glioblastoma Response to AZD2171 Combined with Radiotherapy and Temozolamide
- Molecular Determinants of Glioblastoma Response to BAY 43-9006 (Sorafenib) Combined with Temozolamide and Radiotherapy
- RTOG Research Associates Committee Chair
- RTOG Group Member Agreement
- Fused MR-Based Imaging Datasets Improving Surgical Outcomes and Providing Superior Response Classification System of Malignant Gliomas

Translational Research Studies/Grants

- Clinical Utility of Biomarkers for Stage III Non-small Cell Lung Carcinoma and Stage IV Head and Neck Cancer
- Checkpoint Reduced Cell Sensitivity to High Energy Particles-Induced Killing
- Characterization of the Role of Fhit In Maintenance of Genomic Integrity Following Low Dose Radiation, In Vivo and In Vitro
- Modification of Hyperthermia Response: Project 1 "Sensitization to Thermoradiotherapy in Human Melanoma Xenografts"
- Modification of Hyperthermia Response: Core B "Administration"
- Radiation Therapy Oncology Group Committee Chair
- Modulation of Radiosensitivity in zebrafish
- Radiation Therapy Oncology Group Physicist Chair
- An Emerging Technology Assessment Mechanism for RTOG Protocols
- Modification of Hyperthermia Response: Project 3 "Reduced pHi Inhibits Heat-Induced HSP, Enhances Apoptosis"
- Modification of Hyperthermia Response: Core A "Intracellular pH Regulation"

- Deputy Group Chair of the Radiation Therapy Oncology Group
- Protection from Dose Limiting Toxicity of Chemoradiation for Head and Neck Cancer
- Improvement of Tumor control by Combining a VEGF Blocker, VEGF-Trap, with Radiation Therapy
- Molecular Signatures related to Amifostine Radioprotection
- Evaluation of Fullerene Nanoparticles in a Zebrafish Model
- Microenvironmental control of the Radiation Response
- Vice Chair Translational Research Program
- Nutrigenomics for the Study of Disease Prevention and Intervention
- Protection from Dose Limiting Toxicity of Chemoradiation for Head and Neck Cancer
- Health Research Formula Fund Grant Project 1: Clinical Utility of Biomarkers for Stage III Non-small Cell Lung Carcinoma and Stage IV Head and Neck Cancer
- Enhancement of Tumor Response to Radiation by Use of Vascular Targeting Agent, ZD6126
- Conducting Biomarker, and Proteomics Correlative Research in the Radiation Therapy Oncology Group
- Microenvironmental Control of the Radiation Response After ERBITUX Blockade
- Improvement of Colorectal Tumor Control by Combining ERBITUX with Radiotherapy and Chemotheraputic Agents Oxaliplatin and Irinotecan (CPT-11) PCGA 04-001
- Improvement of Brain Tumor Control by Combining ERBITUX with Radiotherapy and Chemotherapeutic Agents Temozolamide (CPT-11) PCGA 04-025
- Orthogonal Ultrasound for Cancer Detection and Therapy
- Sono-Contrast Induced Functional Imaging/Spectroscopy
- Robot-Assisted Platform for Intratumoral Delivery

Support Groups

Jefferson Kimmel Cancer Center Support Groups, October – December 2008

October

4 **A Place for Me**
A program for children whose parent or grandparent has cancer. Using art, games and other activities, children are helped to understand and to cope with the diagnosis of cancer in the family. A separate group for parents or grandparents is held concurrently.
Time: 10 am – 1:30 pm
Location: Bluemle Life Sciences Building

15 **The Delaware Valley Brain Tumor Support Group**
Time: 7 – 8:30 pm
Location: Bluemle Life Sciences Building, Suite 105

17 **Brain Tumor Caregiver Workshop**
Time: 8 am – 4 pm
Location: Bluemle Life Sciences Building, Suite 101

23 **Facing Breast Cancer**
Screening and Detection
Barbara C. Cavanaugh, MD, Breast Imaging
Time: 12 – 1:30 pm
Location: Hamilton Building, Suite 505

25 **Navigating the New Normal**
(for young adult cancer survivors, ages 18-45)
Cartoon Boot Camp
Christian "Patch" Patchell, Graphic Artist
Time: 2 – 5 pm
Location: Hamilton Building, Suite 210/211

30 **Current Topics**
End-of-Life Issues
Anne Delengowski, RN, MSN, AOCN
Time: 12 – 1:30 pm
Location: Hamilton Building, Suite 505

November

3 **Look Good...Feel Better**
A free program for women who are undergoing cancer treatment to learn to cope with appearance-related side effects of treatment.
Time: 1:30 – 3:30 pm
Location: Gibbon Building, 2nd Floor, Suite 2135

6 **Survivor's Conference**
Life After a Cancer Diagnosis
A patient and family conference on all issues relating to cancer survivorship.
Time: 3:30 – 7 pm
Location: Bluemle Life Sciences Building

13 **Current Topics**
Lung Cancer Awareness Month Program
Benny Weksler, MD, Division of Cardiothoracic Surgery, Section of Thoracic and Foregut Surgery
Time: 12:00 – 1:30 pm
Location: Hamilton Building, Suite 505

19 **The Delaware Valley Brain Tumor Support Group**
Group for individuals diagnosed with a brain tumor and their families. Patients and families share information, gain insight and develop coping strategies to face the challenges associated with living with a brain tumor. For more information, call 215-955-4429.
Time: 7 – 8:30 pm
Location: Bluemle Life Sciences Building, Suite 105

20 **Current Topics**
Jefferson Journaling: A Program for Women Facing Cancer, Janet Ruth Falon
Time: 12:00 – 1:00 pm
Location: Kimmel Cancer Center
Bodine Building, Suite G-312

December

3 **Navigating the New Normal**
(for young adult cancer survivors, ages 18-45). Holiday Happy Hour – an opportunity to network with other survivors your age. $3.00 drink specials, free appetizers and live music (non-alcoholic drinks also available). Friends, partners and other supports are welcome to attend.
Time: 6 – 8 pm
Location: Doc Watson's Pub, 216 S. 11th Street
2nd Floor

11 **Man to Man**
PSA Rising Post-Treatment
Leonard G. Gomella, MD
Chair and Professor, Department of Urology
Time: 12:00 – 1:30 pm
Location: Bluemle Life Sciences Building, Suite 101

17 **The Delaware Valley Brain Tumor Support Group**
Time: 7:00 – 8:30 pm
Location: Bluemle Life Sciences Building, Suite 105

Ongoing Programs

Every Thursday

Radiation Therapy Information Session
Time: 10 – 11:00 am
Location: Kimmel Cancer Center – Bodine, Suite G-312

Learning to Live Better with the Stress of Cancer Research Study
Free 8-week cancer support programs for women, 21 years or older, and diagnosed with cancer or recurrence within three years. Call **215-955-2881** or **1-800-JEFF-NOW**, or visit: **www.JeffersonHospital.org/cim** and click on the study poster.

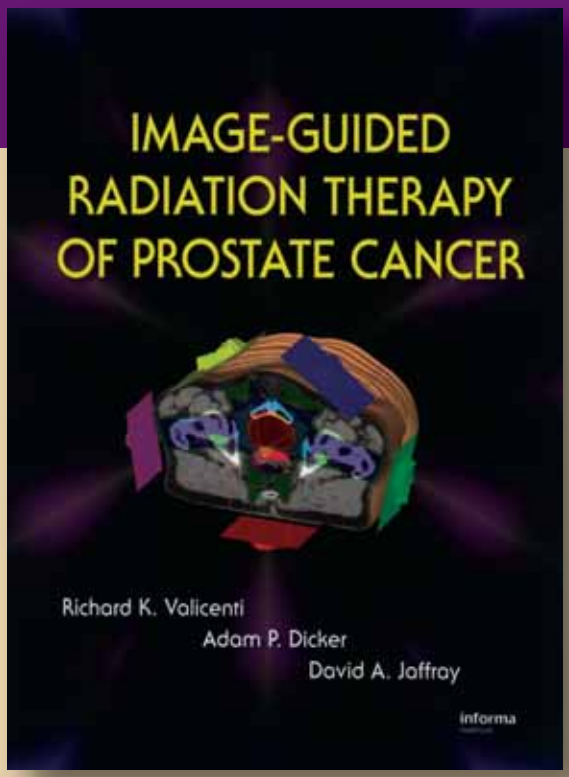

An outstanding new title from Informa Healthcare

Image-guided Radiation Therapy For Prostate Cancer: Principles And Practice

Richard K. Valicenti
Thomas Jefferson University Hospital
Philadelphia, Pennsylvania, U.S.A.

Adam P. Dicker
Thomas Jefferson University Hospital
Philadelphia, Pennsylvania, U.S.A.

David A. Jaffray
Princess Margaret Hospital, Toronto
Ontario, Canada

May 2008 / ISBN-13: 9781420060782
312 pp. / 158 Illustrations / **Price: $229.95**

Answering the need that exists for a single reference to address the practical issues of implementing image guided radiation therapy (IGRT) into prostate cancer treatment, this text provides:

- complete overview of new and exciting technologies
- practical guidance on successfully employing IGRT to improve patient outcomes
- disease stage-specific recommendations which include dosage, fractionation, target volume delineation, and tissue tolerances
- latest novel approaches to radiotherapy of prostate cancer that include intensity modulated radiation therapy (IMRT), hypofractionated radiation therapy, and proton beam radiation therapy

Contents Include:

Ordering Information

PHONE North America 1-800-634-7064
South America 1-859-727-5000
Int'l +44 (0) 1264 343071

FAX North America 1-800-248-4724
South America 1-859-647-4028
Int'l +44 (0) 1264 343005

E-MAIL orders@taylorandfrancis.com
INTERNET www.amazon.com or www.bn.com
MAIL Informa Healthcare
Kentucky Distribution Center
7625 Empire Drive
Florence, KY 41042 U.S.A.


Jefferson™
Kimmel Cancer Center
NCI-designated